

Stephen F. Austin State University

SFA ScholarWorks

Electronic Theses and Dissertations

12-2018

Groundwater Hydrogeolgy and Hydrochemistry of Karst Springs in the Eastern Peninsula of Fort Hood Military Installation

William Scribner Welles

Stephen F. Austin State University, william.s.welles@gmail.com

Follow this and additional works at: <https://scholarworks.sfasu.edu/etds>



Part of the [Environmental Chemistry Commons](#), [Environmental Monitoring Commons](#), [Geochemistry Commons](#), [Hydrology Commons](#), [Natural Resources and Conservation Commons](#), and the [Water Resource Management Commons](#)

Tell us how this article helped you.

Repository Citation

Welles, William Scribner, "Groundwater Hydrogeolgy and Hydrochemistry of Karst Springs in the Eastern Peninsula of Fort Hood Military Installation" (2018). *Electronic Theses and Dissertations*. 217.
<https://scholarworks.sfasu.edu/etds/217>

This Thesis is brought to you for free and open access by SFA ScholarWorks. It has been accepted for inclusion in Electronic Theses and Dissertations by an authorized administrator of SFA ScholarWorks. For more information, please contact cdsscholarworks@sfasu.edu.

Groundwater Hydrogeolgy and Hydrochemistry of Karst Springs in the Eastern Peninsula of Fort Hood Military Installation

Creative Commons License



This work is licensed under a [Creative Commons Attribution-Noncommercial-No Derivative Works 4.0 License](https://creativecommons.org/licenses/by-nc-nd/4.0/).

GROUNDWATER HYDROLOGY AND HYDROCHEMISTRY OF KARST SPRINGS IN
THE EASTERN PENINSULA OF FORT HOOD MILITARY INSTALLATION

By

WILLIAM S WELLES, Bachelor of Science

Presented to the Faculty of the Graduate School of

Stephen F. Austin State University

In Partial Fulfillment

Of the Requirements

For the Degree of

Master of Science in Environmental Science

STEPHEN F. AUSTIN STATE UNIVERSITY

December 2018

GROUNDWATER HYDROLOGY AND HYDROCHEMISTRY OF KARST SPRINGS IN
THE EASTERN PENINSULA OF FORT HOOD MILITARY INSTALLATION

By

William Scribner Welles, B.S.

APPROVED:

Dr. Matthew McBroom, Thesis Director

Dr. Kevin Stafford, Committee Member

Dr. Kefa Onchoke, Committee Member

Pauline M. Sampson, Ph.D.
Dean of Research and Graduate Studies

ABSTRACT

The eastern peninsula of Fort Hood Military Installation is underlain by a complex karst spring network. These springs are a primary water source in a protected habitat for endangered songbirds, which has only recently begun to be fully investigated. These Fredericksburg Group springs express both epigenetic and hypogenetic karst signatures. The study area is part of a paleo reef trend, a hydraulically disconnected segment of the northern section of the Edwards Aquifer. This study utilized standard ion index values, repeated measures, and principal component analyses on the chemical profiles of six perennial springs to classify spring water sources and their chemical composition. Spring water quality was found to be within acceptable limits for TCEQ regulated analytes, with the exception of total dissolved solids. Of the springs sampled the chemical profiles of springs to the north were epigenetic in composition and those to the south expressed more hypogenetic influences.

ACKNOWLEDGEMENTS

This thesis would not have been possible without the assistance of many great people with whom that I have been blessed to have had interactions. The most obvious are those that offered their technical expertise, to my thesis committee, Dr. Matthew McBroom, Dr. Kevin Stafford, and Dr. Kefa Onchoke. I extend my appreciation for your sage advice and direction throughout this project. Thanks are extended to Dr. Mindy Faulkner for her assistance in collecting field water samples and to Mr. Wayne Weatherford of the Soil, Plant, and Water Laboratory at Stephen F. Austin State University for his expertise in laboratory analysis. Charles Pekins, the Wildlife Biologist at Fort Hood Natural Resources Management Branch was the keystone contact for this project, allowing me and other SFASU students and faculty access to Fort Hood Military Installation for this and other projects.

I cannot give thanks enough for my family who provided me with love and allowed me time and space to complete this journey. To my in-laws, Tom and Susan, thank you for offering Jo and me a place to live in Nacogdoches, which allowed us to start our family and send me down the path to completing my degree at SFASU. My parents Gordon and Debbie I thank you for your unending support and making me the adult and parent I am today; you are excellent examples to follow. Oliver and Elliot, my most wonderful children, one only needs to observe your unbridled energy and enjoyment of life to be inspired; thank you my loves.

As this chapter of my life comes to a close, I reflect on those who have passed away in my life and how they have all help guide me to where I am today. I remember my Pop Pop, an avid gardener, who showed me how managing the natural world can bring such joy and happiness to others. I remember his wife, my Nana, who showed me what wonders can be made from that hard work, in the form of her famous strawberry rhubarb pie. I remember my grandfather, who with his analytical mind and his career as a toxicologist in no small part piqued my interest in the sciences at a young age. Also, I remember my father in law Tom, who was an avid outdoorsman and gladly took me under his wing and introduced me to hunting, which is now a large part of my life and motivates me to spend those beautiful early morning hours in the outdoors.

Ultimately, I thank my wife. Jo, you are the best partner, friend, coach and, therapist that I could ask for. Your understanding and willingness to manipulate our schedules and manage the children during this project was critical for its completion. Your words of encouragement, willingness to listen to me ramble on, or to read my manuscripts were all priceless points of support. You are my rock and I cannot wait to see what comes next for us.

TABLE OF CONTENTS

ABSTRACT	i
ACKNOWLEDGEMENTS.....	ii
TABLE OF CONTENTS	iv
LIST OF FIGURES	vii
LIST OF TABLES	xi
TABLE OF EQUATIONS	xiii
1. INTRODUCTION.....	1
1.1 Site Description	3
1.1.1 Study Area	3
1.1.2 Climate.....	4
1.2 Geology.....	5
1.2.1 Geologic Setting.....	5
1.2.2 Stratigraphy.....	12
1.1.1 Karst Geomorphology	15
1.1.2 Karst Hydrology.....	26
1.2 Groundwater Chemistry.....	30
2. OBJECTIVES.....	36
3. METHODS	37
3.1 Field Data Collection	37
3.2 Laboratory Analysis.....	38

3.2.1	Instrumentation	38
3.2.2	Elemental Analysis	40
3.2.3	Anion Analysis.....	41
3.3	Statistical Analysis.....	42
3.3.1	Standard Ion Indexes	42
3.3.1.1	Individual Standard Ion Indices (ISII).....	44
3.3.1.2	Successive Standard Ion Indices (SSII)	45
3.3.2	t-Test.....	45
3.3.3	Repeated Measures Analysis of Variance (ANOVA)	46
3.3.4	Principal Component Analysis (PCA)	46
4.	RESULTS.....	50
4.1	Water Quality Analysis	50
4.2	Standard Ion Indexes	58
4.2.1	Individual Standard Ion Indexes	58
4.2.2	Successive Standard Ion Index	59
4.3	Inferential Statistics	79
4.3.1	Statistical Analysis.....	82
4.3.1.1	Major Ion and Physicochemical Repeated Measures Grouped by Spring	82
4.3.1.2	Trace Metals Repeated Measures Grouped by Spring	86
4.3.1.3	Major Ion and Physicochemical Repeated Measures Grouped by Date	87
4.3.1.4	Trace Element Repeated Measures Grouped by Sample Date	92
4.3.2	Principal Component Analysis	94
4.3.2.1	Soluble Element Principal Component Analysis	94

4.3.2.2	Total Element Principal Component Analysis	101
5.	DISCUSSION	106
5.1	Study Significance	106
5.2	Regulatory Standards Water Quality Review	107
5.3	Karst Hydrogeology Interpretation Using Geochemical Evidence	108
6.	CONCLUSION	112
7.	LITERATURE CITED	114
8.	APPENDIX	119
8.1	Field and Laboratory Results	119
8.1.1	Physicochemical Attributes Data Table	119
8.1.2	Soluble Elements Data Tables	123
8.1.3	Total Element Data Tables	133
8.2	Statistics Data Tables	140
8.2.1	t-test Results	140
8.2.2	Soluble Element PCA Biplots	142
8.2.3	Total Element PCA Biplots	152
9.	VITA	162

LIST OF FIGURES

Figure 1: Fort Hood location and general study area map	2
Figure 2: Fort Hood climate data 2010-2014 monthly rainfall and temperatures (maximum and minimum averages represented as error bars) (National Oceanic and Atmospheric Administration, 2014)	6
Figure 3: Paleogeography of Texas modified from (Blakeley, 2011)	9
Figure 4: Geologic structures of central Texas modified from (Walker, 1979) and (Amsbury, 1984).....	11
Figure 5: Edwards Aquifer and Balcones Fault Zone (George et al. 2011)	14
Figure 6: Stratigraphic units and their relative positions in Bell County (Moore, 1964).....	16
Figure 7: Stratigraphic cross section: vertical facies distribution, Fredericksburg division (Moore, 1964).....	16
Figure 8: Carbonate aqueous speciation diagram Points 1 and 2 indicate pH where the two carbonate species in question are at equal concentrations in solution. Point 3 indicates the pH at which bicarbonate concentration dominates (Univeristy of California Davis, 2014).....	18
Figure 9: Dunham carbonate rock classification ((Dunham, 1962)).....	20
Figure 10: Epigene and hypogene karst diagram (Klimchouk, 2007).	21
Figure 11: Hypogene speleogenesis initiation (Klimchouk, 2000)	24
Figure 12: Evolutionary karst types and speleogenetic environments (Klimchouk, 2007).....	25
Figure 13: Elution profile for 8 compound standards for Dionex ICS-2100 IEC	41
Figure 14: Spring discharge and monthly precipitation for eastern peninsula of Ft. Hood	52

Figure 15: Piper diagram of studied springs from December 2012 to December 2013	54
Figure 16: Standard ion index of major and trace ions for Bear Spring from December 2012 to December 2013.....	60
Figure 17: Standard ion index of major and trace ions for Crayfish Spring from December 2012 to December 2013.....	61
Figure 18: Standard ion index of major and trace ions for Geocache Spring from December 2012 to December 2013.....	62
Figure 19: Standard ion index of major and trace ions for Gnarly Root Spring from December 2012 to December 2013.....	63
Figure 20: Standard ion index of major and trace ions for Nolan Creek Spring from December 2012 to December 2013.....	64
Figure 21: Standard ion index of major and trace ions for East Range Road Spring from March 2012 to December 2013	65
Figure 22: Successive standard ion index for Bear Spring from December 2012 to December 2013.....	67
Figure 23: Successive standard ion index subset for Bear Spring from December 2012 to December 2013	68
Figure 24: Successive standard ion index for Crayfish Spring from December 2012 to December 2013	69
Figure 25: Successive standard ion index subset for Crayfish Spring from December 2012 to December 2013.....	70
Figure 26: Successive standard ion index for Geocache Spring from December 2012 to December 2013.....	71
Figure 27: Successive standard ion index subset for Geocache Spring from December 2012 to December 2013.....	72
Figure 28: Successive standard ion index for Gnarly Root Spring from December 2012 to December 2013.....	73
Figure 29: Successive standard ion index subset for Gnarly Root Spring from December 2012 to December 2013.....	74

Figure 30: Successive standard ion index for Nolan Creek Spring from December 2012 to December 2013	75
Figure 31: Successive standard ion index subset for Nolan Creek Spring from December 2012 to December 2013	76
Figure 32: Successive standard ion index for Road Spring from December 2012 to December 2013	77
Figure 33: Successive standard ion index subset for Road Spring from December 2012 to December 2013	78
Figure 34: Soluble analytes PCA biplot of component 1 (Cl, Na, Mg, and S) and component 2 (pH and - K)	98
Figure 35: Soluble analytes PCA biplot for component 3 (NO ₃ and - C°) and component 5 (Ca, F, and discharge)	99
Figure 36: Soluble analytes PCA biplot for component 4 (TDS) and component 5 (Ca, F, and discharge).....	100
Figure 37: Total metal PCA biplot for component 1 (Al, Fe, Na, and S) and component 2 (- Mg and - K)	104
Figure 38: Total metal PCA biplot for component 3 (B, Zn, and pH) and component 4 (discharge).....	105
Figure 39: Soluble element PCA biplot of component 1 (Cl, Na, Mg, and S) x component 2 (K and inverse pH)	142
Figure 40: Soluble element PCA biplot component 1 (Cl, Na, Mg, and S) x component 3 (N and inverse temperature)	143
Figure 41: Soluble element PCA biplot component 1 (Cl, Na, Mg, and S) x component 4 (conductivity).....	144
Figure 42: Soluble element PCA biplot component 1 (Cl, Na, Mg, and S) x component 5 (Ca, F, and discharge)	145
Figure 43: Soluble element PCA biplot component 2 (K and inverse pH) x component 3 (N and inverse temperature)	146
Figure 44: Soluble element PCA biplot component 2 (K and inverse pH) x component 4 (conductivity).....	147

Figure 45: Soluble element PCA biplot component 2 (K and inverse pH) x component 5 (Ca, F, and discharge)	148
Figure 46: Soluble element PCA biplot component 3 (N and inverse temperature) x component 4 (conductivity)	149
Figure 47: Soluble element PCA biplot component 3 (N and inverse temperature) x component 5 (Ca, F, and discharge).....	150
Figure 48: Soluble element PCA biplot component 4 (conductivity) x component 5 (Ca, F, and discharge).....	151
Figure 49: Total element PCA biplot component 1 (Al, Fe, Na, and S) x component 2 (Mg and inverse K).....	152
Figure 50: Total element PCA biplot component 1 (Al, Fe, Na, and S) x component 3 (B, Zn, and pH)	153
Figure 51: Total element PCA biplot component 1 (Al, Fe, Na, and S) x component 4 (discharge).....	154
Figure 52: Total element PCA biplot component 1 (Al, Fe, Na, and S) x component 5 (conductivity).....	155
Figure 53: Total element PCA biplot component 2 (Mg and inverse K) x component 3 (B, Zn, and pH)	156
Figure 54: Total element PCA biplot component 2 (Mg and inverse K) x component 4 (discharge).....	157
Figure 55: Total element PCA biplot component 2 (Mg and inverse K) x component 5 (conductivity).....	158
Figure 56: Total element PCA biplot component 3 (B, Zn, and pH) x component 4 (discharge)	159
Figure 57: Total element PCA biplot component 3 (B, Zn, and pH) x component 5 (conductivity)	160
Figure 58: Total element PCA biplot component 4 (discharge) x component 5 (conductivity)	161

LIST OF TABLES

Table 1. Testing parameters, limits of detection and standard testing method number.....	39
Table 2: Physicochemical attributes of sampled springs.....	52
Table 3: Soluble cation concentrations of sampled springs.....	55
Table 4: Total cation concentrations of sampled springs	55
Table 5: Anion concentrations of sampled springs.....	56
Table 6: Results compared to level 1 primary contact recreational surface water maximum contaminate level standards for Belton Lake (TCEQ 2012)	56
Table 7: Results compared to aquatic life and human health maximum contaminate level protection standards (TCEQ 2012).....	57
Table 8: Results compared to human health maximum contaminate level protection standards (TCEQ 2012).....	57
Table 9: Mean major ion and physicochemical comparison table for sampled springs and adjacent water sources (mg/L unless specified)	80
Table 10: Mean trace metal comparison table of sampled springs and adjacent water sources (µg/mL).....	80
Table 11: Repeated measures ANOVA and SNK grouping by spring for major cations of sampled springs (mg/L)	84
Table 12: Repeated measures ANOVA and SNK grouping by spring for major anions and physicochemical parameters for sampled springs (mg/L unless noted)	84
Table 13: Repeated measures ANOVA and SNK grouping by spring for trace metals of sampled springs (µg/L).....	89
Table 14: Repeated measures ANOVA and SNK grouping by date for Ca, Mg, and Na spring analyses	90

Table 15: Repeated measures ANOVA and SNK groupings by date for P, K, and S spring analyses	90
Table 16: Repeated measures ANOVA and SNK by date for physicochemical spring data	91
Table 17: Repeated measures ANOVA and SNK grouping by date for anion analyses	91
Table 18: Repeated measures ANOVA and SNK grouping by date for Al, B, Cu and Fe analyses	92
Table 19: Repeated measures ANOVA and SNK grouping for Mn and Zn analyses	93
Table 20: Table of PCA variables for soluble and total element data sets.....	95
Table 21: Soluble elements PCA eigenvalues of the correlation matrix	95
Table 22: Component loadings for soluble PCA	96
Table 23: Total elements PCA dataset	101
Table 24: Total element PCA eigenvalues of the correlation matrix	102
Table 25: Component loadings for retained factors for total element PCA	102
Table 26: Physicochemical attributes	119
Table 27: Major soluble element analysis (mg/L).....	123
Table 28: Soluble anion analysis of sampled springs (mg/L)	126
Table 29: Trace metal soluble element analysis (mg/L)	130
Table 30: Total major element analysis (mg/L)	133
Table 31: Total trace element analysis (µg/L).....	136
Table 32: Major element t-tests among springs	140
Table 33: Trace element t-tests among springs	140
Table 34: Major element t-tests among sample dates.....	141
Table 35: Trace element t-tests among sample dates	141

TABLE OF EQUATIONS

Equation 1: Formation of carbonic acid (Ford & Williams, 2007).....	17
Equation 2: Dissolution of calcium carbonate in the presence of natural water (Ford & Williams, 2007)	18
Equation 3: Pyrite oxidation contributing to carbonate dissolution (Ford & Williams, 2007).....	19
Equation 4: Carbon dioxide gas into aqueous solution reaction	31
Equation 5: Arrhenius equation	33
Equation 6: Standard ion index calculation modified from (Şen, 2011)	43
Equation 7: General formula for calculating principal components modified from (SAS, 2014).....	47
Equation 8: Principal component loading equation	47

1. INTRODUCTION

Fort Hood Military Installation (FH) is located in central Texas (Figure 1). This region is classified as a semi-arid climate. FH is predominated by mixed juniper and oak woodlands interspersed with mixed shrubland. The eastern peninsula of FH is unique in that this region is home to an endangered species of song bird, the Golden-cheeked Warbler (*Setophaga chrysoparia*). The eastern peninsula is also the only known habitat for an undescribed sub-species of salamander (*Plethodon albagula*) which utilizes karst springs as its sole habitat (Pekins, 2007). The protected species utilizing this region as their habitat make this location particularly sensitive. A complete understanding of the region's environmental system is important to protect and manage this habitat. Until recently, there has been little emphasis on understanding the network of karst springs that are found throughout FH. Water is fundamental to life; it is only logical that advancing an understanding hydrology of this region would be of utmost importance for successful management of this sensitive ecosystem.

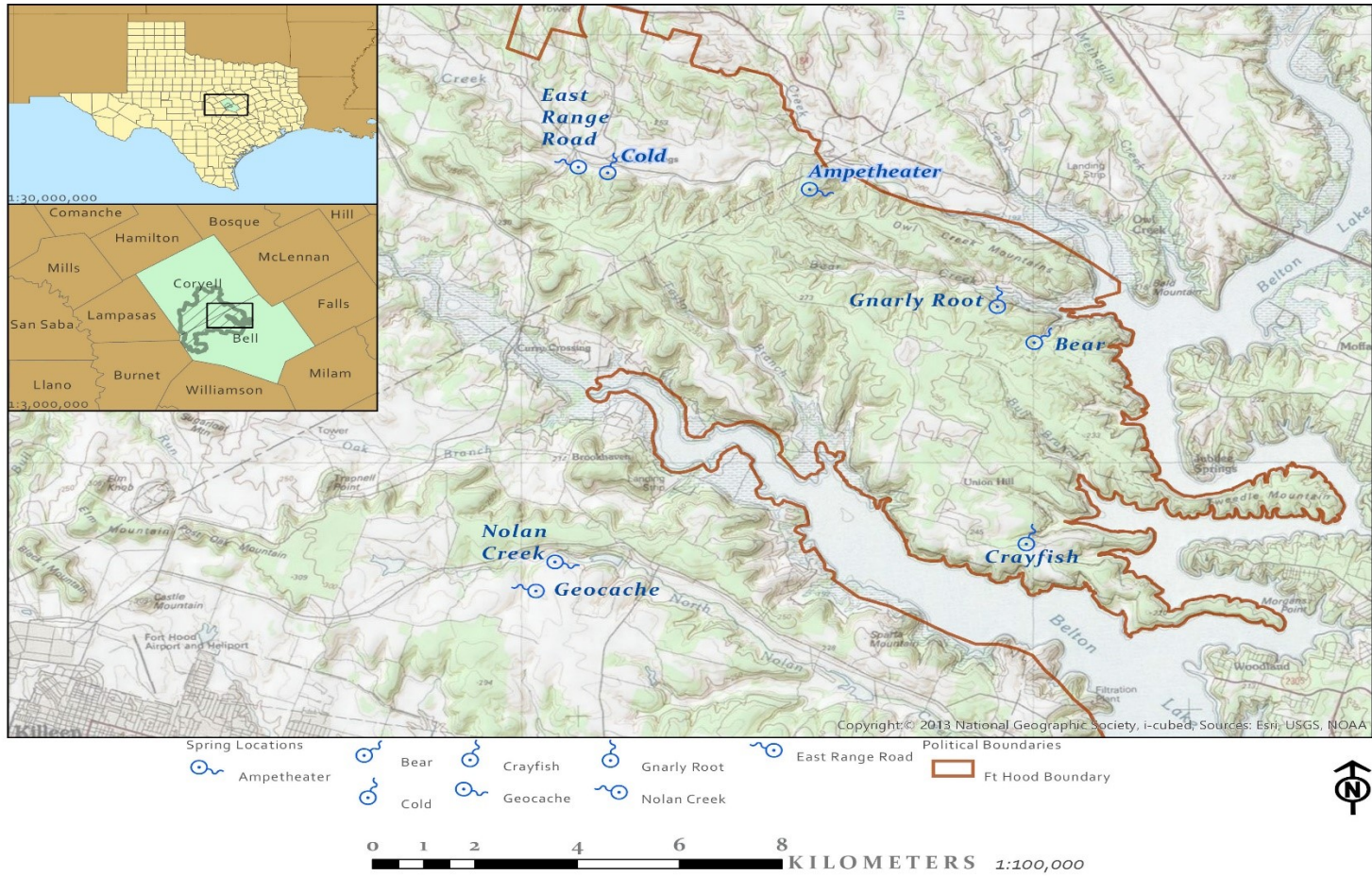


Figure 1: Fort Hood location and general study area map

1.1 Site Description

1.1.1 Study Area

FH straddles Bell and Coryell counties in Central Texas. Geographically speaking, this is the largest U.S. military installation in the world, having an approximate area of 96,921 hectares. FH was officially opened on September 18, 1942 for tank destroyer training and firing center in response to the start of United States military activities in World War 2 (Briuer, 2015). Due to the rapid establishment of FH, over 300 farming families were forced to relocate on a short timetable. To compensate for this, many of those original farming families were allowed to continue grazing their cattle on government property, which is a continued practice today. Fort Hood is the primary garrison for the III Corps, composed of the First Cavalry Division, Fourth Infantry Division (mechanized), and 36th Engineer Brigade with a total base population of over 41,000 soldiers (History of the Great Place, 2007). FH today is utilized for a variety of combat training missions involving infantry, rotary wing aircraft and mechanized armor divisions. The main mission of FH is to maintain a high state of readiness for combat missions and training for the III Corps (Briuer, 2015).

The study area for this project is the eastern-most portion of the FH installation. Specifically, a peninsula reaching out into Lake Belton, within Bell County that is bounded to the north by Preachers Creek, to the south by Cowhouse Creek and to the

east by Lake Belton. There are two outlying springs also studied in this project lying to the south of Cowhouse Creek, along North Nolan Creek. The springs studied are shown in Figure 1. The springs chosen in the study area due to their perennial discharge. They had been known historically to continue to produce water despite the drought Central Texas at the time of study. Topography of the region is quite rugged, characterized by large limestone mesas, comprising the Owl Mountains, and steep valleys covered in thick mixed juniper and oak woodlands. Elevation difference in the study area is approximately 120 meters (from 290 meters above mean sea level (AMSL) to 170 meters AMSL). Soils in the study area are predominantly mollisols and exposed calcareous bedrock. Soils ranges from clay to loamy in texture and are well drained (National Resources Conservation Service, 2014 a). The geology of the region consists predominantly of Lower Cretaceous carbonates modified by karst features such as sinkholes, caves, rock shelters and springs.

1.1.2 Climate

Fort Hood is in a transitional zone between sub-tropical, sub-humid, and sub-tropical humid regions. This region is classified as the North Central Climatic division by the National Climate Data Center (NCDC) (Narasimhan et al.2005). NCDC data indicates seasonal variability in mean monthly rainfall where the greatest precipitation volumes are in the late winter to early spring. The lowest precipitation volumes are in the summer months. Average annual precipitation for region is 88.72 cm (National Oceanic and Atmospheric Administration, 2014). The region has regularly experienced

less precipitation annually within the last 10 years and has fluctuated between minor to severe drought conditions consistently per the National Drought Mitigation Center (MDMC). The annual average temperature for the region is 19.5 °C with mean highs and lows of 25.7 °C and 13.3 °C, respectively, spanning a 12.4 °C range. All climate related averages were calculated over a 30-year period (1980-2010) (National Oceanic and Atmospheric Administration, 2014). In Figure 2 precipitation and temperature data are shown for Ft. Hood locally between 2010 and 2014.

1.2 Geology

1.2.1 Geologic Setting

The geologic strata directly underlying FH are comprised of Lower Cretaceous (Comanchean) aged formations of the Fredericksburg and Trinity groups. The sedimentary formations comprising these groups were deposited in a range of environments from coastal to marine settings. During the Cretaceous, Central Texas depositional environment alternated between transgression and regression of the epicontinental sea, changing the depositional environment of the sedimentary formations of the Lower Cretaceous (Walker, 1979). The geologic region is defined by a regional positive elevation feature known as the Belton High, which is bounded to the

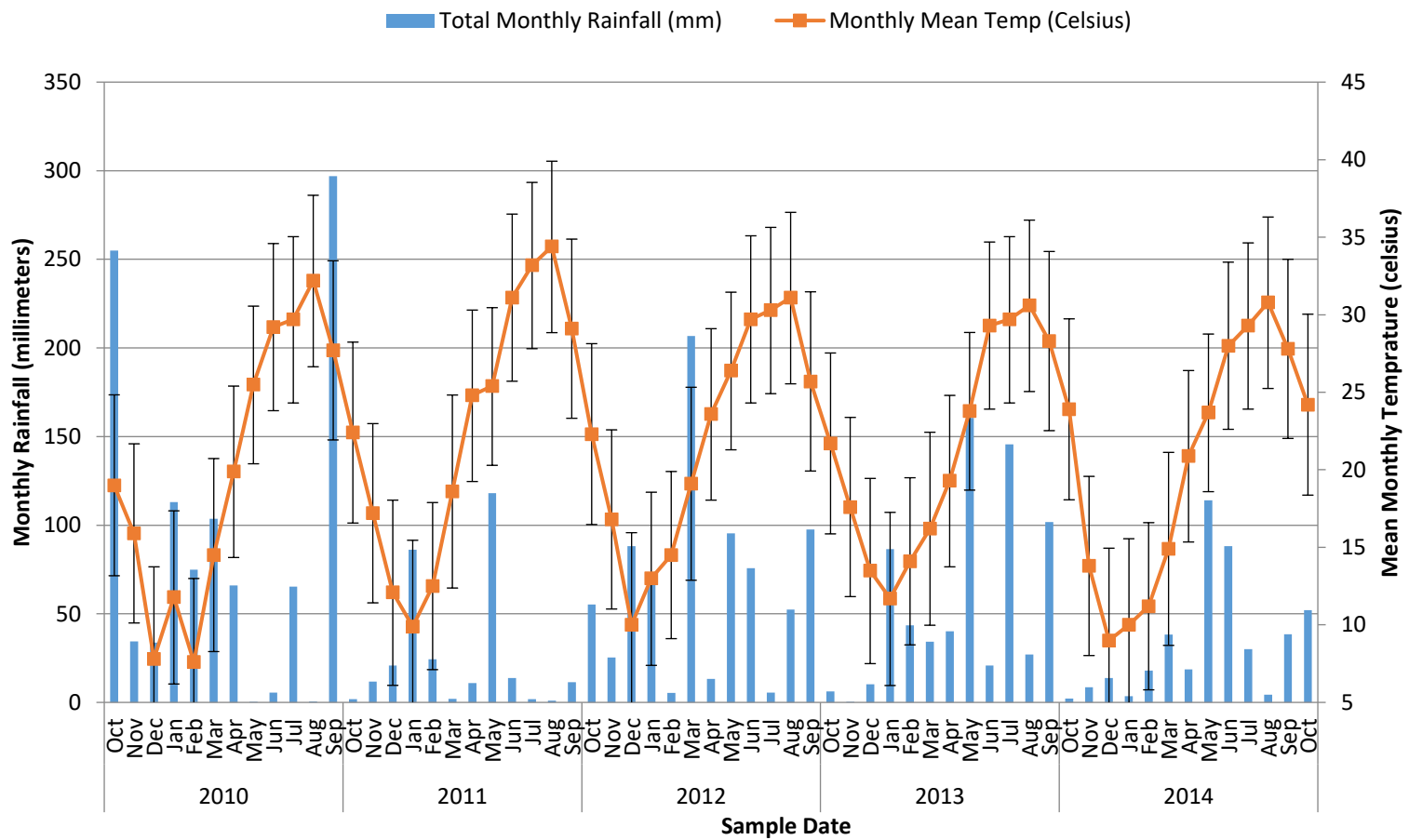


Figure 2: Fort Hood climate data 2010-2014 monthly rainfall and temperatures (maximum and minimum averages represented as error bars) (National Oceanic and Atmospheric Administration, 2014)

northeast by the North Texas -Tyler Basin, to the southwest by the Round Rock Syncline and to the west by the Llano Uplift (Figure 4). The creation of the Belton High is believed to be associated with a reef structure at the northern extent of the main Edwards Reef trend during the Late Cretaceous (Brown, 1972).

Proterozoic rocks within the region are comprised of granites and schists (Sellards, 1930). These formations were subaerially exposed which resulted in significant erosion in the late Precambrian and into the Cambrian (Walker, 1979). During the Cambrian, Central Texas was beginning to be transgressed by an epicontinental sea (Figure 3). During this time, deposition of sediments began across the region and participated in varying rates of subsidence of the sea floor (Walker, 1979). The transgression of the epicontinental sea and deposition of sediments continued into the Ordovician until the Edwards Plateau region was uplifted by the Ouachita Orogeny, and deposition ceased (Figure 3). The Ouachita Orogeny uplift and faulting significantly affected the formations of the Cambrian and Ordovician causing extensive deformation, creating difficulties in determining an exact succession of geologic processes prior to this Pennsylvanian age orogeny (Adkins, 1930).

The Pennsylvanian period is initiated by the Ouachita Orogeny (Figure 3). During this mountain building phase, bedding planes of prior sediments were significantly folded and faulted creating many of the large regional trends such as the Concho Arch and the Central Texas Bend Flexure to the west of Bell County (Figure 4). By the end of the Pennsylvanian, formations in the region were tilted toward the Midland Basin to the west of the study area. This basin was then being supplied alternately

with erosional material by river systems flowing west from the newly formed Ouachita range and marine sediments from a transgressing and regressing sea.

During the Permian, the sea continued to enlarge and migrate west of the Ouachita Range. The early part of the Permian saw the development of marine reefs to the west of the study area (Figure 3). This was followed with the deposition of evaporites. The late Permian continued to see deposition of evaporites as well as the addition of shales.

The Triassic saw the retreat of the sea dominating the region during the Permian. This retreat allowed for erosion of Permian formations across the region (Figure 3); however, the severity of this erosion is not thought to have removed large amounts of material (Walker, 1979). Erosion continued through the Jurassic and into the Cretaceous. The erosional events of the Triassic and Jurassic created a relatively flat, stable depositional surface for Cretaceous sediments, known as the Comanche Shelf (Figure 4).

The Cretaceous is marked by the final epicontinental sea transgressing across Central Texas (Figure 3). This sea began to regress near the end of the Cretaceous in alternating surges of sea level rise and fall. These sequences of transgression and regression of the sea allowed for interbedded layers of sandstone and limestone sediments to be deposited upon the Comanche Shelf, which stretched from Mexico to beyond the northern Texas border in a north-east direction. This shelf throughout the Lower Cretaceous never became a deep marine depositional environment like what was found to the southeast of the Comanche Shelf in the paleo Gulf of Mexico. Along the



550 Ma Precambrian



500 Ma Cambrian



485 -450 Ma Ordovician



430 Ma Silurian



315 Ma Pennsylvanian



260 Ma Permian



230 Ma Triassic



170 Ma Jurassic



115 Ma Early Cretaceous



85 Ma Late Cretaceous



40 Ma Eocene



8 Ma Miocene

Figure 3: Paleogeography of Texas modified from (Blakeley, 2011)

boundary between the deeper ancient Gulf of Mexico and the shallow Comanche Shelf formed a narrow band of coral and algae that spanned the length of the Comanche Shelf known as the Stuart City Reef (Figure 4). The Stuart City Reef protected the leeward side of the reef, creating a low energy depositional environment after its formation. The Comanche Shelf region was relatively flat with regional depth changes and notable depressions to the southwest and northeast, being the Maverick and North Texas-Tyler Basins respectively (Figure 4). Between these depressions was a long shallow region trending northwest named the Central Texas Platform. On the Central Texas Platform and found within the study area is a sub-regional variance in deposition where the Edwards limestone deposition is significantly thicker than found in other areas measured. This sub-regional thickening is believed to be near 6.5 km wide and trends northwest, known as Moffatt Mound. The Moffatt Mound is thought to be an outlying paleo reef associated with the Edwards Group deposition, unique with its oolite and pellet facies as opposed to rudist and milloid facies found in other locations within the area (Amsbury, 1984). The study area shows a similar shoal trend as that of the Moffatt mound as described by (Bryant, 2012) and (Faulkner, 2016). As the Comanchean gave way to the Gulfian midway through the Cretaceous, sea level began to recede and an erosional unconformity is evident between the two series (Walker, 1979). Sediments, however, continued to be deposited in the paleo Gulf of Mexico, creating structural strain forming the basis of the Balcones Fault that roughly trends along with the Comanche Shelf.

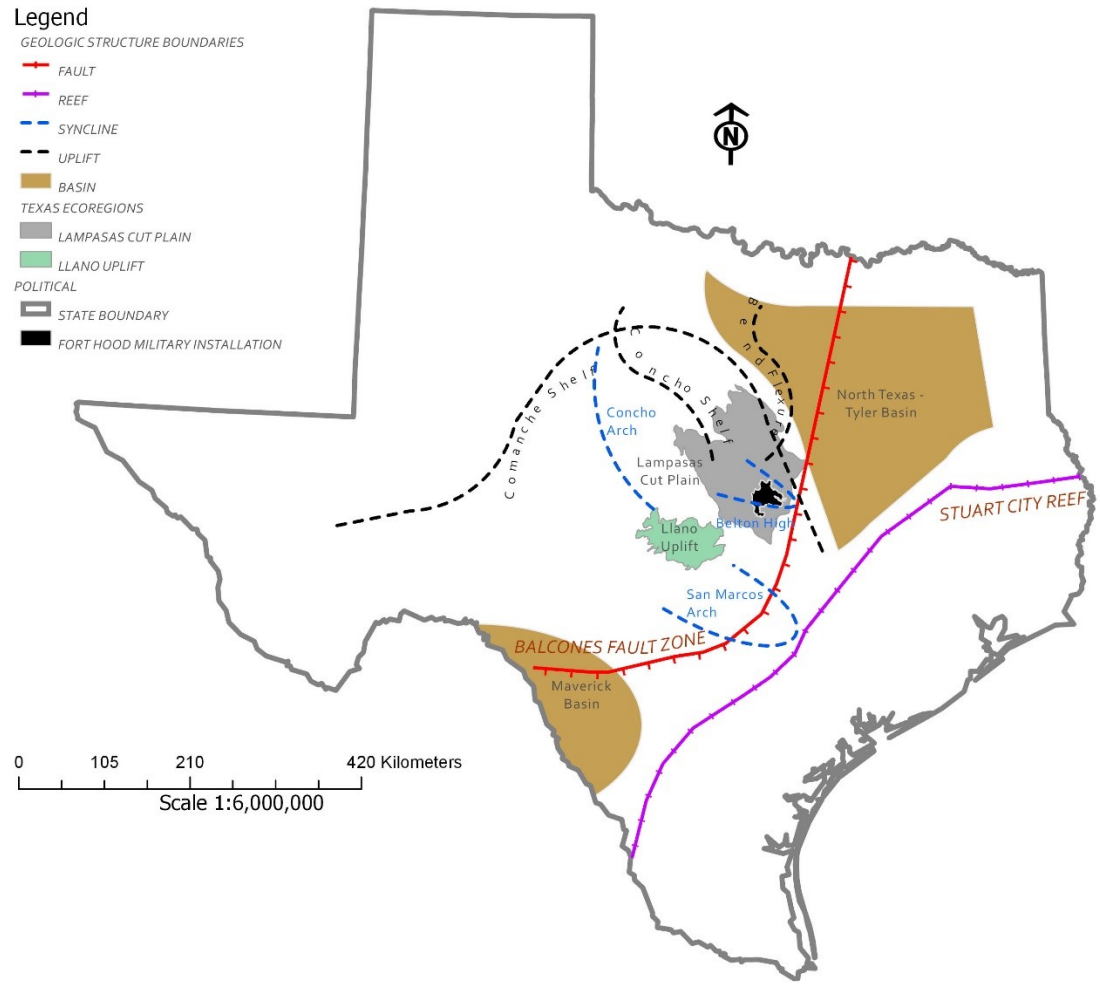


Figure 4: Geologic structures of central Texas modified from (Walker, 1979) and (Amsbury, 1984)

The Balcones Fault continued to develop through the Cenezoic into the Miocene. The Balcones Fault fractured and exposed Cretaceous sediments stretching from Kinney to Bell Counties (Figure 4). Faulting displaced Cretaceous sediments vertically more than 150 m in Bell County from their original depositional location due to the tectonic activity through the Miocene (Adkins, 1930) which down-dropped formations to the southeast forming the Gulf Coastal Plain. Bell County is bisected north to south by a series of prominent, down-to-the- east, normal faults being part of the Balcones Fault Zone. The faulting and subsequent exposure of calcareous sediments to meteoric water allowed for the development of the Edwards Aquifer (Figure 5).

1.2.2 Stratigraphy

There are two Groups within the Comanche Series that crop out in the study area: Trinity and Fredericksburg (Figure 6). The Trinity Division is divided into three formations: Travis Peak Sandstone, Glen Rose Limestone and Paluxy Sand. Three distinct formations comprise the Fredericksburg Division: Walnut, Comanche Peak and Edwards formations. The Comanche Peak and Edwards formations are most prevalent at higher elevations and Walnut is predominantly found in valleys within the study area.

The Glen Rose Formation is comprised of thinly bedded, Miliolid-rich limestone alternating with marl to marly limestone beds (Moore, 1964). The marl is more resistant to weathering which creates a stair-stepped, differential weathering of outcrops. Glen Rose strata are limited to outcropping along Cowhouse Creek predominantly in the western region of Fort Hood (Adkins, 1930).

Fredericksburg Division comprises the remainder of outcropping formations within the study area (Figure 6). The Walnut Formation contains five separate members: Bull Creek Limestone, Bee Cave Marl, Cedar Park Limestone, Keys Valley Marl and Upper Marl, of which only the upper two, Keys Valley Marl and Upper Marl members, are predominantly present in Cowhouse and Owl Creek stream sides (Figure 7). The Keys Valley is both marl and fossiliferous nodular limestone. The fauna within the Keys Valley unit is diverse, containing gastropods, pelecypods, echinoids, oysters, ammonites and a distinct upper boundary of *Gryphaea* (Moore, 1964). The Upper Marl unit is differentiated from Keys Valley in that it is more abundant in limestone, fauna within are less abundant and comprised of *Gryphaea mucronata*, *Exogyra texana*, gastropods, pelecypods, and *Inoceramus* (Moore, 1964). The variations within the Walnut facies were driven by slight variations in depositional environment caused by sea level change during Fredericksburg time (Rose, 1972). Comanche Peak is a nodular massive limestone comprised of shell fragments and micrite in its lower regions which then

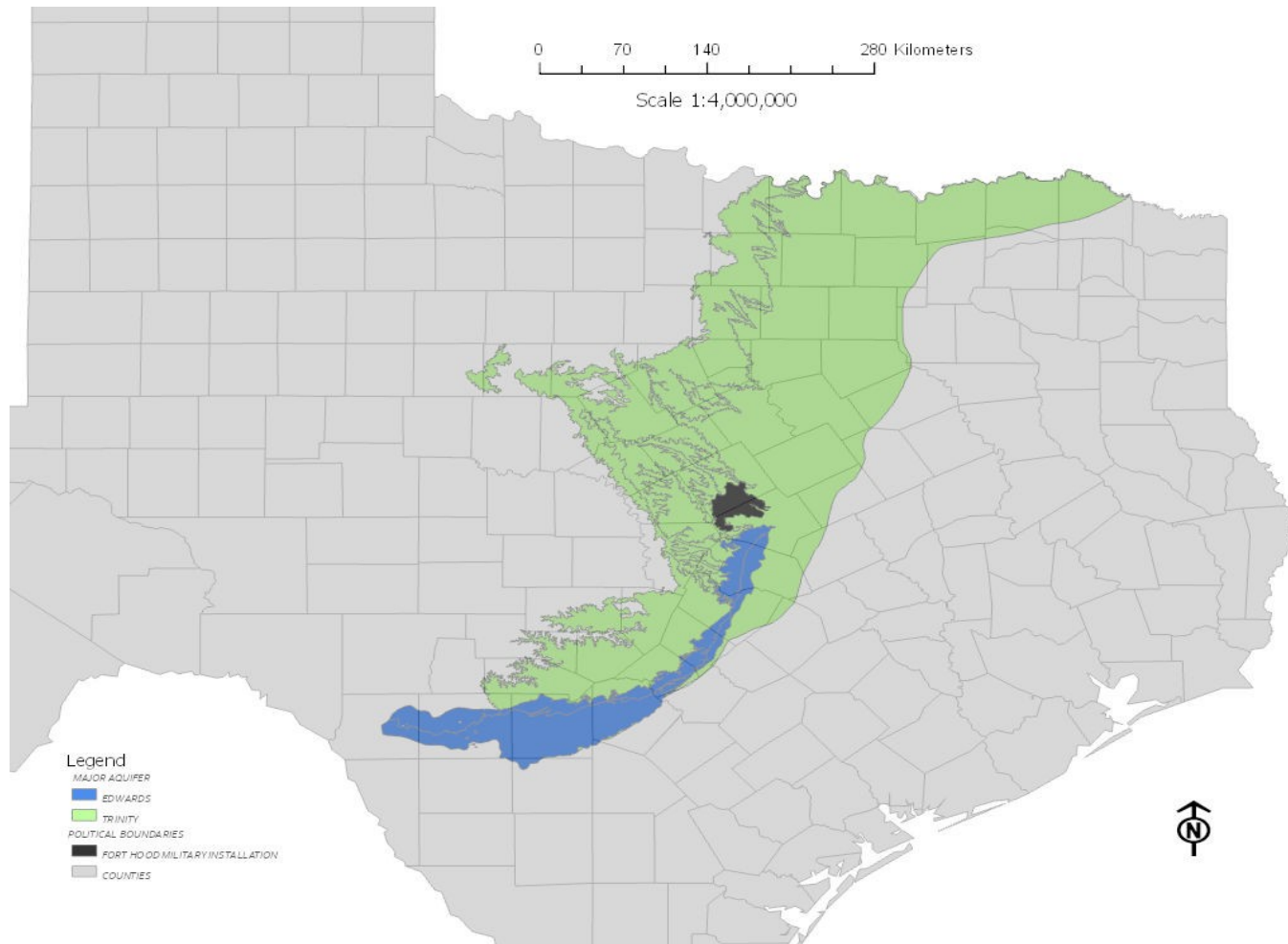


Figure 5: Edwards Aquifer and Balcones Fault Zone (George et al. 2011)

becomes oolite rich and dolomitized in the upper sections (Moore, 1964). The final formation of the Fredericksburg Division is the Edwards. The Edwards Limestone generally thins across Bell County towards Williamson County. However, there is a unique alteration of this trend near the town of Moffat. The Edwards Limestone has deposits of nearly 40 meters thick in this region, which is known as the Moffat Mound (Nelson, 1959). The Edwards is generally described as fossiliferous dolomitized limestone with black chert facies commonly found as caprock (Moore, 1964). In the Moffat Mound region, however, Edwards facies are oolite rich within a grainstone matrix (Amsbury 1984 and Moore 1964). Amsbury concluded that the long and narrow Moffat Mound region (5 km wide and 80 km long trending West-Northwest) is a paleo reef structure separating tidal flat and open marine depositional environments.

1.1.1 Karst Geomorphology

Karst as a term was coined in 1893 by Jovan Cvijić, a Serbian. The term karst has been expanded from its original definition, initially used for describing the geography of the *Kras* region in Europe along the Adriatic Sea from Italy to Slovenia. The term karst is commonly used now to describe any terrain comprised of sinkholes, caves, sinking streams and/or springs. All these features are tertiary modifications to soluble bedrock formations. Karst terrain is commonly formed in carbonate rock formations such as limestone or dolomite. However, karst features also occur in any rock that is comprised of minerals that can be solvated, such as sulfates, halides or even some silicate deposits (Ford & Williams, 2007).

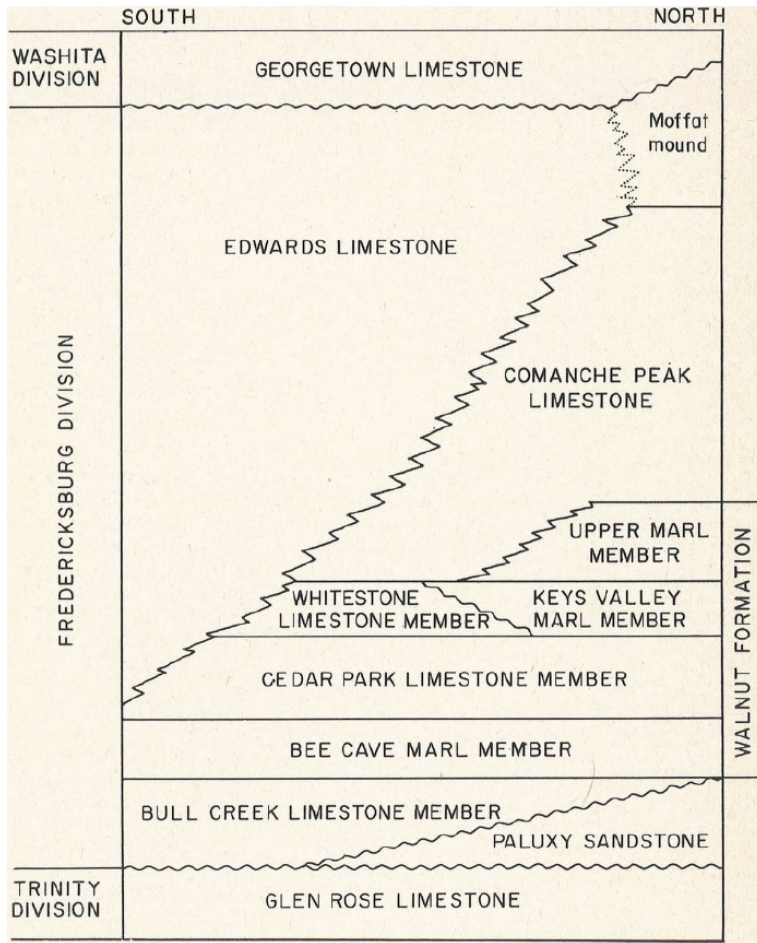


Figure 6: Stratigraphic units and their relative positions in Bell County (Moore, 1964)

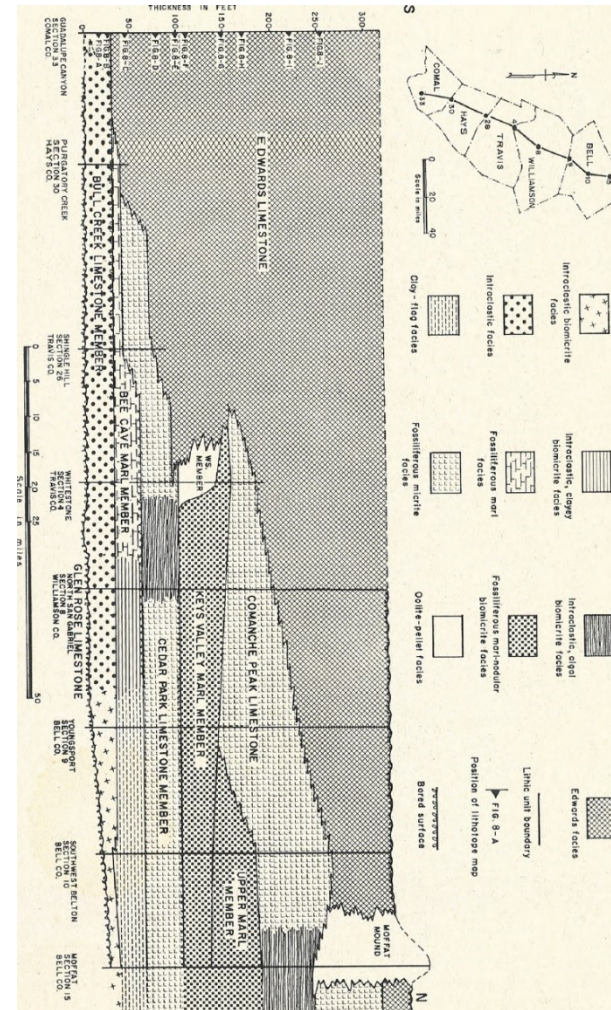
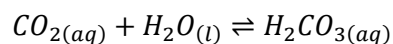
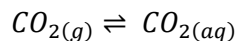


Figure 7: Stratigraphic cross section: vertical facies distribution, Fredericksburg Division (Moore, 1964)

Carbonate karst features develop through interactions between water and rock. The water serves as a dilute aqueous acidic solution capable of precipitating out minerals within rock formations. Water naturally contains trapped gaseous carbon dioxide ($CO_{2(g)}$) and dissolved carbon dioxide ($CO_{2(aq)}$). This mixture is due to pressures atmospheric carbon dioxide exerts on liquid water. Pressure causes a portion of the gas to become trapped in the intermolecular spaces within liquid water. The resulting solution of CO_2 and H_2O then undergoes chemical reaction generating carbonic acid (H_2CO_3) (Equation 1). As carbonate rock is exposed to this dilute carbonic acid, carbonate begins to react with water, being simple dissolution, and carbonic acid, both precipitating bicarbonates in solution (HCO_3^- (aq)) (Equation 2). The concentration of carbonic acid, bicarbonate and carbonate present in the aqueous phase is dependent upon the pH of the system (Figure 8). Carbonic acid dissolution occurs at the highest kinetic rate at or near the soil-bedrock interface, due to the meteoric water being free of carbonates prior to introduction into pores within carbonate rock (Williams, 1983) or in regions where two aqueous solutions mix and chemical equilibria is disturbed, increasing the dissolution potential of carbonic or other acidic agents into solution (Dreybrodt & Eisenlohr, 2000). The dissolution of carbonate out of solid rock and into aqueous solution is the most common method for karst features to form in carbonate rich rock formations.

Equation 1: Formation of carbonic acid (Ford & Williams, 2007)



Equation 2: Dissolution of calcium carbonate in the presence of natural water (Ford & Williams, 2007)

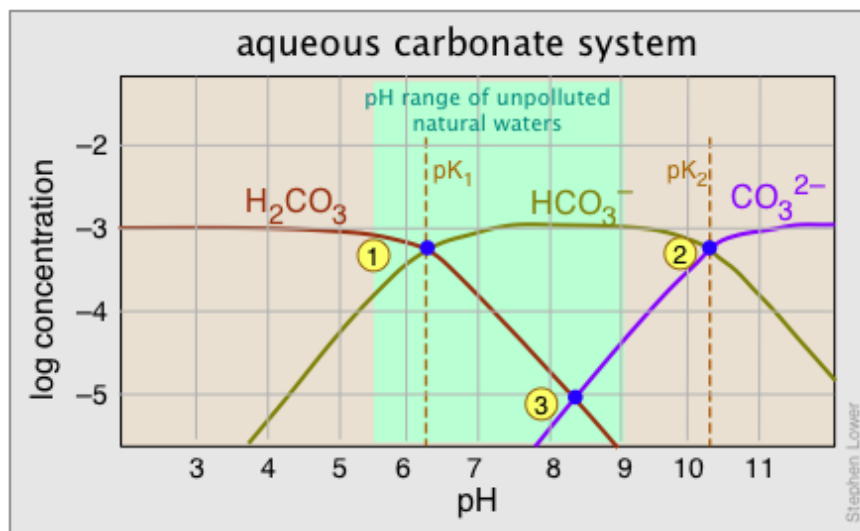
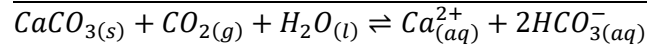
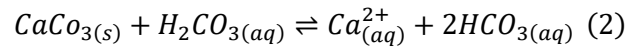
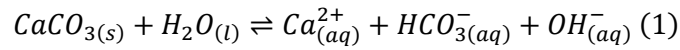
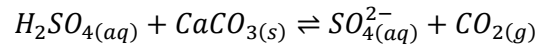
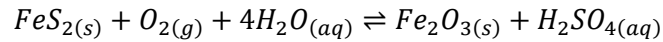


Figure 8: Carbonate aqueous speciation diagram Points 1 and 2 indicate pH where the two carbonate species in question are at equal concentrations in solution. Point 3 indicates the pH at which bicarbonate concentration dominates (University of California Davis, 2014).

Carbonic acid is not the only reagent capable of producing dissolution within formations. Water interacting with minerals at depth can also solvate other acids or form ionic solutions capable of dissolution, such as pyrite (FeS₂) oxidation producing sulfuric acid or geothermal water containing hydrogen sulfide from igneous formations at depth (Equation 3). These processes, over time, begin to produce differential weathering patterns on and within carbonate rocks.




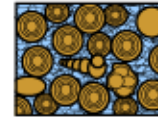
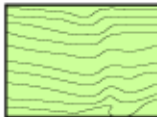
Equation 3: Pyrite oxidation contributing to carbonate dissolution (Ford & Williams, 2007)



Introduction of aqueous acids or ionic dissociation over time develop tertiary dissolution channels within the rock. These tertiary dissolutional features preferentially form along primary permeability features, such as bedding planes. Secondary fractures within soluble formations created through weathering or tectonic movement are also susceptible to tertiary dissolutional modification. Dissolutional features can also form transversely across soluble formations between interconnected pores within a formation's matrix (Klimchouk, 2000). As channels develop, they become the most preferential pathway for water to infiltrate bedrock and enhance water storativity and transmissivity within rock formations, creating viable aquifers (Ford & Williams, 2007).

The bulk composition of a rock can be a predominating factor in development of tertiary features. Proportions of soluble material found within rock formations define the maximum potential for dissolution. Rocks with greater than 70% soluble material globally exhibit the best dissolution potential (Ford & Williams, 2007). High surface area of individual grains that comprise formations are also an essential factor in dissolution potential. There is an inverse correlation between surface area and grain size; therefore, the finer the grain size, the higher the potential for dissolution. This correlation holds until the grains comprising the formation are classified as well-sorted, which allows for better packing of grains, reducing the potential for pores between the sediment grains (Ford & Williams, 2007). Therefore, carbonate rock that is in the wackestone to

packstone classification (Figure 9) would be the best candidate for karst feature development. The Edwards and Comanche Peak Formations in the study area are fine grained and wackestone to packstone in classification. Both candidates for karst formation.

Original components not bound together at deposition				Original components bound together at deposition. Intergrown skeletal material, lamination contrary to gravity, or cavities floored by sediment, roofed over by organic material but too large to be interstices
Contains mud (particles of clay and fine silt size)		Lacks Mud		
Mud-supported		Grain-supported		
Less than 10% Grains	More than 10% Grains			
Mudstone 	Wackestone 	Packstone 	Grainstone 	Boundstone 

C. G. St. C. Kendall, 2005 (after Dunham, 1962, AAPG Memoir 1)

Figure 9: Dunham carbonate rock classification ((Dunham, 1962))

Chemical dissolution can occur under different regimes, either through sub aerial water interaction (meteoric water interaction at the surface) or interaction with water at depth such as from cross-formational or geothermal sources. Karst features developed at the surface are classified as epigene features while hypogene features are developed at depth (Figure 10). Distinct morphological differences occur between hypogene and epigene regimes which are predominantly derived from hydrodynamic differences in the two systems.

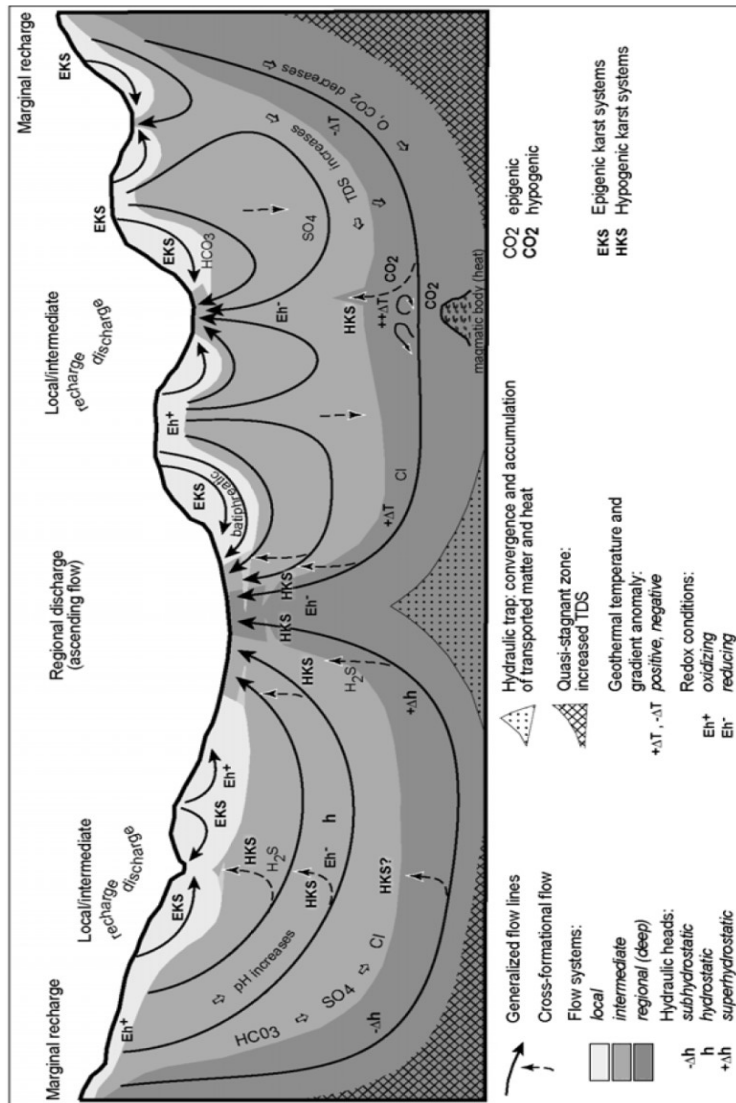


Figure 10: Epigene and hypogene karst diagram (Klimchouk, 2007).

Epigene systems are found in unconfined settings, where channel openings are both exposed at the surface, with their development controlled by hydraulic capacity and available recharge water. In the unsaturated zone of epigene systems water movement is driven by gravity, whereas in the phreatic zone hydrostatic pressure exerted by meteoric water directs the dissolution predominantly downward into soluble formations

(Ford & Williams, 2007). As dissolution conduits are developed and breakthrough, there is a positive feedback on the system allowing for a direct increase in epigenetic speleogenesis, coinciding with increased water flow. Epigenetic speleogenesis develops generally as corrosive waters encounter any void space within a soluble rock formation. These voids can be bedding planes, joints, interconnected matrix pores, or faults. As the corrosive water infiltrates fractures within soluble rock, driven predominantly by gravity, the soluble rock dissolves into solution widening the fractures and creating conduits within the rock formation. There may be many conduits that begin to form, and due to the heterogeneity of the rock matrix and the fractures within, some conduits will form preferentially faster than others. After a conduit has broken through into a more permeable formation or becomes subaerially exposed, conduit development accelerates along this flow path and slows on other competing secondary conduits. Over time secondary conduits may begin to interconnect with the primary conduit that achieved breakthrough either by elongation of their flow path or through continued expansion of the primary conduit.

Alternatively, the development in hypogene systems is not as intuitive. The prevailing factor that determines hypogene development is hydraulic head differences between two adjacent layered aquifers separated by a leaky soluble confining unit. Hypogene karst development is classified by an overall upward direction of water flow, moving transverse to the bedding plane of a formation (Figure 10). The transverse movement of water within a hypogene segment of a karst aquifer commonly connects layered aquifers through confining beds (Klimchouk, 2014). During initiation of

hypogene speleogenesis the soluble unit is commonly an upper leaky confining bed of an adjacent aquifer (Figure 11). As the pressure of the aquifer below begins to drive water into pore spaces of the soluble unit above, multiple competing conduits begin to form, transversely across the soluble unit. All competing conduits will develop at relatively similar rates, which is due in part to the relatively slow initiation of conduit development that favors uniformity (Klimchouk, 2000). Some conduits may even exhibit lateral development along the soluble unit though still exhibiting a transverse progression overall. These multiple competing conduits can create a complex branching maze like network (Klimchouk, 2007). When a conduit achieves breakthrough into the adjoining aquifer above, the upper aquifer will most likely have a permeability greater than that of the non-modified soluble unit; however, it will still not be greater than the newly formed conduits. After breakthrough is achieved some of the competing conduit development may slow, resulting in dead end terminations for conduits. After breakthrough there may be some increase in flow through the “successful” conduit initially but will stabilize to the newly entered formations permeability limit. This output control on hypogene karst allows for all competing conduits to continue developing uniformly within a soluble unit due to the pressure head differences between the units above and below the soluble unit being relatively similar (Klimchouk, 2000). When hypogene systems break through to another soluble member, their feedback is regulated by the lowest permeable member in the system, thus creating a control on flow rates in hypogene systems. This cross-formational interaction allows for potential mixing of water inputs and varied mineral contact, thus altering chemical equilibrium. Waters from different formations mix and their chemical composition changes and moves chemical

composition farther from equilibrium, thus more favorable for speleogenesis (Klimchouk, 2014).

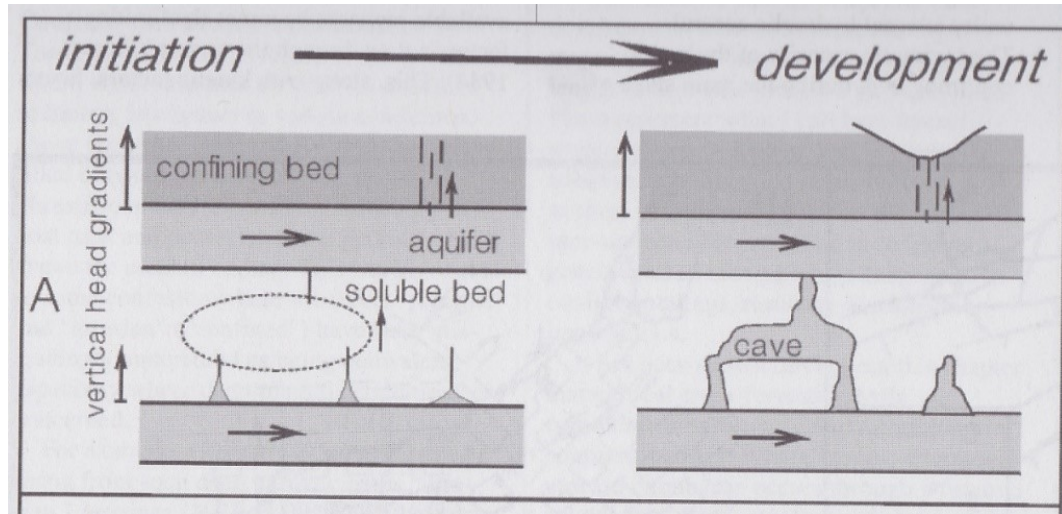


Figure 11: Hypogene speleogenesis initiation (Klimchouk, 2000)

In naturally occurring systems it is common to find karst features that exhibit both epigene and hypogene speleogenesis. Karst development is episodic; a function of water interacting with soluble rock, over geologic time scales, differently depending upon the current geologic position of a series of formations. As a formation is deposited, buried and outcrops again on the surface, speleogenesis can occur at any phase of this sequence and will exhibit different karst features brought on by either or both speleogenetic regimes.

Eogenetic karst networks are the most simplified, where speleogenesis begins soon after deposition, prior to deep burial and epigene speleogenesis regime dominates. Telogenetic karst development occurs after burial, where by hypogene upward movement of water prevails speleogenetic activity. As a soluble formation is uplifted and

or the overlying formations erode, eogenetic features can modify historical telogenetic features adding greater complexity to the karst network. Commonly identified formations exhibiting hypogenetic features have been decoupled from the hydrologic network that developed them and have been reconnected with a different epigenetic hydrologic system, exposing the network to the surface prior to human observation (Klimchouk, 2007). The evolution of karst features is depicted below in Figure 12.

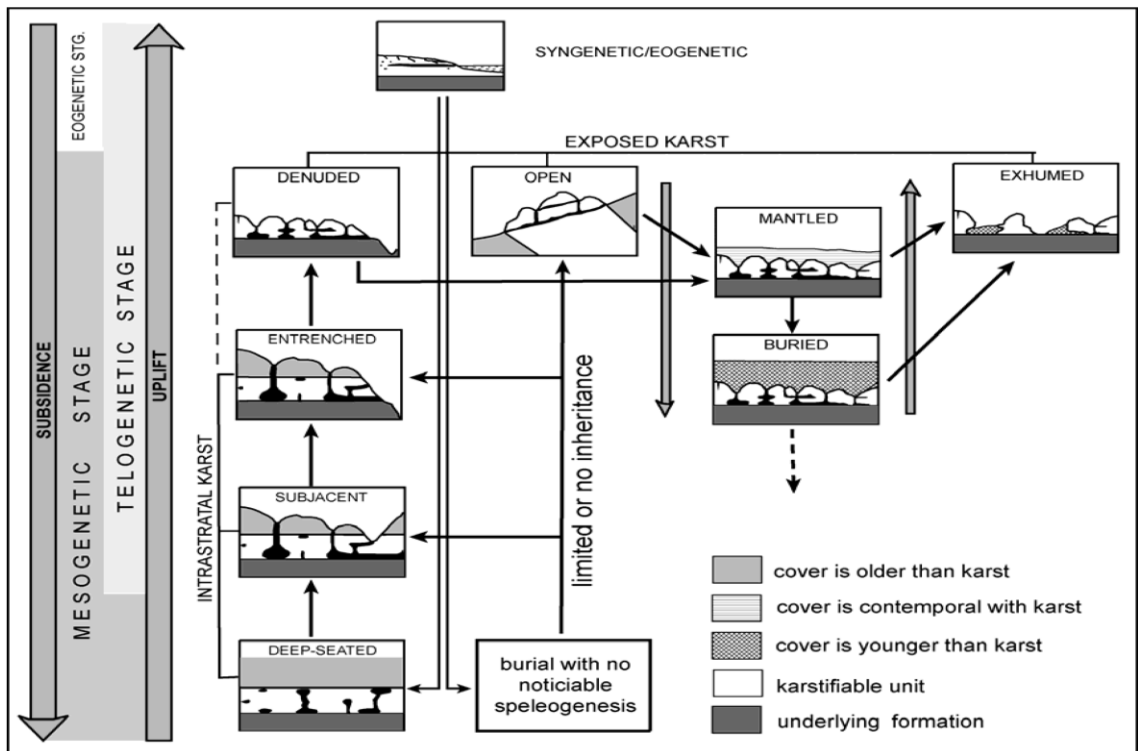


Figure 12: Evolutionary karst types and speleogenetic environments (Klimchouk, 2007)

1.1.2 Karst Hydrology

Porosity, the availability of void spaces within rock, and permeability, the interconnected nature of those pores, are of equal importance for the presence of water to develop into a viable groundwater source. Aquifers are groundwater bodies that have sufficient volumes and flow rates to provide sufficient water for an intended purpose. Therefore, aquifer is a relative designation for a water body; an aquifer sufficient to supply a single domicile might not be considered an aquifer if being drawn upon for a municipality.

The way in which the primary porosity (matrix), secondary porosity (fractures) and dissolution modification (tertiary) are connected is a major determining factor to how a karst aquifer behaves hydraulically. In all karst aquifers there is some level of connectedness between these porosities. Commonly one porosity regime will be dominant over the others. The empirical discharge data are truly a result of diagenesis and morphology of the basin. Variations in flow are due to the narrow pore throats that groundwater must infiltrate and migrate through (the tortuosity) as well as length of flow paths taken within the host formation.

In epigene karst where the dissolution channels and or fractures are well-developed and highly interconnected, hydrologic response to infiltrating water into the system can be rapid, resulting in discharge of water at springs or wells with short lag times, on the order of minutes to days (Kresic et al. 2010). Rapid response times are due to the large diameter dissolution channels' (compared to matrix interstitial spaces) ability to move volumes of water rapidly driven by gravity and atmospheric pressure.

Similar rapid response times are also possible in formations that have a high functional porosity, resulting from high interconnectivity between pore spaces within the matrix, such as can be seen commonly in non-soluble sand formations (Ford & Williams, 2007).

Hypogene systems are two or more transmissive formations interconnected by soluble leaky confining formations. As the confining soluble material begins to precipitate into the groundwater, karst structures begin to form. Over time phreatic pressure drives groundwater upward through geostatic, thermobaric, or compressive forces towards the soluble confining formation (Klimchouk, 2014). Geostatic forces are generated by subsiding structures, which exert pressure on water filled voids. Thermobaric pressure is created in deep seated formations where the pressure gradient is sufficient to increase trapped water temperatures, thus further pressurizing groundwater. Pressure exerted by folded and faulted formations is classified as compressional force. All three hypogenic forces drive groundwater towards areas having lower pressure gradients, generally higher in strata elevation. Strata above water bearing units commonly have lower pressure heads due to reduced overburden, thus reducing geostatic pressure. Formation and breakthrough of hypogene systems are commonly found in regions where surficial erosion has removed overburden material, such as near incising streams (Klimchouk, 2000).

In cases where there is appreciable primary, secondary and tertiary porosity, the system will exhibit multiple flow regimes. In practice, it can be difficult to differentiate between secondary and tertiary porosity; commonly they are considered jointly. As conduits are drained, the matrix pores that were also filled with water, during infiltration,

will begin to release this water into the larger fractures and dissolution channels over time. The slow release of water from pores in the rock matrix is expressed as less discharge per unit of time, over larger lengths of time (Kresic et al. 2010). During large water inputs into epigene aquifers that are fractured or have developed dissolution morphology, there will be a sharp rise in discharge through the system, with a duration of discharge comparable to the duration of water application from the source. This direct control of karst discharge by the source is characteristic of true epigene systems (Ford & Williams, 2007). Hypogene systems are comprised of one or more soluble formations sandwiched between water bearing formations; discharge is controlled by the upper confining bed (Klimchouk, 2000). This condition occurs because the permeability of the formations below are significantly higher than that of the uppermost minimally modified confining bed, thus the uppermost confining unit is the limiting factor in discharge for the network.

Regardless of which classification best fits a spring network, the initial surge of water detected at the outlet will be water that resided within the aquifer for some time prior to any flushing storm events. The first increase in discharge detected at an outlet will be resident water previously retained within the aquifer that was flushed out of the system through the hydrostatic pressure exerted on the aquifer from infiltrating water. After some period, the highly transmissive zones of the aquifer will be flushed of “old” resident water and the infiltrated water will begin to be observed at the outlet. The rate at which each aquifer exhibits this flushing mechanism will be dependent upon the composition of the aquifer and the physical structure of the drainage network.

Observation of water flushing from the aquifer and collection of water quality data can indicate the origins of water contributing to a spring outlet. Water collected from a spring that contains certain mineral signatures can indicate origins of the sample. Spring locations that are monitored regularly and show variations in mineral concentrations or compositions may show changes in water source. Mineral content variations over time may also indicate residence time changes within the aquifer or mixing with other sources.

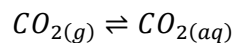
Spring water discharges associated with a storm event can be evidence of different karst morphologies. The speleogenetic regime, aquifer matrix, channel structure, duration, and intensity of the storm event will all be significant factors in discharge rate and volume. Well-developed epigene channel networks behave as underground streams showing storm discharges characterized by a sharp peak and short duration, characteristic of the dominant channel flow regime (Ford and Williams 2007). Karst aquifers with poorly developed channel networks or hypogene systems that are highly regulated by their semipermeable members express storm discharge events more gradually (Klimchouk, 2007). The discharge will have poorly defined peaks and occur over a larger period, respective of the storm event duration. The cause for the longer residence time is the increase of path length, greater tortuosity, low permeability and/or low effective primary porosity.

1.2 Groundwater Chemistry

The chemistry of karst groundwater is much richer than its predecessor, meteoric water, due to its interaction with the aquifer rock matrix, surrounding geological formations, and soil horizons. As water encounters these materials, loose particles can become suspended in the water. Chemical reactions also occur that dissolve constituents into the water. Nearly all materials are soluble in water, to varying degrees, which gives water a composition that reflects the environments to which it has been exposed. In carbonate aquifers, the most prevalent water constituents are bicarbonate, calcium, and magnesium. This is a result of limestone (CaCO_3) and dolomite ($\text{CaMg}(\text{CO}_3)_2$) being the main sedimentary rocks in carbonate formations. Other major ionic constituents of groundwater are potassium, sodium, sulfate and chloride. These major ion constituents form a large portion of the ionic character of natural waters (Drever, 1997). Concentrations of major ions in natural waters are useful in determining groundwater sources. Bicarbonate waters, which are also rich in calcium and magnesium, are associated with carbonate groundwater (Kresic et al. 2010). Sulfate waters, also rich in high levels of magnesium, are normally associated with evaporites or igneous groundwater sources. Chloride waters, which are also found to have high alkali ion concentrations, can be associated with surface water sources, evaporites or deep saltwater aquifers (Ford & Williams, 2007). The minor ionic constituents of natural waters are predominantly trace metals and anthropogenic compounds.

In karst aquifers, however, groundwater is not always found at equilibrium due to the reaction kinetics of carbonate with natural water. The reaction kinetics for carbon dioxide gas to become aqueous are quite rapid, occurring in under a minute. The reaction of aqueous carbon dioxide to form carbonic acid occurs in milliseconds, which then dissociates as rapidly into hydrogen ions and bicarbonate. This essentially allows for natural waters to almost instantaneously begin the reaction with carbonate sediments. However, reaction kinetics for carbonates occurs over days (Morse & Arvidson, 2002). The kinetics of carbonate essentially does not allow for rapidly flushing carbonate aquifer water to reach equilibrium with the source rock. Due to this non-equilibrium situation, calculations can be done to assist in determining the relative age of spring water based upon its carbonate concentration.

Equation 4: Carbon dioxide gas into aqueous solution reaction



Another useful chemical analysis that can be conducted on karst aquifers is to calculate the calcium to magnesium ratio. The Ca/Mg ratio can assist in identifying the composition of the aquifer. Ratios in the range of 6-8 are indicative that the aquifer is primarily comprised of limestone. However, if the ratio is less than this range, the aquifer is comprised of dolomite as well as limestone (White W. B., 2010).

Saturation index is another calculation that can be conducted based upon the measured activity product of calcium and carbonate species present in spring water. These calculations help to quantify how far the spring water sample is from equilibrium.

Values that are found to be above the equilibrium constant for carbonate are super saturated and those below are considered to be under saturated (Drever, 1997).

Fundamental chemical and physio-chemical properties are an efficient way to identify and classify water sources. Critical water quality parameters that are commonly utilized for assessment of water bodies are temperature, pH, dissolved oxygen and conductivity. Each of these parameters is easily collected in the field and can assist in rapid classification of a water body.

Temperature of natural waters is a fundamental water quality parameter. Generally, an increase in temperature will increase chemical reaction rates as described in the Arrhenius equation in Equation 5 (Laidler, 1984). Biological activity within an aquatic system will also increase with temperature (Chang, 2006). Surface waters can have rather large temperature swings throughout a water year; groundwater will maintain a more constant temperature due to the insulation factor of bedrock substrates, resulting in temperatures close to annual air temperature averages, except for situations where there is a geothermal contribution to the groundwater system. These differences in temperatures can allow for qualitative observations that allow analysts to determine potential sources of groundwater. Groundwater that is found to be above average annual regional temperatures is likely to coincide with deep water geothermal mechanisms or be part of an epigenetic karst system with short allogenic recharge flow paths during summer months. Groundwater that is at or below regional temperatures can be attributed to shallow groundwater storage or again be a part of an epigenetic system with short flow paths but during winter months (Kresic et al. 2010). Groundwater

of intermediate or varying temperatures is not as conclusive, whereby the source could be meteoric or deeper seated groundwater that is sourced from mixed aquifers being flushed through channels either by storm event, sinking stream, or transverse hypogene flow.

Equation 5: Arrhenius equation

$$k = Ae^{\frac{-E_a}{RT}}$$

The acidity of a water body is also another useful property for analysis. The acidity or alkalinity of a water sample is measured by pH. The pH measurement is the hydronium ion concentration within a sample (H_3O^+). This concentration is expressed as an inverse logarithm of the hydronium concentration ($-\log [\text{H}_3\text{O}^+]$). Natural waters on average have pH ranging from 6.0-8.5. However, in some extreme situations, thermal springs have been found to have pH readings at the limits of the pH range (Hem, 1985). Meteoric water generally has a more acidic characteristic being 5.6 or lower (Charlson & Rodhe, 1982). Surface water pH is regulated by the dissolved ion content generated by water/sediment interaction and biological interaction. Groundwater pH is also modified based upon its interaction with the aquifer rock, sediments the inflowing water percolated through, biological activities within the aquifer and dissolved gasses trapped within the inflowing water. Surface water interaction with sediment/bedrock that generates substantial negatively charged ions (carbonates, phosphates, nitrates, *etc.*) will create a buffer solution allowing for acidic material, such as meteoric water, to be mixed with groundwater without decreasing pH drastically.

Dissolved oxygen is critical for biota to thrive in natural waters. High dissolved oxygen levels within a water body allow aquatic organisms to be sustained in that system and promote biological diversity. Dissolved gas concentrations (such as oxygen or carbon dioxide) have an inverse relationship with the temperature of the water body, the lower the temperature the greater the potential a gas has for dissolving into liquid water. However, the total gas concentration within a water body is dependent upon the partial pressure of said gas available within the atmosphere surrounding the water body. As water is drawn into an aquifer the partial gas pressure of oxygen effectively reduces to zero due to the liquid water filling the interstitial spaces within the substrate, driving out gases. Groundwater then will initially have dissolved oxygen concentrations similar to its source. Decreased oxygen levels in groundwater systems can be an indicator of long retention times for an aquifer. Deoxygenation through bacterial activities, as well as chemical reactions with the aquifer substrate, are both mechanisms for oxygen level reduction in groundwater (Hem, 1985).

Electrical conductivity measurements are another simple but effective measure of water quality. Conductivity measurements are an indirect measure of total dissolved solids within a water sample. Dissolved solids can be measured in this way because many inorganic solids that are soluble in water are electrolytic compounds (those that conduct electricity). Using this information, total dissolved solid (TDS) measurements can be calculated based upon the conductivity of a water sample. However, TDS measurements are not exact because there can be organic constituents within the water sample as well that are dissolved but produce no electrical charge. These non-

electrolytic compounds are considered minor constituents of whole natural environments however. Conductivity measurements for water range from 5.5×10^{-6} Siemens per meter (S/m) for pure water to 5 S/m for salt water (Lenntech, 2013). Freshwater streams range from 1 S/m to 0.2 S/m in conductance. Meteoric water conductivity measurements range from 2×10^{-4} to 4.2×10^{-3} S/m (State Water Resources Board, 2007).

2. OBJECTIVES

The goal of this project is to obtain a better understanding of the karst spring network of the eastern peninsula of Fort Hood. Understanding of the spring network was enhanced in the following ways:

- Identified water input into studied springs via allogenic, autogenic, or cross-formational sources.
- Increased understanding of the hydrochemical composition of groundwater within the eastern peninsula of FH and its relationship to karst development.

3. METHODS

3.1 Field Data Collection

Groundwater grab samples were collected monthly from springs selected from the study area. On each sampling run, one 500 mL sample was collected for each spring location. Springs were selected due to their historical consistency in discharge through the year. Springs studied were: Amphitheatre, Bear Spring, Cold Spring, Crayfish Spring, Gnarly Root Spring, Geocache, Nolan Creek Spring and Road Spring (Figure 1). Between determination of springs to be included in the study and initiation of monthly sampling Amphitheatre and Cold Spring ceased consistent discharge, thus were excluded from the sample data set. Eagle Picher certified clean PTFE polycarbonate 500 mL bottles were used to collect samples. Spring water was collected as close to the spring orifice as possible. The sample bottle was filled to the maximum to minimize headspace within the bottle to reduce the potential interaction of the samples and trapped ambient air at the time of sampling. Each sample was recorded and immediately placed on ice to maintain a maximum temperature of 4°C. Each set of samples was delivered to Stephen F. Austin State University Soil, Plant and Water Laboratory for laboratory analysis within 48 hours of sample collection. If this maximum

time was exceeded, the samples were frozen, as a preservation technique, until the samples were processed.

Field measurements were also recorded utilizing an YSI multi-probe and a FH950 electromagnetic flow meter. The YSI is equipped with probes that are capable of measuring temperature, pH, total dissolved solids (TDS), and dissolved oxygen. These measurements were also taken at each spring as close to the spring orifice as possible. A minimum of 25 measurements recorded from each spring were averaged by the sampling instrument to report the average for the event. The electromagnetic flow meter was also used at each spring to quantify the flow velocity from each spring.

3.2 Laboratory Analysis

3.2.1 Instrumentation

A Thermo Scientific iCAP 7400 inductively coupled plasma optical emission spectroscope (ICP) was utilized for the analysis of both water-soluble metals and total metal concentrations. ICP is a rapid and accurate analytical technique that allows for multiple emission bands to be analyzed instantaneously when a sample is excited within the plasma excitation source. Limits of detection (LOD) for each analyte are listed in Table 1. The variations within the limits of detection are due to the unique spectral signature of each element and how the spectral background was interfering with measurement. Ion exchange chromatography (IEC) was utilized to analyze fluoride,

sulfate, chloride, and nitrate concentrations within spring water samples. Dionex ICS-2100 IEC with a Dionex IonPac AS22 4x250 mm column and a suppressed conductivity detector was used. The IEC was run at 1200-2300 psi producing a 0.25 mL per minute flow rate. Bicarbonate analysis was carried out by a sulfuric acid titration and pH meter. Water quality measurements were compared to state and national standards for the parameters tested (Table 1). Based upon the comparison of data collected and standards regulators have set forth, any parameters that exceed standards were identified and potential causes of exceedance are discussed below, with respect to potable human use as well as for impact on ecological quality.

Table 1. Testing parameters, limits of detection and standard testing method number.

Chemical Formula	Name	EPA Method	Limit of Detection	Analytical Method
Al	Aluminum	EPA 200.7	12 ppb	ICP-OES
As	Arsenic	EPA 200.7	48.3 ppb	ICP-OES
B	Boron	EPA 200.7	4.8 ppb	ICP-OES
Ca	Calcium	EPA 200.7	58.5 ppb	ICP-OES
Cu	Copper	EPA 200.7	6.6 ppb	ICP-OES
Fe	Iron	EPA 200.7	4.2 ppb	ICP-OES
K	Potassium	EPA 200.7	82.2 ppb	ICP-OES
Mg	Magnesium	EPA 200.7	8.4 ppb	ICP-OES
Mn	Manganese	EPA 200.7	0.90 ppb	ICP-OES
Na	Sodium	EPA 200.7	17.10 ppb	ICP-OES
P	Phosphorus	EPA 200.7	35.10 ppb	ICP-OES
Pb	Lead	EPA 200.7	43.50 ppb	ICP-OES
S	Sulfur	EPA 200.7	33.90 ppb	ICP-OES
Zn	Zinc	EPA 200.7	0.60 ppb	ICP-OES
Cl ⁻	Chloride	EPA 300.0	4.0 ppb	IEC
F ⁻	Fluoride	EPA 300.0	2.0 ppb	IEC
NO ₃ ⁻	Nitrate	EPA 300.0	3.7 ppb	IEC
SO ₄ ²⁻	Sulfate	EPA 300.0	18 ppb	IEC
PO ₄ ³⁻	Phosphate	EPA 300.0	14 ppb	IEC
HCO ₃ ⁻	Bicarbonate	EPA SM 2320	2 mg/L	Titration

3.2.2 Elemental Analysis

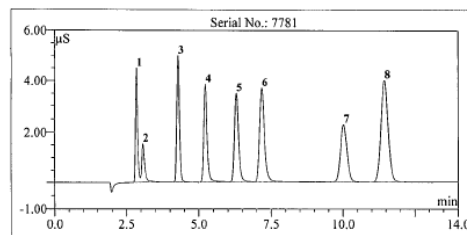
Upon sample arrival at the laboratory, 100 mL aliquots of each sample were filtered through a 0.45 μ m filter for water soluble elemental analysis. Another 100-mL aliquot was analyzed for both water soluble and suspended solid metals within the samples. Total metal analysis, prior to ICP injection, requires 1000 μ L of concentrated nitric acid (1:1) and an additional 500 μ L of hydrochloric acid (1:1) to be added to each aliquot. These samples were then placed on a heating block and raised to 85°C and left to flux for a minimum of 30 minutes to allow the volume to reduce to approximately 20 mL. After the volume was reduced, the aliquot was brought back to 100 mL and mixed vigorously following the adopted USEPA method 200.7 (Martin et al. 1994). After sample preparation for both the total recoverable and aqueous analytes ICP was conducted immediately.

A high and low standard, as well as a laboratory blank, were run for each set of samples processed. The high and low standard were certified reference materials used to verify instrumentation measurements and calibration. These quality controls were implemented to validate the method. Results obtained from ICP analyses were generated based upon means obtained from three sample injections. The mean values obtained from each sample were then be compared to limit of detection (LOD) values for each element separately. The method outlined above is EPA 200.7 method for determination of metals and trace elements in water by ICP (Martin et al. 1994). Concentrations of elements tested were compared to state and national regulations.

Analyses of major and minor ions concentration results were conducted utilizing various statistical methods outlined below

3.2.3 Anion Analysis

An aliquot of 10 μL of each sample was injected into the Thermo Fisher Dionex IEC-2100 for analysis. For each set of samples, the Dionex 7 anion calibration standard was utilized for calibration of each sample run. The elution profile created was used as a calibration chromatogram, to quantify the results. The concentrations and retention times for the standard chromatogram are shown below in Figure 13. This method of analysis is EPA 200.7 determination of inorganic anions by ion chromatography (Pfaff, 1993). Bicarbonate / carbonate analysis was conducted via sulfuric acid titration of 50 mL aliquots of spring water. The titration was conducted to an inflection point of pH 4.5 for bicarbonate. Based upon the volume of sulfuric acid utilized the bicarbonate concentrations of each sample were calculated.



No.	Peak Name	Ret.Time (min)	Asymmetry (ATA)	Resolution (EP)	Efficiency (EP)	Concentration (mg/L)
1	Fluoride	2.84	1.9	1.60	8216	5.0
2	Acetate	3.07	n.a.	7.51	5930	20.0
3	Chloride	4.28	1.4	5.09	10936	10.0
4	Nitrite	5.22	1.4	4.67	10072	15.0
5	Bromide	6.30	1.4	3.22	9960	25.0
6	Nitrate	7.18	1.4	7.95	9326	25.0
7	Phosphite	10.02	1.2	3.26	9123	40.0
8	Sulfate	11.45	1.1	n.a.	10119	30.0

Figure 13: Elution profile for 8 compound standards for Dionex ICS-2100 IEC

3.3 Statistical Analysis

After laboratory and field measurements were compiled, standard ion indices, t-tests, repeated measures ANOVA and principal component analysis (PCA) were conducted to identify variations between sampled springs. T-tests were conducted between soluble and total element results for each analyte to determine if there was any statistical difference among the analytical results. Repeated measures ANOVA assisted in identifying which elements had similar contributions to the variance of an individual sample location as well as to the variance between springs on a sampling date. Principal component analysis allowed for the visualization of multiple variables and their effects on variability within the data set. Statistical Analysis Software (SAS) version 9.2 was utilized for all statistical analyses. The General Linear Model (GLM) procedure was run to produce ANOVA results with a 95% significance level. The Principal Component procedure in SAS was used to group analytes based upon their significance to the variation of spring characteristics.

3.3.1 Standard Ion Indexes

The standard ion index (SII) statistical approach was employed on the ion concentrations for all the springs in two ways (Şen, 2011). The first method identified ionic composition changes comparatively between all samples individually. Each ion's individual contribution to the sample was studied. The second method compared ion

concentration for springs individually and indicates, graphically, how ion concentrations evolve over time.

The SII is a method of comparing the effect of multiple analytes on the overall ionic character of a water sample or successive water samples with dimensionless standard values. The SII is created by converting all analyte values into molar concentrations, determining the molar average and standard deviation for each water sample followed by dividing the difference between the analyte and the molar average for the sample by the standard deviation of the sample (Equation 6). Standardizing the concentrations obtained from analytical analyses by this method creates dimensionless values with a zero mean and a standard deviation of 1 for each sample. The modification of the analytical results allows for equitable comparisons of the sampled ions. Chemical analysis results that were below the analytical limit of detection were excluded from SII analysis. The SII magnitude indicates the contribution a specific analyte gives to the overall ionic character of the sample. The sign of the SII value indicates analyte contribution being more (positive) or less (negative) than the average ion contribution to the overall ionic character of the sample.

Equation 6: Standard ion index calculation modified from (Şen, 2011)

$$x_i = \frac{(x_i - \bar{X})}{S_X}$$

analytes in sample ($X_1, X_2, X_3, \dots, X_n$)

3.3.1.1 Individual Standard Ion Indices (ISII)

SII values are then plotted as the ordinate ratio value over each nominal analyte value along the abscissa for each spring location. The graphs generated indicate the ISII for each analyte at each spring. Comparing each monthly sample at a specific spring assists in determining compositional variations in spring water over time. ISII graphs allow us to apply the following assumptions about the data:

- Positive SII values indicate the analyte is in greater abundance in the sample than the average ion concentration.
- Negative SII values indicate an analyte has less than average ion contribution to the sample.
- Ions that are nearer to the zero mantissa are less ionically significant to the overall character of the sample.
- Ions that fluctuate between positive and negative values between sampling events are an indication of instability in the overall ion character of the spring, which could be caused by changes in the spring waters source.
- Ions that exhibit spreading in the vertical direction indicate variation in the ion concentration through the sampling interval.

3.3.1.2 *Successive Standard Ion Indices (SSII)*

SSII are created by comparing one month's sample to the following month's sample for each spring, plotting the initial sample on the ordinate and the following sample on the abscissa. The plots generated show analytes differentiated into clusters that in an ideal situation should center on a line through the origin with a 45° slope. Longitudinal spreading along the ideal line for analytes indicate consistent incremental change to the SII; lateral dispersion of clusters along the ideal line indicate fluctuations in the SII between the successive samples. SII values in the lower left and upper right quadrants of the plot indicate the analytes contribute less or greater, respectively, to the samples composition consistently between sequential sampling events. Sample points that appear in the upper left (quadrant 4) or lower right quadrants (quadrant 2) of plots indicate that the analyte fluctuated, high to low or low to high SII values respectively, between sequential sampling events.

3.3.2 **t-Test**

T-testing was performed to compare concentration averages among each spring between soluble and total element analyses as well as among sample dates. However, before t-tests were conducted, an F-test was used to determine if the data sets variances were normally distributed. The normalcy was then used to determine if the two sample t-test was to be run assuming equal or unequal variance. All analyses were conducted at the 95% confidence interval.

3.3.3 Repeated Measures Analysis of Variance (ANOVA)

Repeated measures ANOVA was conducted for each spring sampled. Each spring was considered a repeated measures subject, classifying each successive sample date as a treatment in the statistical design. The repeated measures analysis of variance is used to determine differences in chemical composition among sample dates, as well as among each sampled spring. Results from spring water analysis that were below the limit of detection for all sampling events were excluded from ANOVA testing. Those results that were intermittently below the LOD were still considered in ANOVA testing, reporting concentrations below the LOD as half the method detection limit. Student-Newman-Keuls (SNK) comparison tests were utilized to identify subgroups of springs.

3.3.4 Principal Component Analysis (PCA)

A principle component analysis (PCA) was conducted on the sample data to assist in reducing the number of variables and to determine if there are groups of variables that are correlated and similarly effect the variance found in the dataset. PCA reduces the number of variables within a dataset by generating several synthetic variables equal to the number of subjects in the analysis, those being the sample events in our study. Each of these synthetic variables, principal components (PC), are composed of a linear summation of each analyte multiplied by an optimized coefficient that indicates the weight, or impact, that the analyte has on the principal component variation (Equation 7). The first PC is a vector that has been optimized to describe the

largest covariance of dataset. Each successive PC describes the next largest covariance of the data set while being orthogonal, or uncorrelated, to other PC. The PCA uses an eigenequation to determine the optimized coefficient (eigenvalue) and eigenvectors for each analyte which are used to calculate analyte loadings for each principal component. Each variable collected at a sampling event has a representative loading on each PC calculated by Equation 8. The loading magnitude explains the variables influence on a given PC and the sign of the loading indicates the increasing or decreasing value of the variables that are weighted heavily on the PC. Review of the eigenvalues and the variable loadings on each of factor will determine which of the factors are significant for analysis.

Equation 7: General formula for calculating principal components modified from (SAS, 2014)

$$c_n = \sum_1^p b_{np}(x_p)$$

c_n = subject score on PC_n

b_{np} = regression coefficient (weight) for variable p which was used in creating PC_n

x_p = subject's value for variable p

Equation 8: Principal component loading equation

$$\text{Variable Loading} = \text{Eigenvector} \times \sqrt{\text{Eigenvalue}}$$

There are multiple methods of determining which factors are meaningful: the eigenvalue one, scree plot analysis, and percent contribution tests. The eigenvalue one test is the simplest to implement; those PC with eigenvalues of one or greater should be

retained. However, this method is only recommended if communalities (the sum of squared factor loadings for a specific variable) are greater than 0.70 in datasets having fewer than 30 variables (Stevens, 1986) which this data set matches. A scree test is a review of the scree plot whereby the analyst identifies where the eigenvalues begin to level off on the plot. Any factors with higher eigenvalues than the break point on the plot are to be retained (Cattell, 1966). A percent contribution test would recommend retaining any eigenvalues that are greater than either 5% or 10% of the total contribution to the dataset variance. In best practice it is recommended to use a combination of all methods to determine the number of components to retain. If there are eigenvalues that are on the cusp of a cutoff, it is worthwhile to also evaluate those values to determine if their inclusion enhances the interpretation of results. The retained components should also total a minimum of 70% of the total variance for the dataset to ensure valid results.

Determining which eigenvectors significantly load on a factor is determined by identifying those loadings that have the highest absolute values with respect to the loadings of other variables on the factor. Determining the exact eigenvector values to include in a factor is up to the analyst. Depending upon which variables are loading at what value, as well as which variables would logically be correlated, are all important for determining which variables should be loaded onto a factor.

All variables that were above the analytical limit of detection and were determined to be statistically significant in ANOVA testing were included in the PCA. To ensure the reliability of results, it is recommended that the number of samples, or subjects, be a minimum of five times the number of variables contained in the PCA

(SAS, 2014). Being that this dataset has 22 variables and 70 samples, the PCA was conducted on the soluble (13 variables / 70 samples) and total elements (13 variables / 70 samples) separately to ensure the ratio of variables to samples is sufficient.

4. RESULTS

4.1 Water Quality Analysis

One of the objectives of this project is to classify the perennial spring waters that are produced in and around the eastern peninsula of Ft. Hood. The Owl Mountain region on the eastern peninsula of Fort Hood is predominantly a protected endangered species wildlife area with limited human activity. Since these springs will have little use as a human drinking water source utilizing Texas Commission on Environmental Quality (TCEQ) surface water standards (TCEQ 2012) is more appropriate than the Environmental Protection Agency (EPA) drinking water standard. TCEQ assigns surface water standards for water bodies based upon location and usage of the waterbody. The studied springs are in the Belton Lake's watershed, which is segment number 1220 within the Brazos River basin. Segment 1220 is classified as a level 1 primary contact recreation area, with a high aquatic life use, and is also used as a public water supply. The designation of level 1 primary contact recreation is given to any perennial water body that has the potential for recreational uses where people have direct contact with water but are not likely to ingest high quantities of water while doing so, such as boating or fishing. The classification of high aquatic life use indicates that there is high diversity of regionally expected species while also having sensitive aquatic indicator species

present (TCEQ 2012). The assumed human use and native fauna's reliance on these spring waters are in line with the level 1 primary contact classification and were used as the maximum contaminate level guideline for this project.

General water quality measurements were recorded at each of the subject springs including pH, TDS, spring discharge, and temperature (Table 2). The pH over the course of the project was relatively constant for each spring with occasional acidic outliers for each spring, but no discernible pattern arose from those variations. Temperature was also consistent ($\approx 19 \pm 1$ °C) at near average annual air temperatures for the region, being approximately 18.75 °C (NOAA 2014), for all sampled springs. Discharge varied across time at each spring with each exhibiting spikes in discharge volume that could be due to past rain events; however, there was no consistent discharge increase across multiple springs that could be definitively attributed to a storm event (Figure 14). TDS measurements for all springs but Crayfish and Geocache ranged from 451.30 to 471.46 ppm. Crayfish TDS was slightly higher at 493.75 ppm and Geocache had an average of 594.00 ppm. The increase in TDS measures agrees with chemical analysis results. Five or more analyzed elements at Crayfish and Geocache had higher than average concentrations. The chemical analyses are further presented in the following sections.

Table 2: Physicochemical attributes of sampled springs

Spring Name	n	pH		TDS		Discharge		Temp		Dissolved O ₂		LSI	Saturation	Ca/Mg Ratio
		σ	ppm	σ	cm ³ /sec	σ	C°	σ	%					
Bear	13	7.03	0.49	461.92	104.96	2514.68	1227.37	19.24	0.76	77.23	5.46	-0.34	Under	11.35
Crayfish	12	7.05	0.62	493.75	111.62	522.06	581.81	19.42	0.63	81.51	9.98	-0.26	Under	4.20
Geocache	9	6.79	0.61	594.00	135.16	171.96	101.36	18.97	0.60	75.14	15.19	-0.63	Under	2.64
Gnarly Root	13	6.95	0.62	461.08	128.46	5463.21	5038.85	19.04	1.39	75.98	6.11	-0.41	Under	6.23
Nolan Creek	13	6.96	0.53	471.46	114.54	601.35	295.32	19.46	1.05	74.77	8.57	-0.42	Under	3.10
East Range Road	10	6.56	0.42	451.3	91.62	27.71	17.47	19.59	1.64	69.03	16.75	-0.81	Under	24.94

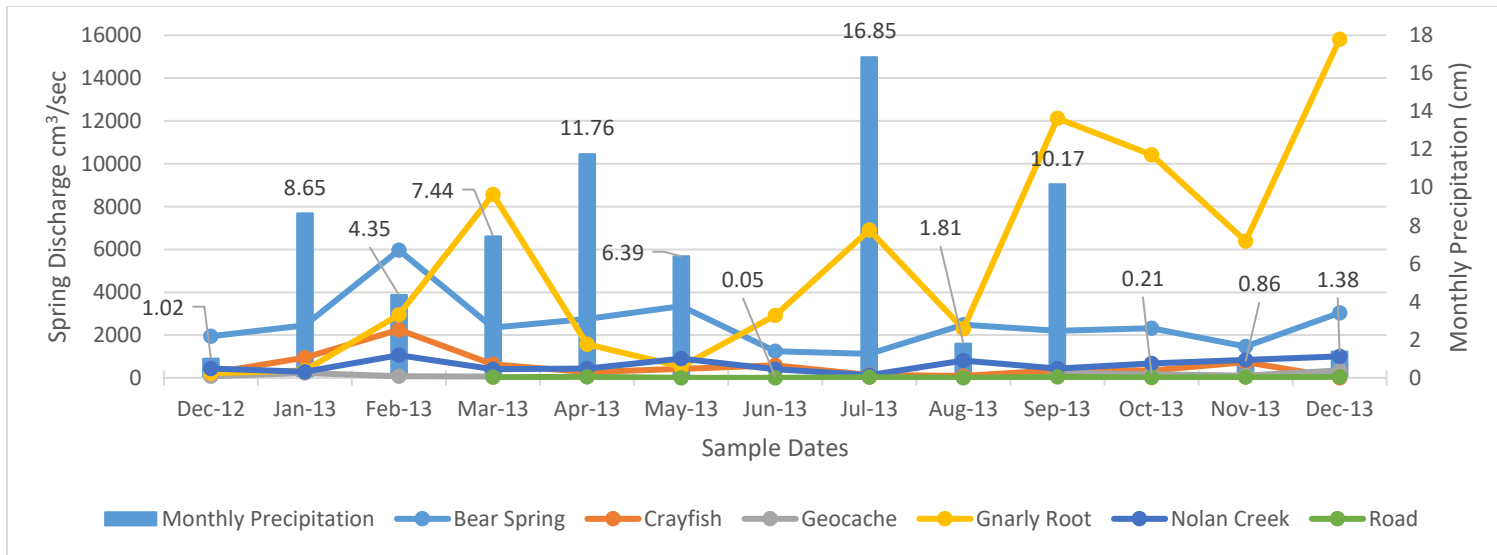


Figure 14: Spring discharge and monthly precipitation for eastern peninsula of Ft. Hood

$\text{Ca}^{2+}/\text{Mg}^{2+}$ ratios and Langelier saturation indexes (LSI) were calculated for the sampled springs (Table 2). $\text{Ca}^{2+}/\text{Mg}^{2+}$ ratios were used to determine the dolomitic character of water. The water samples with $\text{Ca}^{2+}/\text{Mg}^{2+}$ ratio below 6:1 are dolomitic (Drever, 1997). The $\text{Ca}^{2+}/\text{Mg}^{2+}$ ratios range from 25:1 to 2.6:1 for East Range Road and Geocache respectively. Nolan Creek, Geocache, and Crayfish are classified as being dolomitic. The remaining springs, Bear, Gnarly Root, and East Range Road had much higher $\text{Ca}^{2+}/\text{Mg}^{2+}$ ratios and were considered to have a more limestone characteristic. The trend of the springs to the north (Bear, Gnarly Root, and East Range Road) being less Mg saturated than those to the south (Nolan Creek, Geocache, and Crayfish) is visually represented in Figure 15. The LSI is a measure of the dissolution potential of calcium carbonate by a water sample. The average LSI value for all springs was under saturated (negative LSI values) with respect to calcium carbonate dissolution.

The water samples reported in Table 2, Table 3, Table 4, and Table 5 are of the averages for each analyte across the entire project at each spring location. The detailed report of results from each sampling event are available in the appendix (Field and Laboratory Results). For each analyte, the average spring concentration was below the level 1 primary contact recreational maximum contaminant level (MCL) standard except for TDS (Table 6). The TDS concentration most likely exceeded the TCEQ MCL for level 1 primary contact recreational use due to the standard being set for surface water bodies and not turbid springs. The chemical composition of groundwater will commonly have greater concentrations of dissolved compounds due to increased water pressure and prolonged contact with karst strata allowing for spring water to have higher

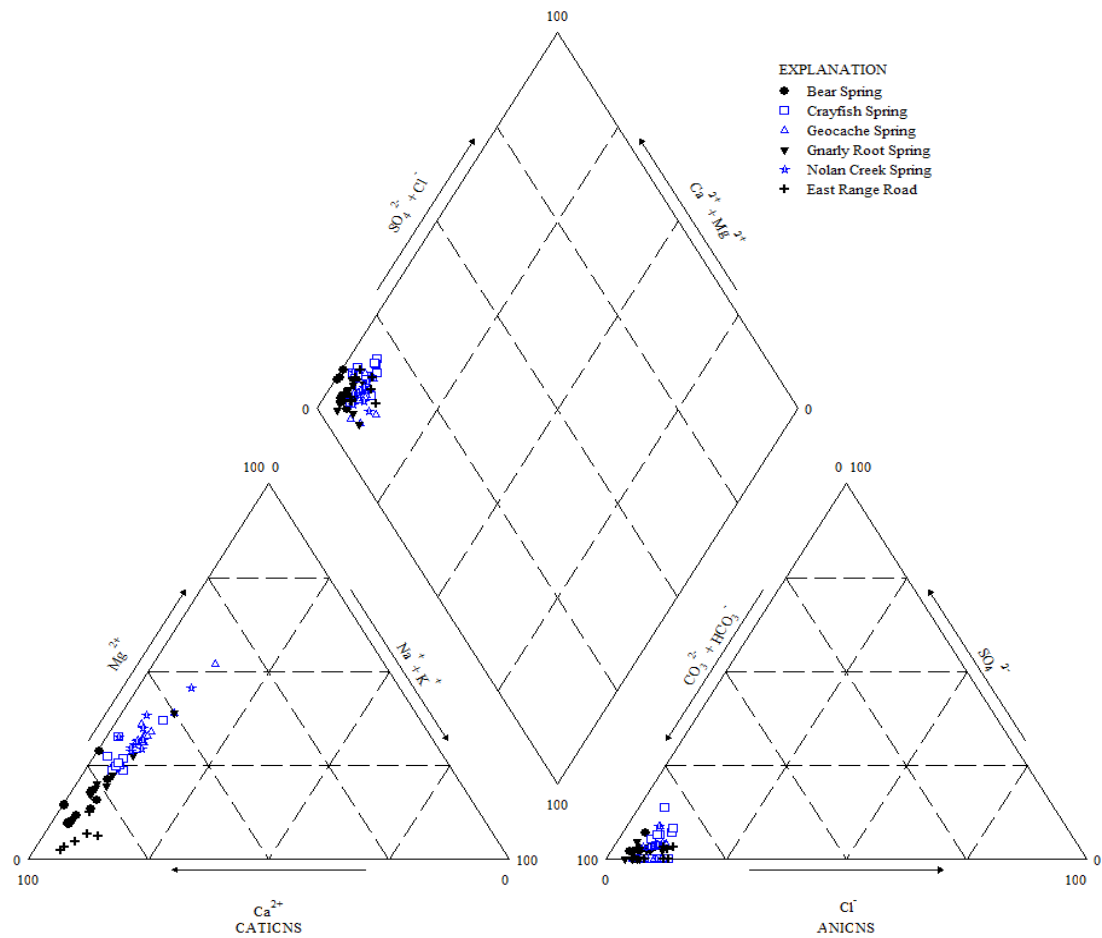


Figure 15: Piper diagram of studied springs from December 2012 to December 2013

concentrations of solutes in a groundwater system. In contrast for Belton Lake, pressure on water is decreased to atmospheric pressures which over time allows for solutes to precipitate out of solution, lowering TDS, in this open pressure system. Additionally, meteoric water inputs to Belton Lake also contribute to decreasing TDS.

The results for spring concentrations for regulated analytes for human or aquatic concern (Table 7 and Table 8) seem to indicate the springs are within acceptable ranges with the exception of Pb. The results for Pb were found below the LOD while still being above the MCL set by TCEQ. Due to this fact determinations of safety, with respect to these two elements, would need additional analysis using instrumentation capable of detecting below the MCL set forth by the TCEQ.

Table 3: Soluble cation concentrations of sampled springs

Spring Name	n	Ca		Mg		Na		K		S	
		mg/L	σ	mg/L	σ	mg/L	σ	mg/L	σ	mg/L	σ
Bear	13	109.68	24.46	10.35	3.23	5.23	3.28	0.64	0.19	3.74	0.80
Crayfish	12	110.59	16.69	26.62	2.92	10.19	4.57	2.61	2.96	8.10	1.47
Geocache	9	87.39	26.04	33.09	5.84	13.37	4.46	2.93	3.14	5.47	1.45
Gnarly Root	13	98.27	21.96	16.08	1.92	6.63	1.57	1.91	2.96	3.08	0.55
Nolan Creek	13	91.42	17.26	29.58	3.06	10.54	3.95	2.43	2.35	5.14	0.68
East Range Road	10	102.73	27.23	5.62	3.19	6.78	2.84	2.11	3.46	3.77	0.55

Table 4: Total cation concentrations of sampled springs

Spring Name	n	Ca		Mg		Na		K		S	
		mg/L	σ	mg/L	σ	mg/L	σ	mg/L	σ	mg/L	σ
Bear	13	124.53	18.42	9.34	4.58	6.78	1.39	0.47	0.07	3.40	0.51
Crayfish	12	127.65	34.39	26.17	6.05	12.25	2.77	0.89	0.32	7.35	1.66
Geocache	9	105.24	23.75	36.65	7.63	16.50	3.72	1.04	0.22	5.56	0.92
Gnarly Root	13	119.19	29.43	19.88	3.88	8.17	1.57	0.56	0.63	3.11	0.49
Nolan Creek	13	101.33	15.85	31.09	4.97	12.49	1.99	1.42	0.41	4.49	0.78
East Range Road	10	146.28	62.16	8.59	3.09	9.01	3.51	0.36	0.13	4.59	3.19

Table 5: Anion concentrations of sampled springs

Spring Name	n	Cl ⁻		F ⁻		HCO ₃ ⁻		NO ₃ ⁻		SO ₄ ²⁻		PO ₄ ³⁻	
		mg/L	σ	mg/L	σ	mg/L	σ	mg/L	σ	mg/L	σ	mg/L	σ
Bear	13	10.12	1.99	0.375	0.27	254.13	43.10	4.37	1.25	4.49	3.18	1.61	2.90
Crayfish	12	15.53	2.45	0.624	0.21	259.43	40.02	7.90	2.40	12.05	9.14	3.97	7.19
Geocache	9	16.89	5.52	0.558	0.29	285.10	30.10	3.26	1.91	6.42	9.72	3.46	6.11
Gnarly Root	13	9.96	2.69	0.609	0.29	264.95	38.22	5.65	1.13	3.41	2.66	1.67	3.44
Nolan Creek	13	15.09	2.63	0.506	0.21	267.51	30.40	3.83	0.90	7.16	5.66	2.58	5.89
East Range Road	10	13.73	4.40	0.288	0.15	242.83	43.66	4.37	2.88	4.24	2.73	1.62	4.54

Table 6: Results compared to level 1 primary contact recreational surface water maximum contaminate level standards for Belton Lake (TCEQ 2012)

Spring Name	Cl ⁻ (mg/L)		SO ₄ ²⁻ (mg/L)		TDS (PPM)		Dissolved Oxygen (mg/L)		pH (SU)		Temperature (°C)	
	Sample	MCL	Sample	MCL	Sample	MCL	Sample	Standard	Sample	Standard	Sample	Standard
Bear Average	10.12	100.00	4.49	75.00	461.92	500.00	9.21	5.00	7.03	6.5-9.0	19.24	33.89
Crayfish Average	15.53	100.00	12.05	75.00	493.75	500.00	9.17	5.00	6.90	6.5-9.0	19.45	33.89
Geocache Average	16.89	100.00	6.42	75.00	594.00	500.00	9.17	5.00	6.67	6.5-9.0	19.44	33.89
Gnarly Root Average	9.96	100.00	3.41	75.00	461.08	500.00	9.23	5.00	7.22	6.5-9.0	19.14	33.89
Nolan Creek Average	15.09	100.00	7.16	75.00	471.46	500.00	9.20	5.00	6.83	6.5-9.0	19.29	33.89
East Range Road Average	13.73	100.00	4.24	75.00	451.30	500.00	8.99	5.00	7.01	6.5-9.0	20.47	33.89

Table 7: Results compared to aquatic life and human health maximum contaminate level protection standards (TCEQ 2012)

Spring Name	Al (µg/L)		As (µg/L)		Pb (µg/L) ¹		Zn (µg/L) ²	
	Sample	MCL	Sample	MCL	Sample	MCL	Sample	MCL
Bear Average	7.12	991	< 48.30	340	< 43.50	8.84	3.22	15.22
Crayfish Average	58.68	991	< 48.30	340	< 43.50	8.75	5.04	15.66
Geocache Average	24.19	991	< 48.30	340	< 43.50	8.8	2.88	15.46
Gnarly Average	13.18	991	< 48.30	340	< 43.50	8.85	6.47	15.18
Nolan Average	14.5	991	< 48.30	340	< 43.50	8.8	6.46	15.44
Road Average	7.55	991	< 48.30	340	< 43.50	8.88	6.95	14.94

1: $Pb_{Aquatic\ Standard} = (1.46203 - \ln(hardness^*)) \times we(1.273 \ln(hardness^*) - 1.460)$

2: $Zn_{Aquatic\ Standard} = 0.978we(0.8473 \ln(hardness^*) + 0.884)$

*: $hardness_{total\ as\ CaCO_3} = 2.5[Ca^{2+}] + 4.1[Mg^{2+}]$

w = site specific variable for waterway, none set so a value of (1) was used

Table 8: Results compared to human health maximum contaminate level protection standards (TCEQ 2012)

Spring Name	As (µg/L)		F (µg/L)		Pb (µg/L)		NO ₃ ⁻ µg/L	
	Sample	MCL	Sample	MCL	Sample	MCL	Sample	MCL
Bear Average	< 48.30	10	375.48	4000	< 43.50	1.15	4365.33	10000
Crayfish Average	< 48.30	10	623.96	4000	< 43.50	1.15	7904.97	10000
Geocache Average	< 48.30	10	558.1	4000	< 43.50	1.15	3257.5	10000
Gnarly Average	< 48.30	10	609.22	4000	< 43.50	1.15	5648.65	10000
Nolan Average	< 48.30	10	505.82	4000	< 43.50	1.15	3832.16	10000
Road Average	< 48.30	10	288.28	4000	< 43.50	1.15	4365.22	10000

4.2 Standard Ion Indexes

4.2.1 Individual Standard Ion Indexes

Review of each spring's overall individual SII index graph shows similar ionic composition general trends between springs (Figure 16 through Figure 21). The ions that contribute the most to the ionic composition of subject springs in descending order of influence are: HCO_3^- , Ca^{2+} , Mg^{2+} , Na^+ , and Cl^- . HCO_3^- had the largest influence on the ionic character of the samples, with the SII value having the general trend of decreasing influence over the sampling period. Geocache, Gnarly Root, and Nolan Creek Springs are the only three springs that at some point during the sampling interval had measured Ca^{2+} contribution less than the average ionic contribution, thus resulting in a negative Ca^{2+} SII value in the sample. The observed Ca^{2+} concentrations exhibit a large vertical variation with respect to the other analytes. Ca^{2+} SII values decrease to negative or near negative values in March 2013 for Bear, Geocache, Gnarly Root, and Nolan Creek Springs, and again in November 2013. The large vertical variation in SII values is an indicator of a fluctuating water source (Şen, 2011). In both situations, there was a precipitation increase months prior which may have led to the decrease in Ca^{2+} concentration. However, there was no definitive increase in spring discharge directly coupled to these spring chemical changes, with only Gnarly Root spring having an increase in discharge over its average discharge, indicating a more complex relationship

between the sampled springs discharge and precipitation (Figure 14). Mg^{2+} SII values for Bear, Road, and Gnarly Root Springs were generally negative, while Geocache, Nolan Creek, and Crayfish springs were positive, with nearly the same contribution to the overall SII value as calcium for many sample events. The high Mg^{2+} contribution for those springs in the southern portion of the study area are consistent with the water quality analysis of Ca^{2+}/Mg^{2+} ratios. Na^+ SII values for Geocache began with above average contribution for roughly the first half of the sampling interval and moved to less than average for the remaining months of sampling. Road Spring also indicated a higher than normal (positive) Na^+ SII value until March, while for the remainder of the sampling interval Na^+ SII values were negative. This change in SII value for Na^+ is a possible indicator of change in water source from a more deeply seated hypogenetic regime to a more epigenetic regime, where residence time within the aquifer does not allow for higher concentrations of Na^+ to accumulate. The remaining elements analyzed in the individual SII index did not fluctuate significantly during the sampling period.

4.2.2 Successive Standard Ion Index

The general chemical concentration trends for each sampled spring were relatively consistent with most analytes having similar ionic contribution from month to month, which was indicated in the successive standard ion index (SSII) values being in the lower left and upper right quadrants of the graphs below (Figure 22 to Figure 33). Many of the analytes trend along the ideal line of the plots, with some lateral dispersion and vertical dispersion. Variation patterns such as these indicate the chemical composition

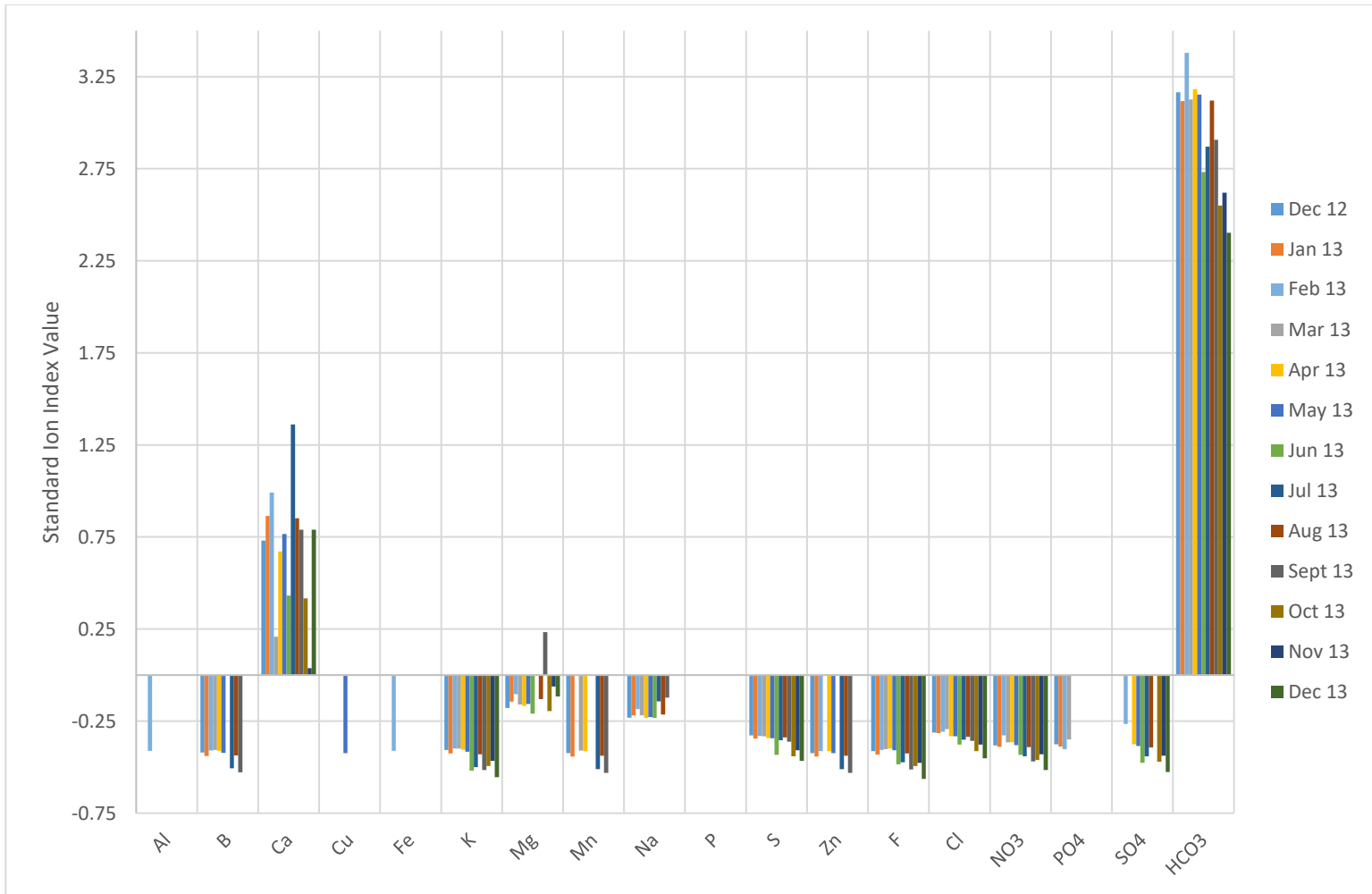


Figure 16: Standard ion index of major and trace ions for Bear Spring from December 2012 to December 2013

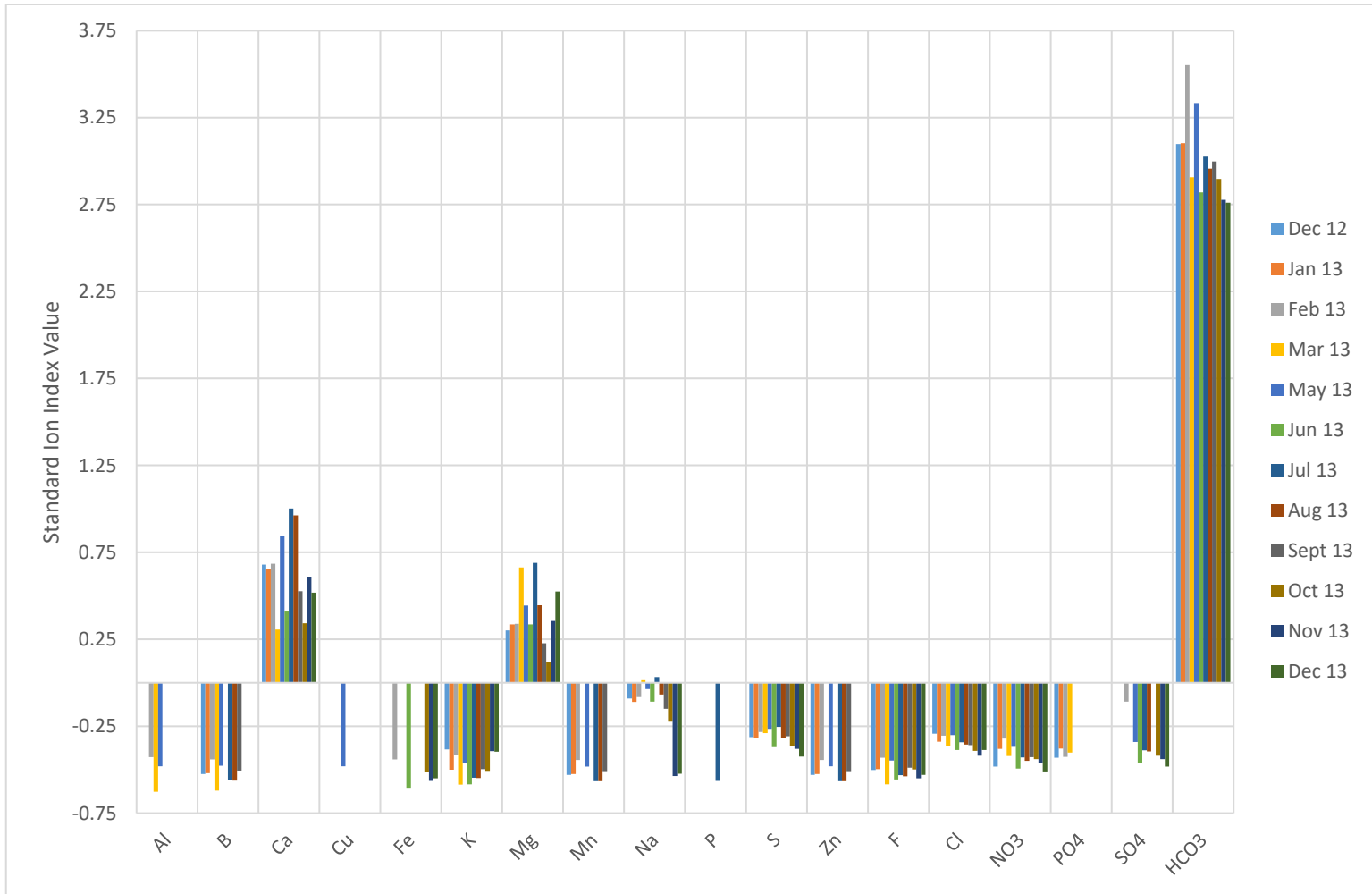


Figure 17: Standard ion index of major and trace ions for Crayfish Spring from December 2012 to December 2013

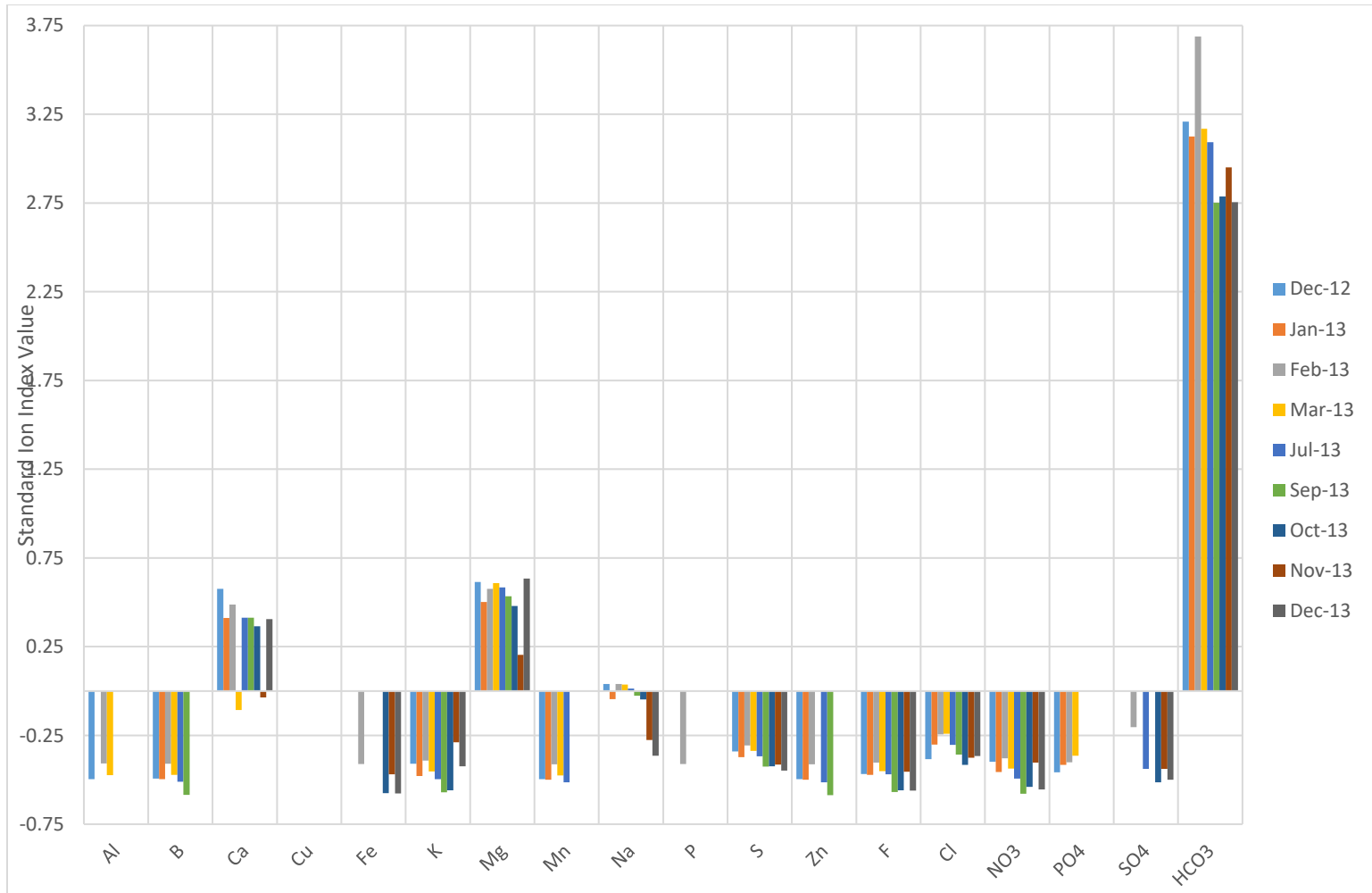


Figure 18: Standard ion index of major and trace ions for Geocache Spring from December 2012 to December 2013

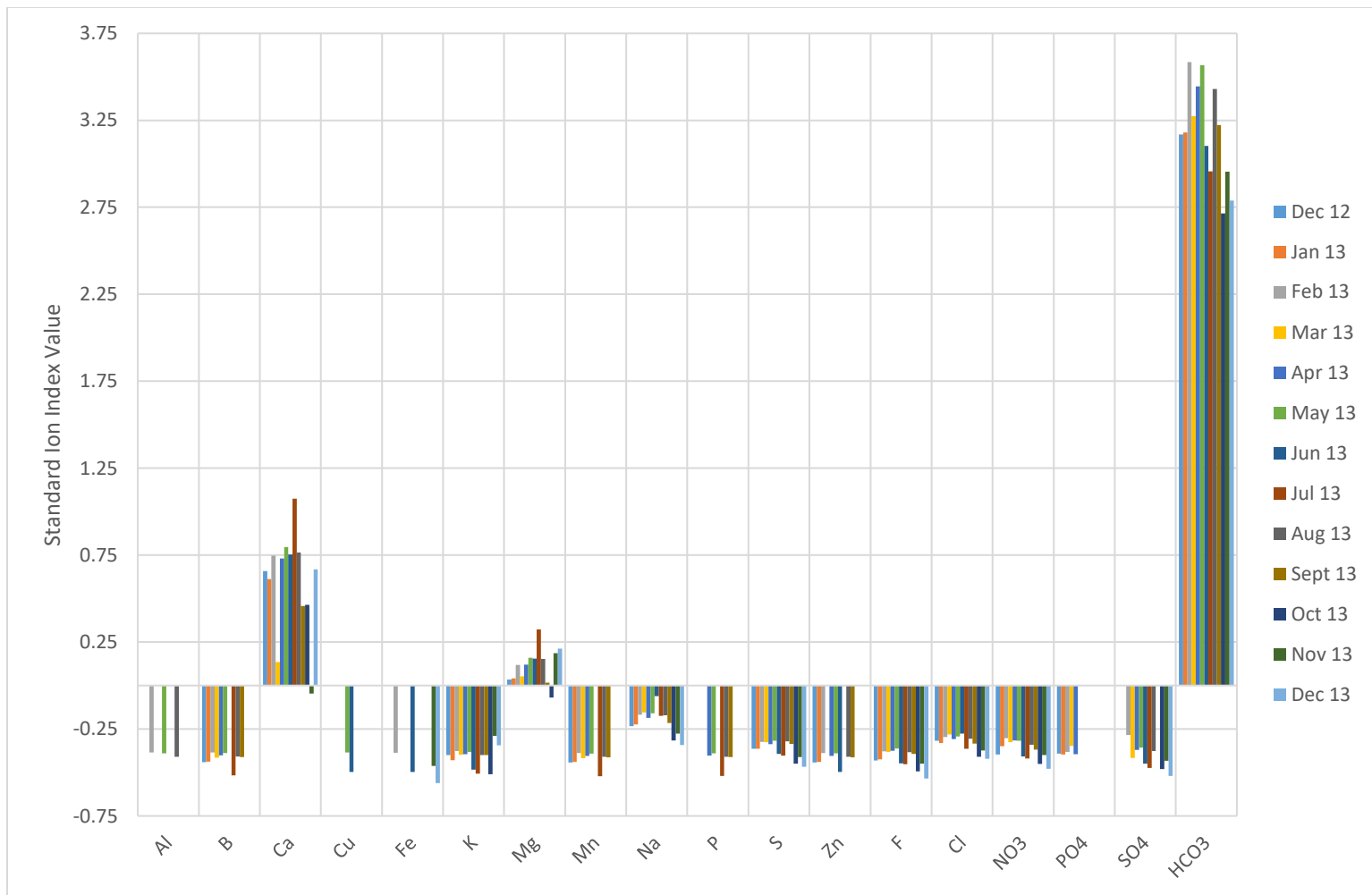


Figure 19: Standard ion index of major and trace ions for Gnarly Root Spring from December 2012 to December 2013

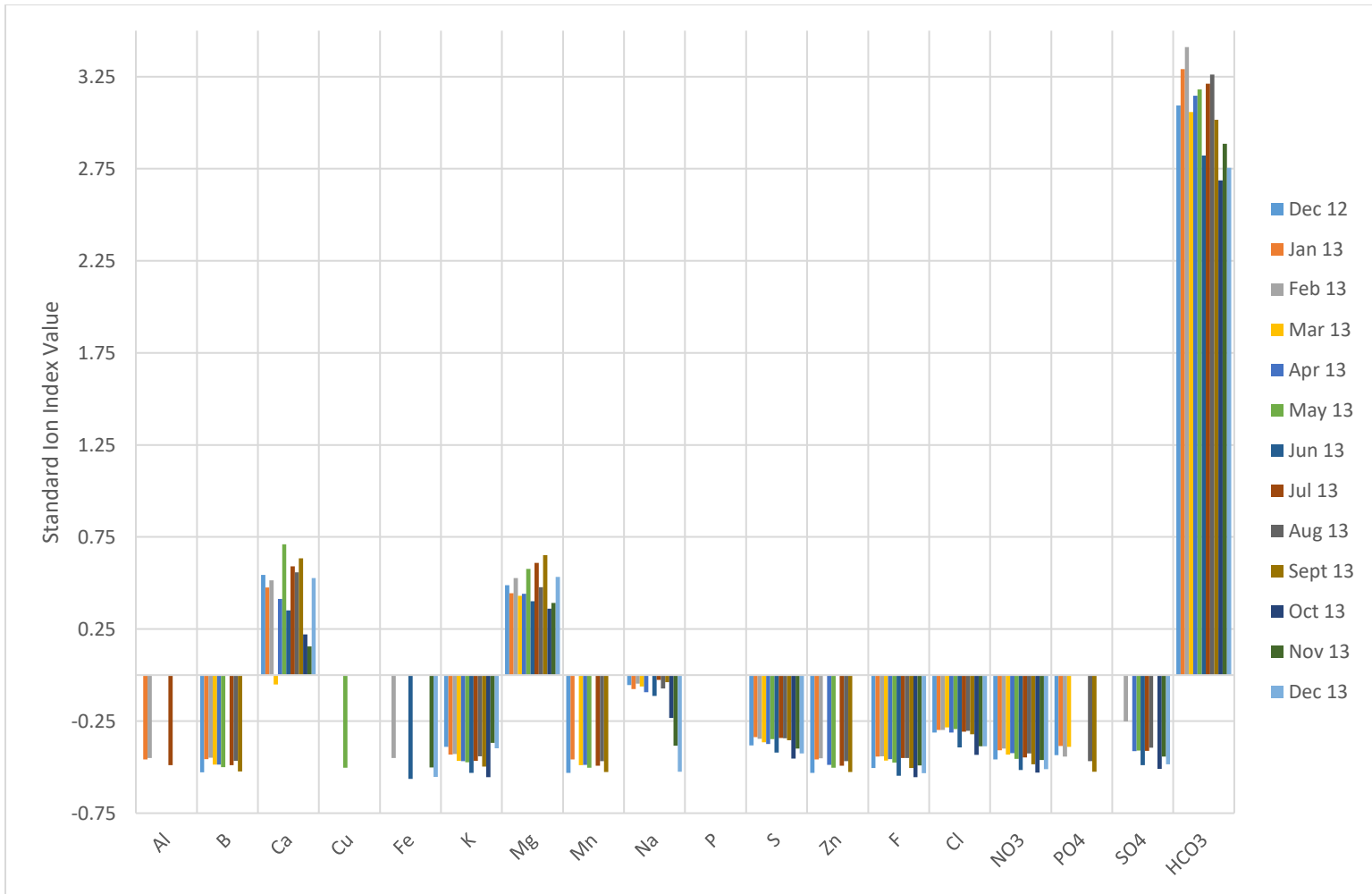


Figure 20: Standard ion index of major and trace ions for Nolan Creek Spring from December 2012 to December 2013

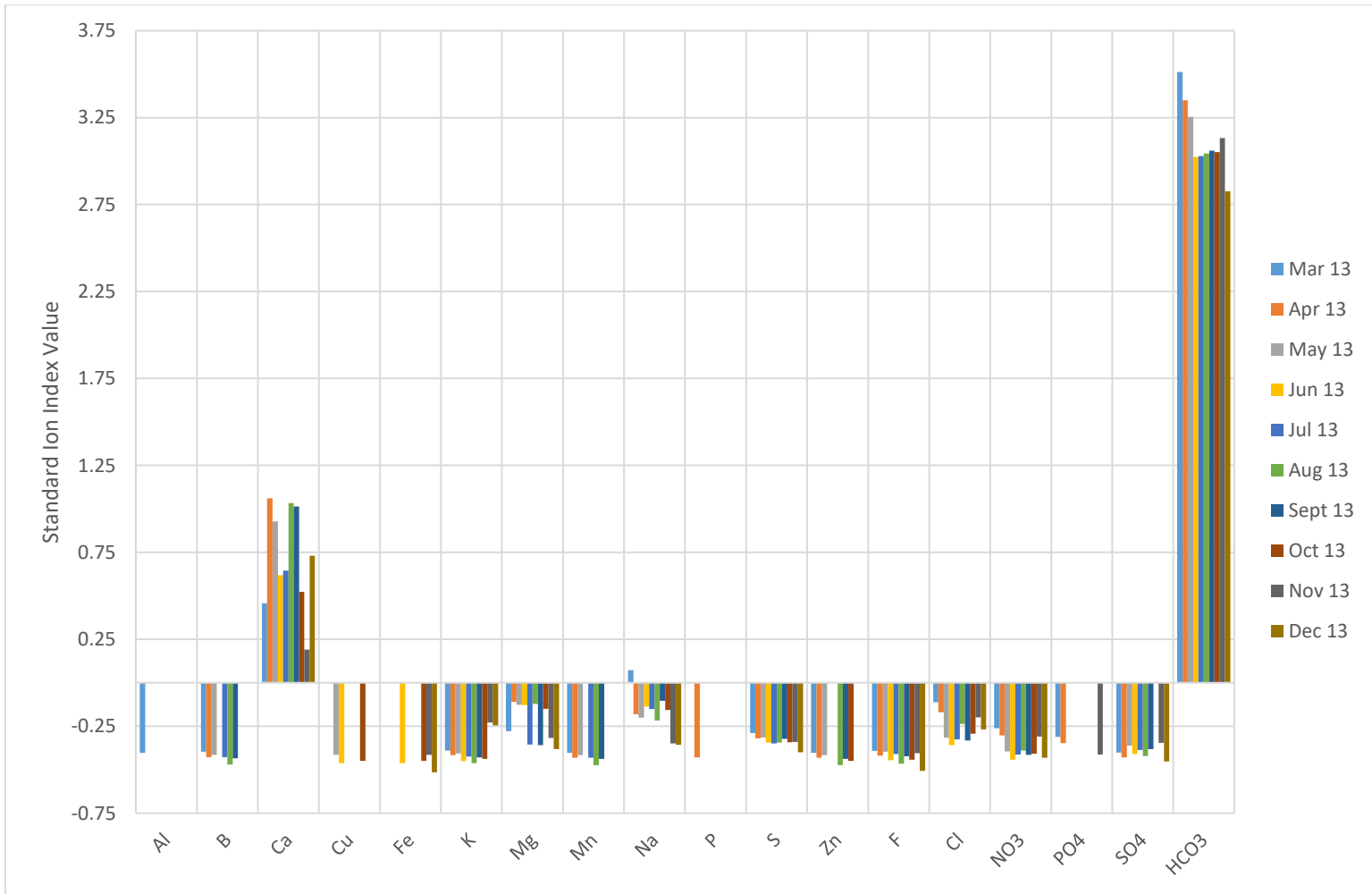


Figure 21: Standard ion index of major and trace ions for East Range Road Spring from March 2012 to December 2013

of the spring water samples does vary incrementally across time, which would be expected in natural systems. However, there were some SSII values that indicate significant ion contribution variation.

Ca^{2+} , Mg^{2+} , and Na^+ are the only three analytes that exhibited SSII fluctuations of positive to negative, or vice versa, between successive samples, indicated by points lying in the upper left (quadrant 4) and lower right (quadrant 2) quadrants of the graphs below. Results lying in quadrant 2 and 4 are sampling events that transitioned from either more than or less than the average contribution to the overall ionic character of the sample to the reverse from one month to the next. Fluctuations of this magnitude point to varying or complex water sources of differing chemical compositions. Crayfish (February to March and July to August, negative to positive changes) Na^+ concentrations had drastic contribution differences to the overall ionic character of samples between sample dates. Geocache also had SSII sign changes for Na^+ values in the December 2012 to January 2013 sample interval, as well as July to September sample interval. For Road Springs March to April both springs had positive to negative value changes. Bear (August negative to September positive) and Gnarly Root (September positive to October negative) springs both had these large contribution swings in Mg^{2+} and concentrations in the late summer to early fall. Geocache (February to March and October to November both positive to negative change), Gnarly Root (October positive to November negative), and Nolan Creek (February positive to March negative) springs all had sign changes for Ca^{2+} SSII values.

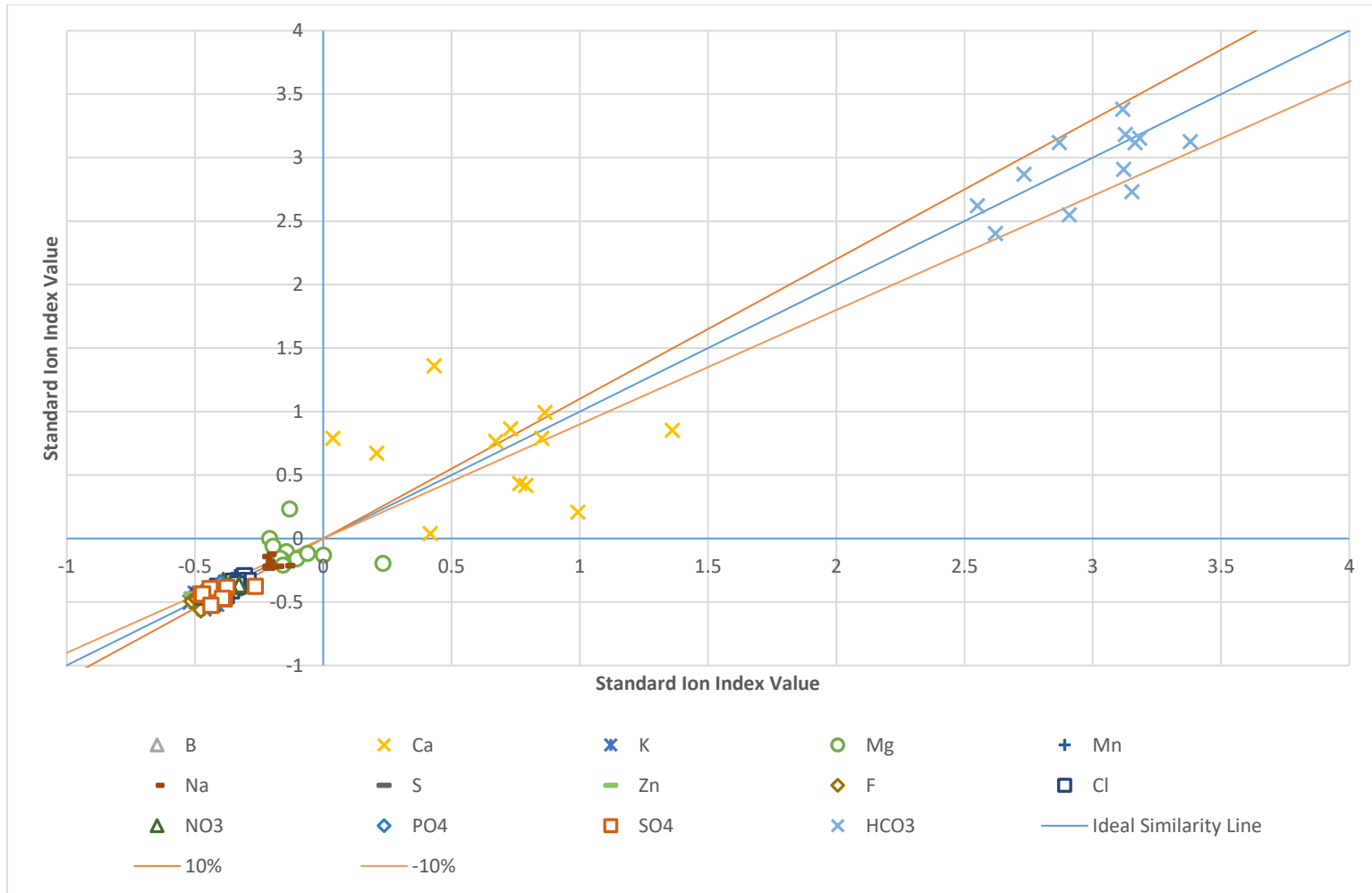


Figure 22: Successive standard ion index for Bear Spring from December 2012 to December 2013

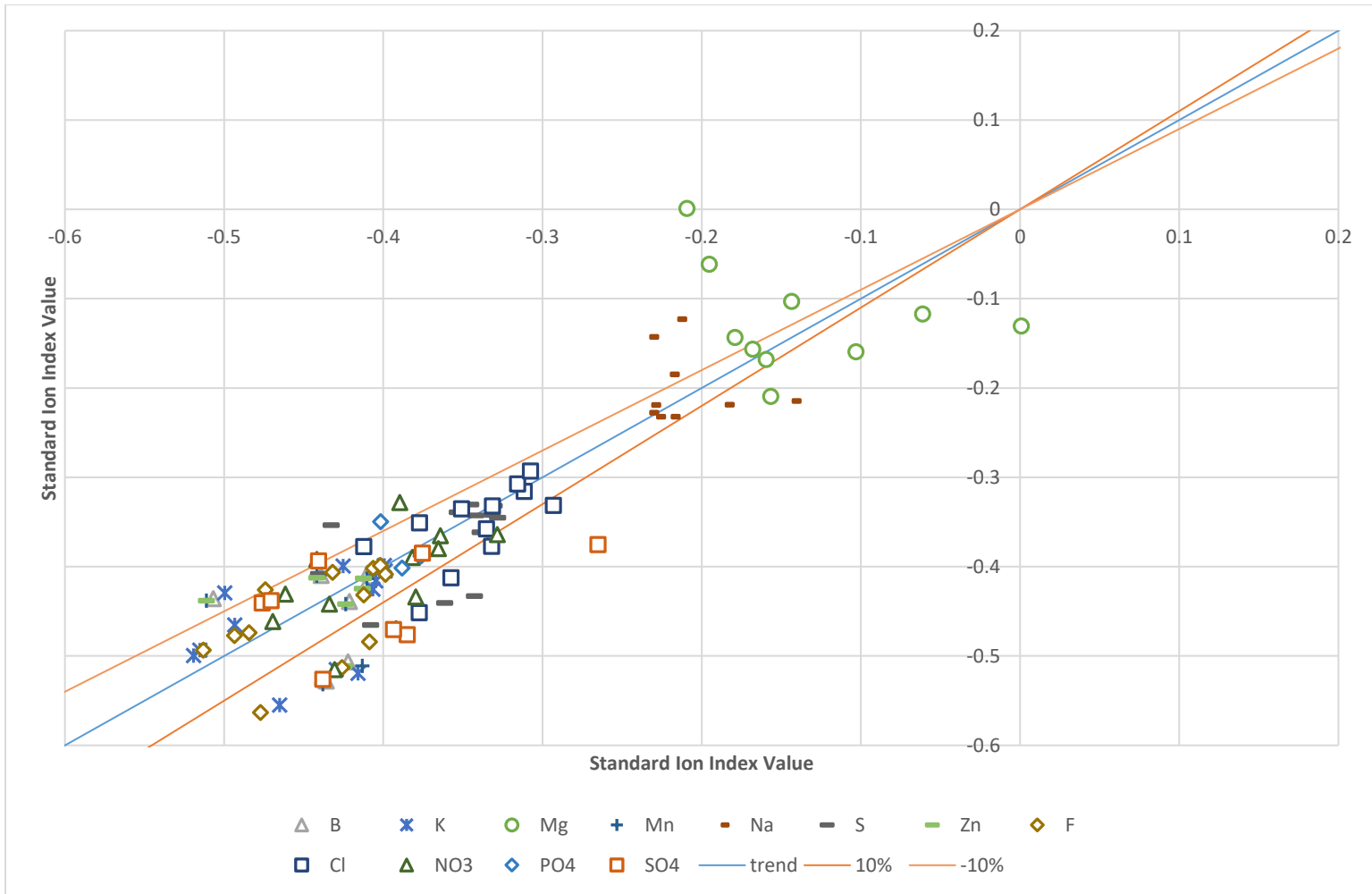


Figure 23: Successive standard ion index subset for Bear Spring from December 2012 to December 2013

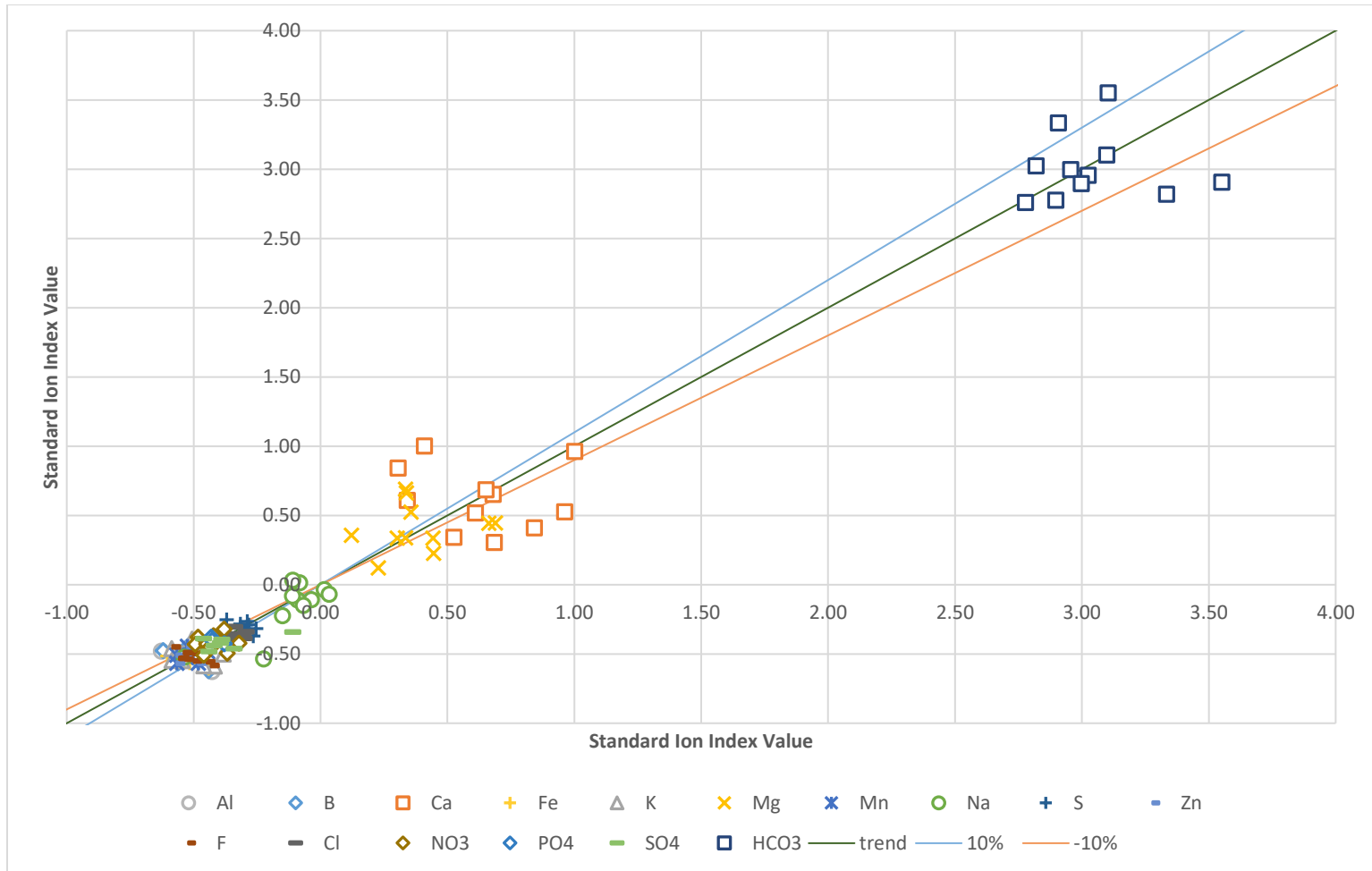


Figure 24: Successive standard ion index for Crayfish Spring from December 2012 to December 2013

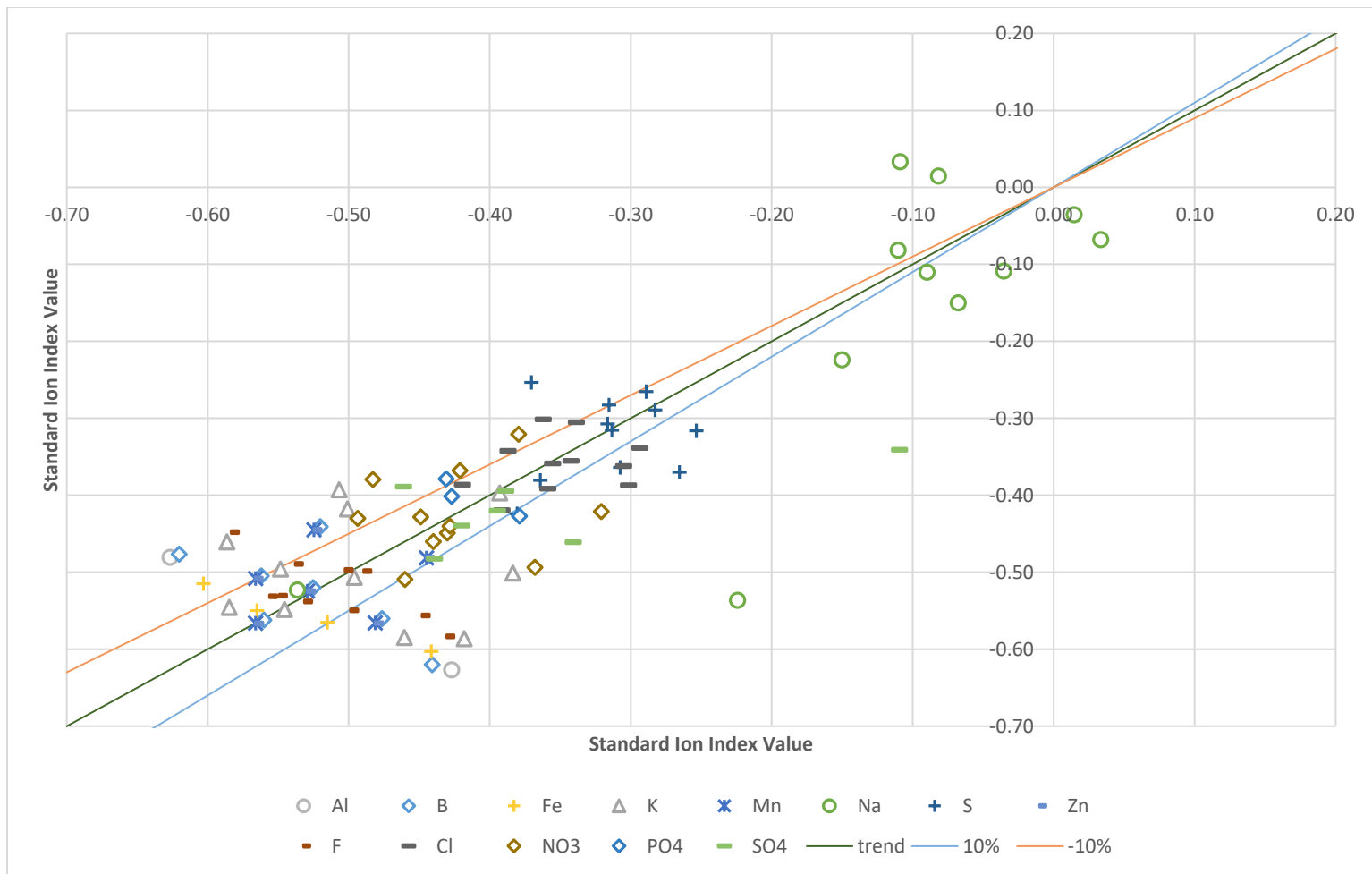


Figure 25: Successive standard ion index subset for Crayfish Spring from December 2012 to December 2013

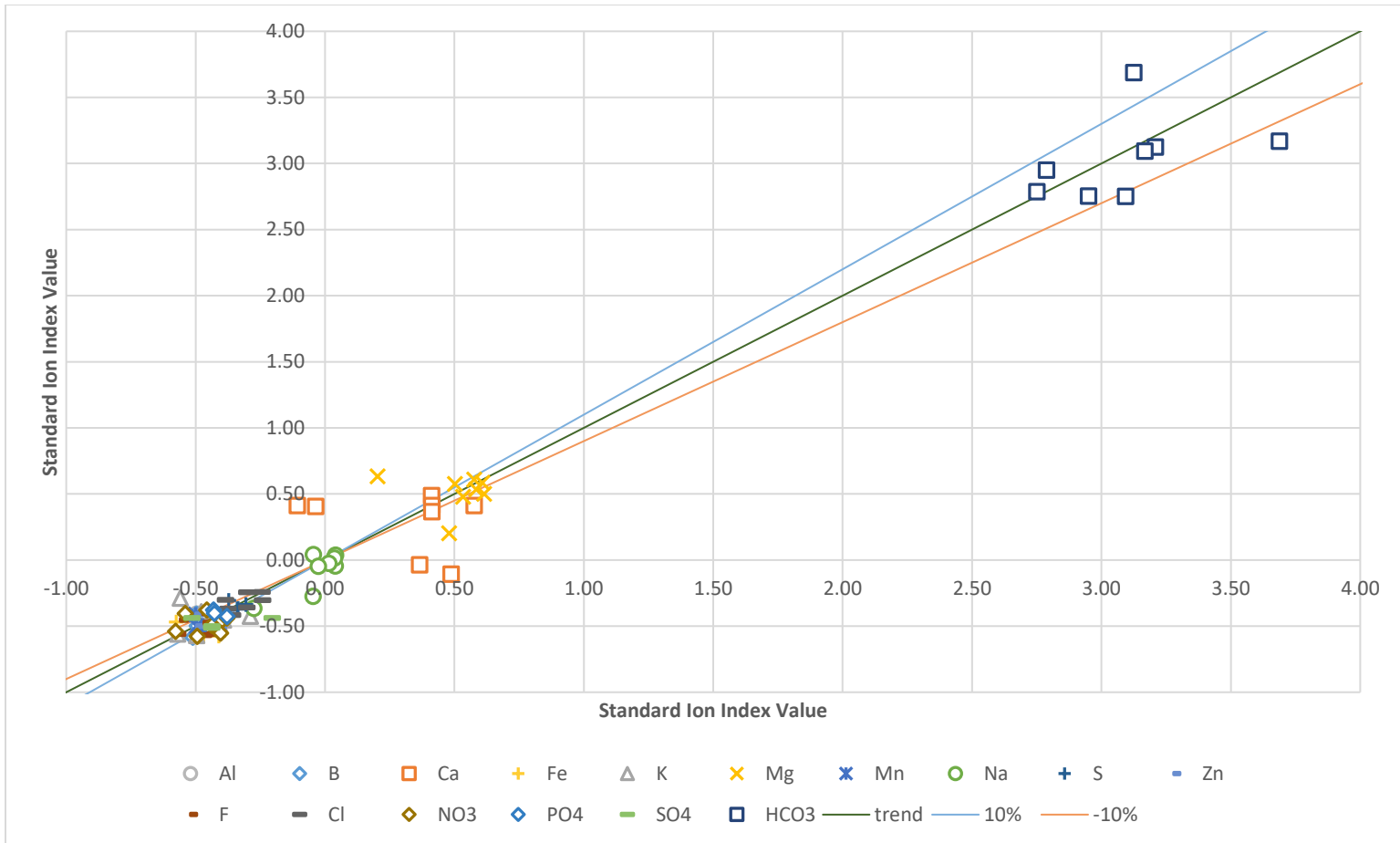


Figure 26: Successive standard ion index for Geocache Spring from December 2012 to December 2013

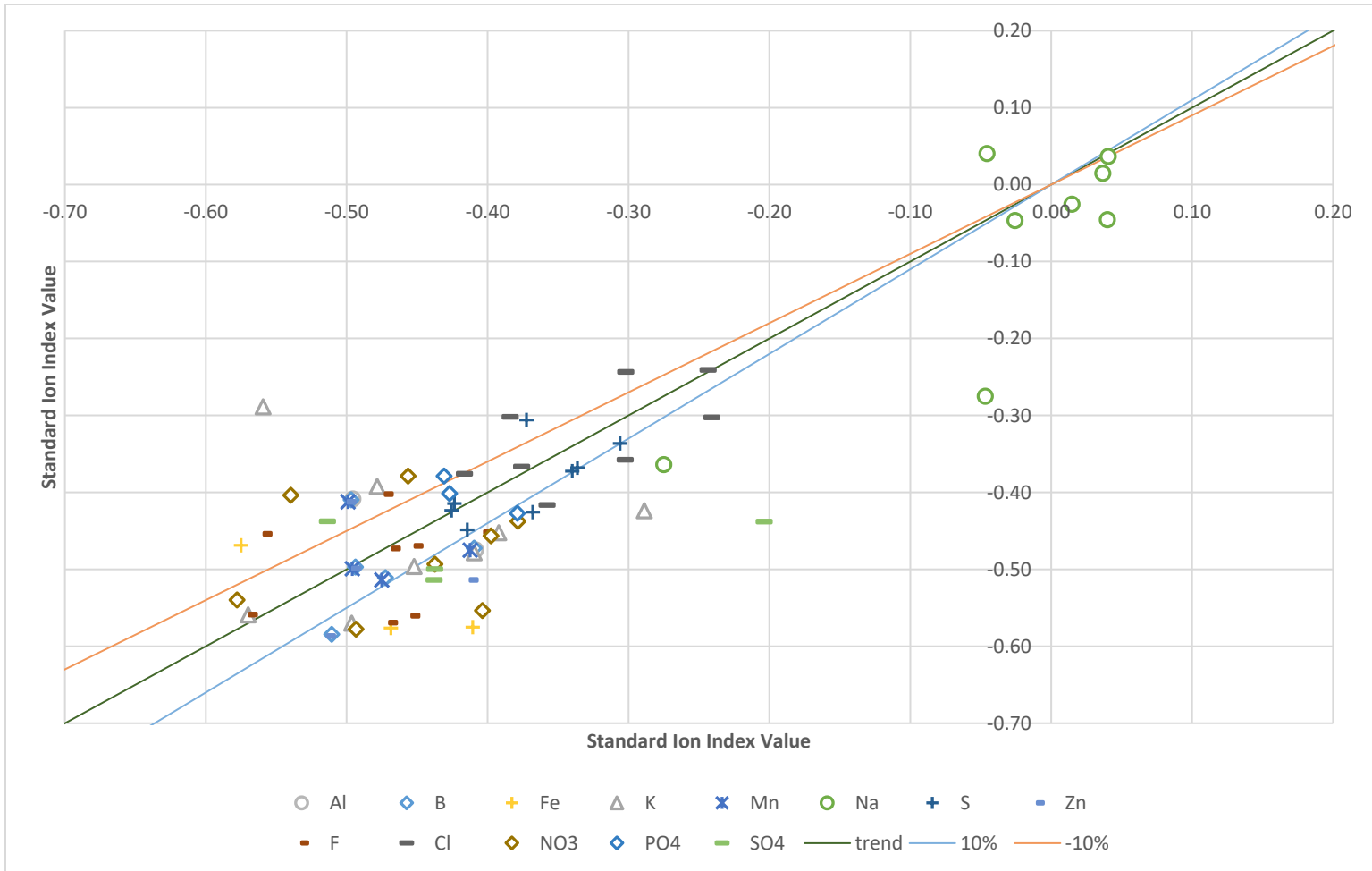


Figure 27: Successive standard ion index subset for Geocache Spring from December 2012 to December 2013

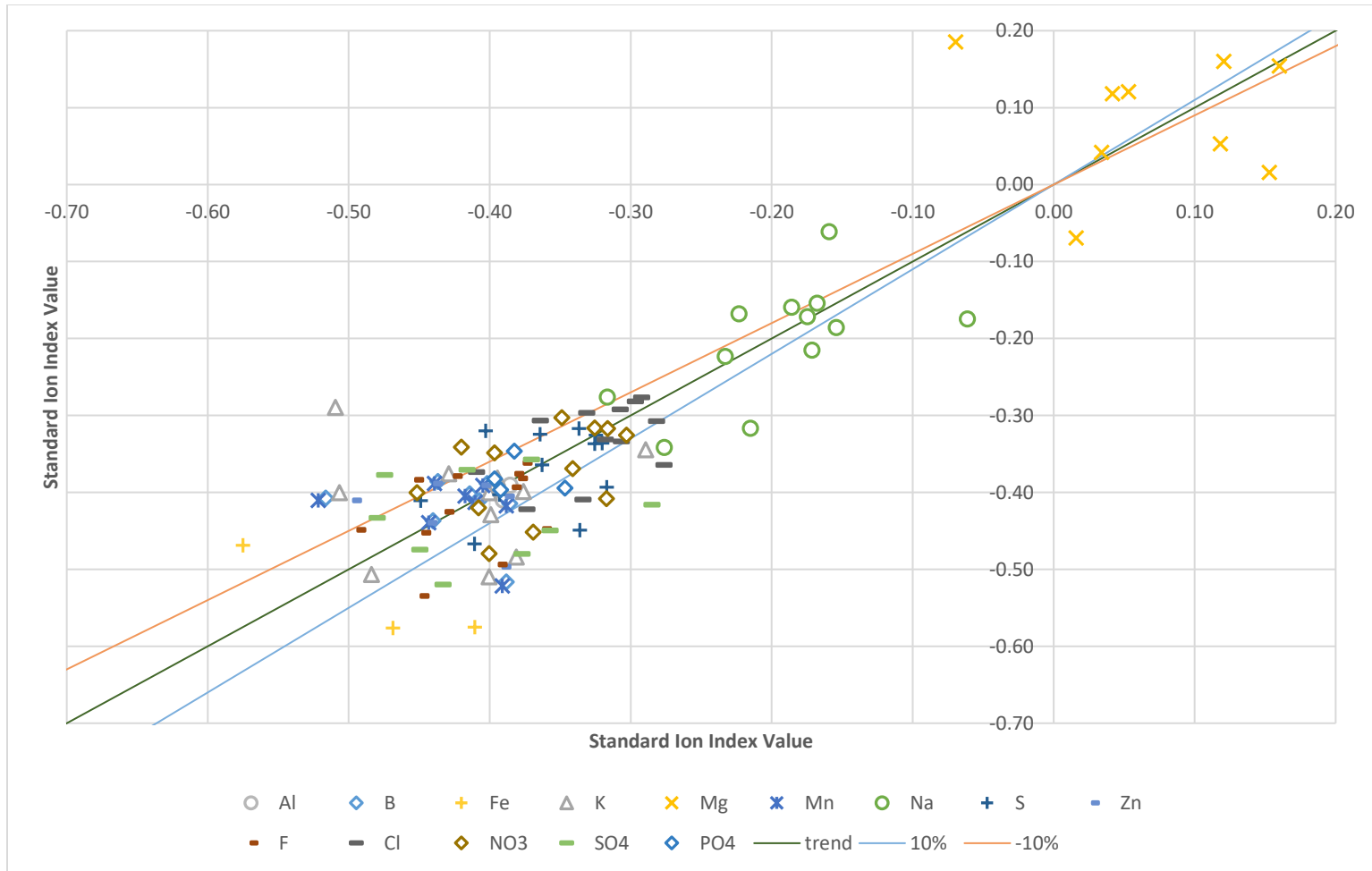


Figure 29: Successive standard ion index subset for Gnarly Root Spring from December 2012 to December 2013

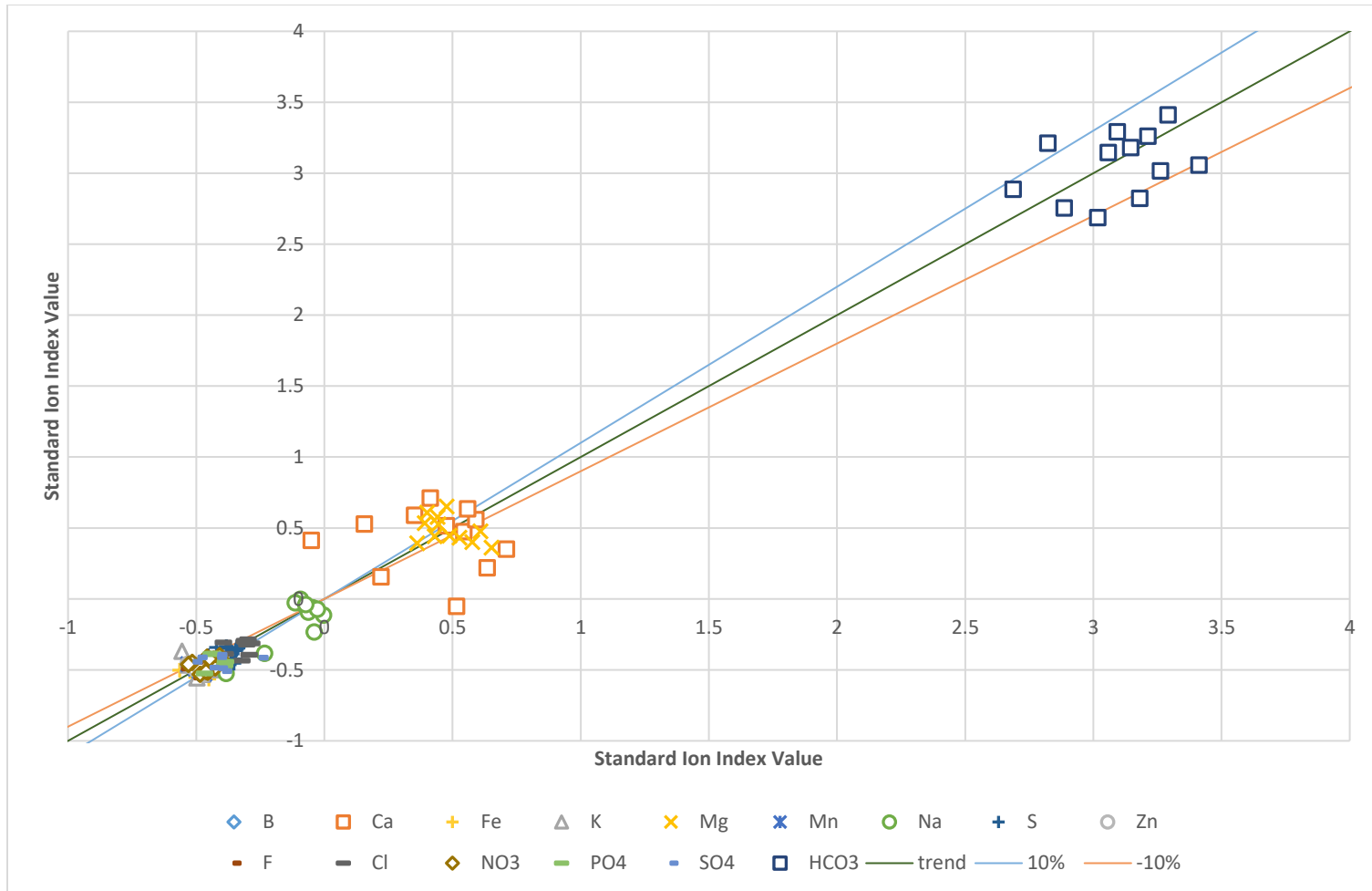


Figure 30: Successive standard ion index for Nolan Creek Spring from December 2012 to December 2013

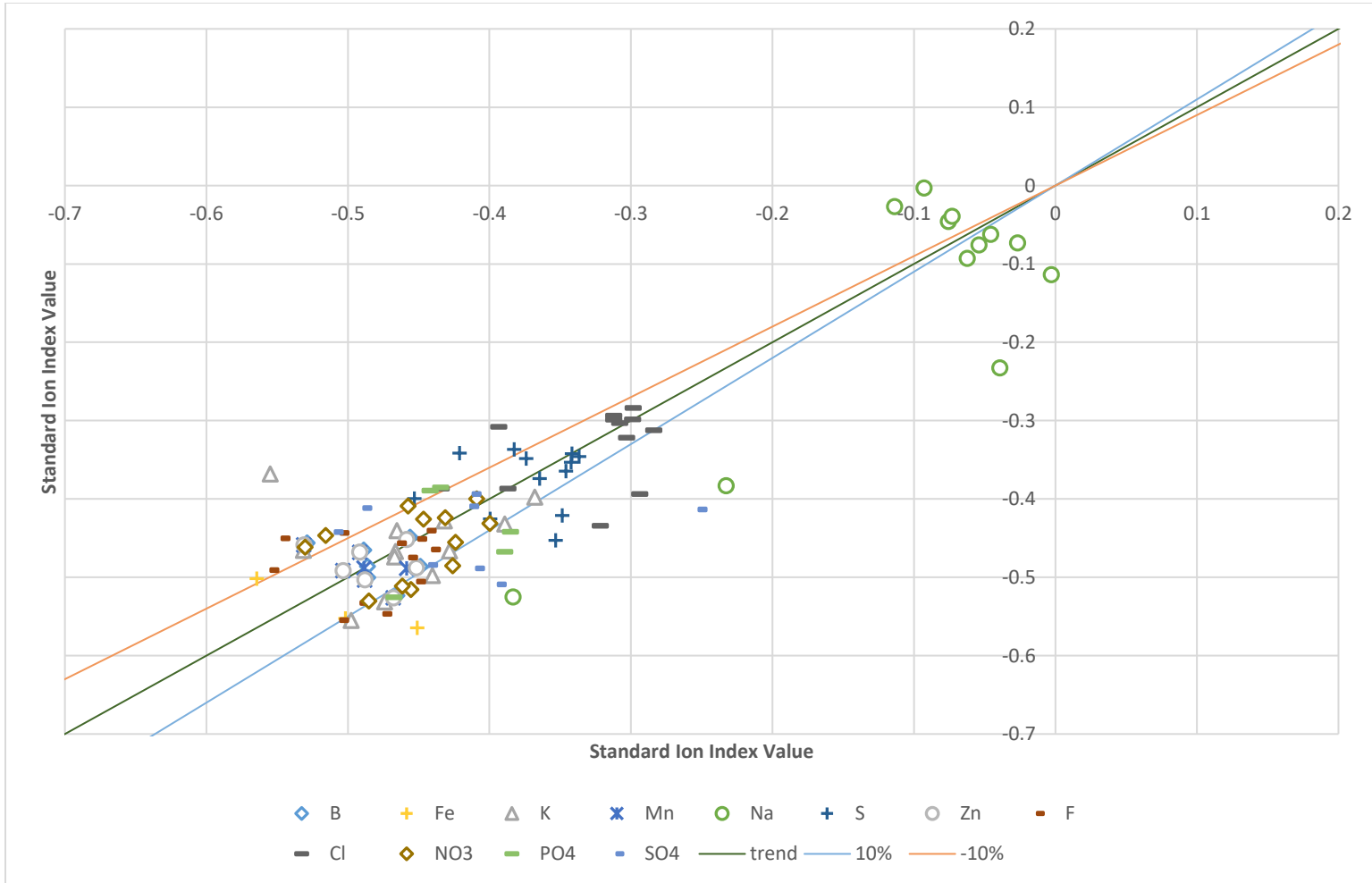


Figure 31: Successive standard ion index subset for Nolan Creek Spring from December 2012 to December 2013

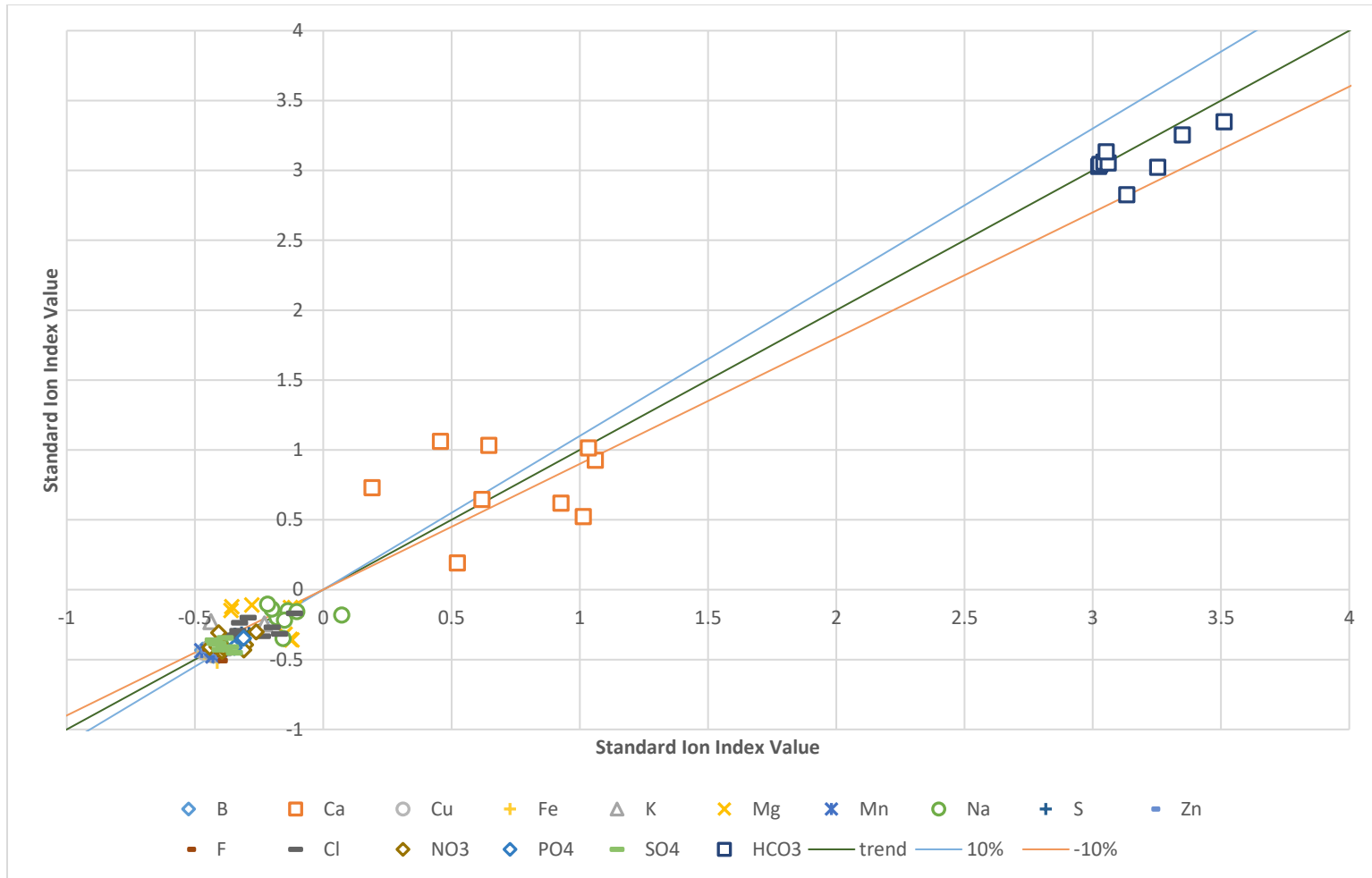


Figure 32: Successive standard ion index for Road Spring from December 2012 to December 2013

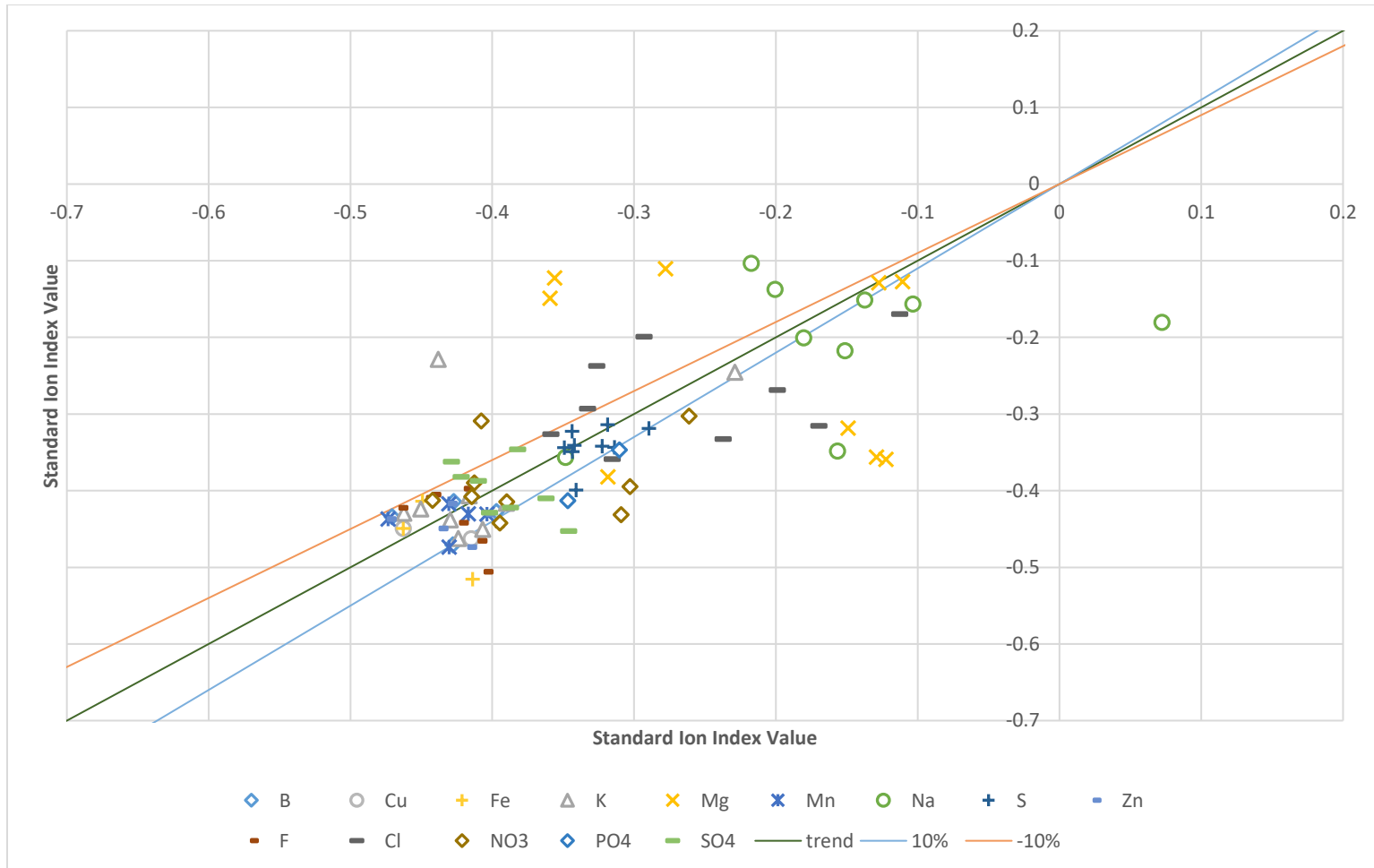


Figure 33: Successive standard ion index subset for Road Spring from December 2012 to December 2013

4.3 Inferential Statistics

Table 9 and Table 10 show the mean spring values. Included in the tables are data collected from regional water suppliers (Bell County 2013, Belton, City of 2013, Temple, City of 2013, and U.S. Army 2013), a water well collecting from the Trinity Division Hensell Sand member of the Travis Peak Formation which is directly under the Fredericksburg Division (Groundwater Database, 1995-2007), and general rainfall averages for the region (Junge et al. 1958). These adjacent water sources are included as a reference to assist in characterizing and inferring similarities and differences of the sampled spring data. The chemical composition differences between the three comparative water sources and sampled springs are thus illustrated.

Major ion concentrations in rainfall were the lowest of the water source references. This is to be expected being that residence time is a major factor in increasing chemical concentrations in natural waters. Residence time of water in the various segments of the water cycle, precipitation residence time on the order of days (van der Ent and Tuinenburg 2017), surface residence time months, and ground water residence time can be centuries (Ford and Williams 2007), lead to the increasing chemical complexity of each water cycle segment. Along with residence time the surrounding environment plays a significant role in the water chemistry. The studied

Table 9: Mean major ion and physicochemical comparison table for sampled springs and adjacent water sources (mg/L unless specified)

Spring Name	Ca	K	Mg	Na	HCO ₃ ⁻	F	Cl	NO ₃ ⁻	SO ₄ ²⁻	pH	°C	TDS (ppm)
Bear	109.68	0.64	10.35	5.23	254.13	0.38	10.12	4.37	4.49	7.03	19.24	461.92
Crayfish	110.59	2.61	26.62	10.19	259.43	0.62	15.53	7.90	12.05	6.90	19.45	493.75
Geocache	87.39	2.93	33.09	13.37	285.10	0.56	16.89	3.26	6.42	6.67	19.44	594.00
Gnarly Root	98.27	1.91	16.08	6.63	264.95	0.61	9.96	5.65	3.41	7.22	19.14	461.08
Nolan Creek	91.42	2.43	29.58	10.54	267.51	0.51	15.09	3.83	7.16	6.83	19.29	471.46
East Range Road	102.73	2.11	5.62	6.78	242.83	0.29	13.73	4.37	4.24	7.01	20.47	451.30
Spring Avg.	100.47	2.05	20.02	8.59	261.09	0.50	13.33	4.97	6.29	6.96	19.47	488.92
Well	1.83	4.83	2.36	446.00	333.89	2.15	237.67	0.19	255.67	9.27	24.23	N/A
Surface	48.60	N/A	9.71	23.57	135.50	0.21	23.85	0.26	31.30	7.30	N/A	411.00
Rainfall	1.75	1.75	N/A	0.40	N/A	N/A	0.37	N/A	1.80	0.00	N/A	N/A

Table 10: Mean trace metal comparison table of sampled springs and adjacent water sources (µg/mL)

Spring Name	Al	As	B	Cu	Fe	Mn	Pb	Zn
Bear	7.12	< 48.3	25.23	8.34	2.83	1.54	< 43.50	3.22
Crayfish	58.68	< 48.3	39.90	8.12	88.31	4.45	< 43.50	5.04
Geocache	24.19	< 48.3	25.84	3.30	28.83	2.67	< 43.50	2.88
Gnarly Root	13.18	< 48.3	27.81	34.44	13.85	2.78	< 43.50	6.47
Nolan Creek	14.50	< 48.3	25.26	5.77	12.62	1.79	< 43.50	6.46
East Range Road	7.55	< 48.3	26.02	20.49	12.72	3.25	< 43.50	6.95
Spring Avg.	20.87	< 48.3	28.34	13.41	26.53	2.75	< 43.50	5.17
Well	8.67	1.53	916.00	3.74	32.00	10.67	2.33	17.93
Surface	22.80	N/A	N/A	11.40	N/A	1.38	1.37	43.25

concentrations are to be expected due to the spring waters' sustained interaction with marine sedimentary rock susceptible to dissolution, e.g. limestone and dolomite. NO_3^- concentrations of spring water may also be increased due to meteoric water interaction with detritus or cattle manure prevalent in the region prior to percolation into the groundwater system or as runoff into the spring outlet pools where sampling occurred.

The Hensell Sand at 770 feet below surface level is the water bearing unit of the Trinity Formation being compared (Groundwater Database, 1995-2007). The well in the Trinity Formation has higher concentrations of K, Na, HCO_3^- , F, Cl, SO_4^{2-} , and B. The increases in groundwater element concentrations at greater depth is a sign of a longer residence time for water within the Trinity Formation. The nearest outcrop of the Hensell Sand at the surface is over 75 km from the study site (United States Geological Survey, 2018). The significant distance from the closest outcropping of the formation to the study site indicates a longer residence time for the Hensell Sand than the springs in the study whose formations outcrop within the study area. The longer water remains in contact with a substrate, the closer to equilibrium water will reach with the substrate it is contained within. Belton Lake major ion concentrations were intermediate between the Trinity well and the studied springs for all ions except for HCO_3^- , which was lower than the other two water sources (Table 9).

Trace metal concentrations for the studied springs were compared to the Trinity Aquifer well and Belton Lake (Table 10). Of the trace metals tested, As and Pb were found below the LOD for the spring locations, which limits the significance of those

results. The Trinity Aquifer well had the highest concentration of B and Mn of all locations reviewed, which again can be an indicator of longer residence time, allowing water to reach closer to equilibrium with the surrounding rock strata. Belton Lake contained the highest Zn concentration, which is likely from anthropogenic sources such as runoff from surrounding impervious road surfaces that collect debris from vehicular traffic and is flushed into the lake.

4.3.1 Statistical Analysis

4.3.1.1 Major Ion and Physicochemical Repeated Measures Grouped by Spring

Repeated measures and t-tests were conducted on sampled springs and summary results are shown in Table 11 and Table 12. Soluble and total Ca averages among springs were found to have means that were statistically different in t-testing. Result differences between soluble and total Ca analyses indicates that there is significant suspended solid Ca being carried from the aquifer to the surface. Bear and Crayfish Spring locations showed high soluble Ca concentrations where East Range Road, Bear and Crayfish Springs showed high total Ca concentrations. This chemical transport has been a historical occurrence and is evidenced at Bear Spring in the large tufa formations adjacent to the spring. Geocache Spring has the lowest soluble Ca concentration; Nolan Spring has the lowest total Ca concentration. However, these two springs have the highest Mg concentrations. This relationship is an indication of more dolomitized limestone interaction.

Total and soluble K analyses were statistically different with t-test analyses (Table 11). For soluble K, only Bear spring is differentiated by SNK grouping having the lowest concentration of the sampled springs. Total K results were more differentiated with Geocache and Nolan Springs being the highest concentrations; Bear and East Range Road Spring having the lowest concentrations. While K is commonly attributed to impurities found in clay minerals, it is possible that the springs to the north (Bear and East Range Road) have less clay characteristic to their aquifer composition than those to the south (Geocache and Nolan Creek). It is also worth noting that both Geocache and Nolan Creek have associated cave features with the springs where soils are present and could easily be incorporated into the spring discharge with fluctuations in flow through the cave. The total K concentrations were found to be less than the soluble K concentrations for all springs sampled, which reduces the reliability of conclusions drawn from the analysis.

Soluble and total Mg analyses were not significantly different at the 95% confidence level in t-tests (Table 11). This result indicates that the measured Mg in the samples collected was predominately dissolved in solution. SNK groupings for both soluble and total analyses support this observation. Groupings are relatively consistent between the two t-tests. All soluble Mg concentrations were separated by SNK testing among springs. Total Mg results showed Crayfish and Nolan Creek Springs grouped together with higher concentrations and Bear and Road Springs grouped with lower concentrations. Concentration of soluble and total Mg does appear higher to the south of the study area and lower to the north.

Table 11: Repeated measures ANOVA and SNK grouping by spring for major cations of sampled springs (mg/L)

Spring Name	Ca		Mg		Na		P		K		S											
	Soluble*	Total*	Soluble*	Total*	Soluble*	Total*	Soluble*	Soluble*	Total*	Soluble*	Total*											
Bear	109.7	A	135.36	AB	10.35	E	8.92	D	5.23	C	6.89	B	0.02	B	0.64	B	0.46	C	3.74	C	3.44	CD
Crayfish	110.6	A	139.92	AB	26.62	C	28.64	B	10.2	B	12.95	B	0.02	B	2.61	A	0.9	AB	8.1	A	7.61	A
Geocache	87.39	D	116.66	BC	33.09	A	38.87	A	13.4	A	17.44	A	0.02	B	2.93	A	1.12	A	5.47	B	5.62	B
Gnarly Root	98.27	BC	125.64	BC	16.08	D	17.37	C	6.63	C	6.99	D	0.03	A	1.91	A	0.66	BC	3.08	D	2.78	D
Nolan Creek	91.42	CD	106.51	C	29.59	B	32.07	B	10.5	B	12.86	B	0.02	B	2.43	A	1.23	A	5.14	B	4.52	BC
East Range Road	102.7	AB	154.83	A	5.62	F	5.69	D	6.78	C	8.79	C	0.02	B	2.11	A	0.37	C	3.77	C	4.61	BC
ANOVA P	<0.0001		<0.0001		<0.0001		<0.0001		<0.0001		<0.0001		0.0077		0.0019		<0.0001		<0.0001		<0.0001	
t-test P	0.00407				0.8153				0.32306						0.00792				0.9086			

* SNK groupings are done by letter assignment where multilettered assignments are in multiple SNK groups

Table 12: Repeated measures ANOVA and SNK grouping by spring for major anions and physicochemical parameters for sampled springs (mg/L unless noted)

Spring Name	F ⁻		Cl ⁻		NO ₃ ⁻		PO ₄ ³⁻		SO ₄ ²⁻		HCO ₃ ⁻		pH*	°C*	TDS (ppm)*		Discharge*				
	Soluble*		Soluble*		Soluble*		Soluble*		Soluble*		Soluble*				cm ³ /sec						
Bear	0.38	B	10.12	B	4.37	BC	1.61	A	4.49	B	254.1	A	7.03	B	19.2	B	461.92	B	2515	B	
Crayfish	0.62	A	15.53	A	7.91	A	3.97	A	12.1	A	259.4	A	6.9	BC	19.5	B	493.75	B	583	B	
Geocache	0.56	A	16.89	A	3.26	C	3.46	A	6.42	B	285.1	A	6.67	D	19.4	B	594.00	A	154	B	
Gnarly Root	0.61	A	9.96	B	5.65	B	1.67	A	3.41	B	265	A	7.22	A	19.1	B	461.08	B	5462	A	
Nolan Creek	0.51	A	15.09	A	3.83	BC	2.58	A	7.16	B	267.5	A	6.83	C	19.3	B	471.46	B	601	B	
East Range Road	0.29	B	13.73	A	4.37	BC	1.62	A	4.24	B	242.8	A	7.01	B	20.5	A	451.30	B	27.7	B	
ANOVA P	<0.0001		<0.0001		<0.0001		0.0167		<0.0001		0.2245		<0.0001		0.002		0.0025		<0.0001		

* SNK groupings are done by letter assignment where multilettered assignments are in multiple SNK groups

Na analyses, as with Mg, were not statistically different using t-tests between soluble and total analyses (Table 11). Crayfish and Nolan Springs were similar in SNK grouping for soluble Na. Bear, Gnarly Root and Road Springs were grouped by SNK in soluble Na analysis. Bear, Crayfish, and Nolan Springs exhibit similar total Na concentrations. Results indicate the trend of springs to the north and south are differentiated in Na concentrations, as with Mg concentrations. Higher concentrations of Na to the south and lower to the north.

T-tests indicate there is no significant difference in the findings of soluble and total S analysis, indicating the majority of sampled S was dissolved in solution. Crayfish and Geocache Springs had the highest soluble S and SO_4^{2-} concentrations with Gnarly Root Spring having the lowest soluble S levels (Table 11 and Table 12). Lithology studies in the area by Bryant (2012) indicate there are pyrite inclusions in the Comanche Peak and Edwards formations which may be a source of S.

Crayfish, Gnarly Root, and Geocache Spring NO_3^- concentrations were significantly different, with Crayfish having the highest and Geocache being the lowest in concentrations with Gnarly Root being intermediate between the two (Table 12). At Crayfish Spring there were often signs of cattle feces, which during storm events may be washing into the spring pool. This circumstance may be associated with the increase in NO_3^- concentration.

Bear and East Range Road Springs have lower F^- concentrations with respect to the other springs. Cl^- concentration analysis differentiates Bear and Gnarly Root

Springs; with lower concentrations with respect to the other sampled springs (Table 12). Despite these variations in Cl⁻ and F⁻ concentrations, the sampled springs appear to have concentrations similar to those that were reviewed from Belton Lake studies (Temple, City of, 2013), which would indicate short residence time within the aquifer.

Soluble P concentrations were below LOD across all springs, apart from a small peak at Gnarly Root Spring (Table 11). There was no significant concentration difference in HCO₃⁻ concentrations among the spring sample sets (Table 12). The pH averages of all springs ranged from 6.67-7.22, with Crayfish, Nolan Creek, and Geocache being slightly more acidic. Temperature averages for spring outlet waters were consistent across all springs at 19°C ± 1°C. East Range Road was the exception with an average of 20.5°C. The increase in temperature is most likely due to the spring outlet pool being exposed to greater incident solar heat than the other springs. TDS among springs was also consistent, apart from Geocache having higher ppm values than the other sampled springs (Table 12).

4.3.1.2 Trace Metals Repeated Measures Grouped by Spring

T-tests were conducted on soluble and total trace metal pairs for each element. The only two trace elements that were different in soluble and total concentration results were Al and Fe (Table 13). The other tests, with results above the LOD, did not have significant concentrations of suspended trace elements.

Soluble Al concentrations among sampled springs were not significantly different. This was true for total concentrations of Al as well except for Crayfish Spring which had

a higher concentration of total Al (Table 13). The increase in total Al may be due to suspended clays in the spring.

Crayfish Spring was the only spring with significantly higher B concentrations (Table 13). The increase in B concentration from Crayfish Spring may be an indicator of hypogenetic water influence since Trinity Formation waters were found to have higher B concentrations (Groundwater Database, 1995-2007). Geocache Spring is the only sampled spring with a higher total Zn concentration, which may be an indicator of similarity with surface water. There was no significant difference in concentration among springs for Cu, Fe, or Mn concentrations.

4.3.1.3 Major Ion and Physicochemical Repeated Measures Grouped by Date

Ca was the only major ion that was significantly different among sample dates based on t-test results (Table 14). The remaining ions with analytical results above the LOD (K, Mg, Na, and S) were not significantly different among sample dates.

Ca concentrations among dates were not statistically different apart from March and November sampling dates for soluble concentrations, which were lower than the other sampling dates (Table 14). Total Ca concentration in July was the only statistically differentiated result from the sample set. Mg, Na, and TDS measurements were also at their highest for the July sampling, being an indicator of a flushing event; however, there was no increase in flow coinciding with this event (Table 14 and Table 16).

Soluble K concentrations were higher in November and December 2012 and 2013 when there were no statistical differences in total K concentrations (Table 15). The

soluble and total element analyses were not differentiated using t-test and SNK groupings, but there is variance in the soluble among dates' ANOVA data and not in the total ion among the dates' ANOVA results. Soluble Mg concentrations were highest in July and lowest in April (Table 14). Total Mg concentrations also followed this pattern with a peak in July with decreases in December 2012 and April 2013. This correlation between soluble and total Mg results are supported by the t-test results identifying the two analytes as not significantly different.

Soluble and total Na concentrations both peaked in July (Table 14). Lower than average soluble values were found in April, November and December 2013 samplings. Total Na values were lower than the average for sampled springs in February, April, May, June, and August. The SNK groupings between the soluble and total ion analyses for Na are not different which would be expected from the t-testing of results of the two analyses, further supporting these comparisons.

P and PO_4^{3-} results were only intermittently above LOD, limiting the inferential utility of these parameters (Table 15). Soluble S concentrations peaked in September and were lowest in April and November. SO_4^{2-} values were higher in February when the remaining winter months of 2012-2013 were the lowest sampled. The pH in fall 2013 was higher than the remainder of the sample set (Table 16). Spring water temperatures were warmer in the late summer and early fall of 2013 and cooler in the winter to early spring of 2012-2013. TDS was lowest in the spring-summer of 2013 apart from the highest measurement of the data set occurring in July.

Table 13: Repeated measures ANOVA and SNK grouping by spring for trace metals of sampled springs (µg/L)

Spring Name	Al		B		Cu		Fe		Mn		Zn									
	Soluble*	Total*	Soluble*	Total*	Soluble*	Soluble*	Total*	Soluble*	Soluble*	Total*										
Bear	7.12	B	53.25	B	25.23	B	33.54	B	8.34	A	2.83	B	40.80	B	1.54	A	3.22	A	8.85	B
Crayfish	58.68	A	324.24	A	39.90	A	51.90	A	8.12	A	83.31	A	208.42	A	4.45	A	5.04	A	6.50	B
Geocache	24.19	B	45.46	B	25.84	B	32.81	B	3.30	A	28.83	B	34.37	B	2.67	A	2.88	A	14.31	A
Gnarly Root	13.18	B	111.13	B	27.81	B	33.77	B	34.44	A	13.85	B	116.44	B	2.79	A	6.47	A	7.15	B
Nolan Creek	14.50	B	135.78	B	25.26	B	34.46	B	5.77	A	12.62	B	75.24	B	1.79	A	6.46	A	6.48	B
East Range Road	7.55	B	138.76	B	26.02	B	34.66	B	20.49	A	12.72	B	148.21	B	3.25	A	6.95	A	3.86	B
ANOVA P	0.3561		0.0014		< 0.0001		<0.0001		0.3883		0.1674		0.0368		0.5990		0.1180		0.0005	
T-test P	0.0423		0.0523		0.0351		0.1277													

* SNK groupings are done by letter assignment where multilettered assignments are in multiple SNK groups

Table 14: Repeated measures ANOVA and SNK grouping by date for Ca, Mg, and Na spring analyses

Date	Ca				Mg				Na			
	Soluble*		Total*		Soluble*		Total*		Soluble*		Total*	
12/1/2012	108.5	A	122.08	B	20.97	AB	25.57	B	10.06	AB	11.13	BC
1/1/2013	105.1	A	114.6	B	21.35	AB	23.17	BC	9.58	AB	10.23	BC
2/1/2013	103.3	A	102.44	B	20.95	AB	21.25	BC	9.22	AB	9.36	C
3/1/2013	57.43	B	116.07	B	20.41	AB	18.7	BC	11.22	AB	10.14	BC
4/29/2013	113.5	A	120.6	B	15.58	B	16.5	C	7.54	B	7.8	C
5/17/2013	115.1	A	127.22	B	16.83	AB	18.47	BC	8.21	AB	8.91	C
6/22/2013	102.5	A	127.24	B	19.25	AB	18.82	BC	11.33	AB	8.81	C
7/11/2013	120	A	209.42	A	22.49	A	30.97	A	11.56	A	16.09	A
8/25/2013	115.3	A	121.34	B	17.3	AB	17.25	BC	8.23	AB	8.32	C
9/16/2013	112.1	A	119.14	B	21.53	AB	21.89	BC	11	AB	10.82	BC
10/1/2013	103.4	A	128.33	B	21.28	AB	23.71	BC	8.84	AB	11.11	BC
11/1/2013	60.62	B	119.74	B	17.58	AB	18.24	BC	2.76	C	10.85	BC
12/1/2013	101.4	A	140.28	B	22.74	A	23.23	BC	2.66	C	13.11	B
ANOVA P	<0.0001		<0.0001		0.0847		0.0005		<0.0001		<0.0001	
T-test P	0.0064				0.2587				0.0764			

* SNK groupings are done by letter assignment where multilettered assignments are in multiple SNK groups

Table 15: Repeated measures ANOVA and SNK groupings by date for P, K, and S spring analyses

Date	P		K			S					
	Soluble*		Soluble*		Total*	Soluble*		Total*			
12/1/2012	0.02	B	3.97	B	0.81	A	5.32	ABC	4.68	A	
1/1/2013	0.02	B	0.94	C	0.96	A	4.92	ABCD	4.43	A	
2/1/2013	0.02	AB	0.9	C	0.81	A	3.98	DE	5.04	A	
3/1/2013	0.02	B	1	C	0.87	A	5.33	ABC	4.22	A	
4/29/2013	0.04	A	0.67	C	0.48	A	3.63	E	3.39	A	
5/17/2013	0.03	AB	0.69	C	0.72	A	4.56	BCDE	4.36	A	
6/22/2013	0.02	B	0.84	C	0.64	A	5.55	AB	4.44	A	
7/11/2013	0.02	AB	0.73	C	0.97	A	5.78	AB	6.51	A	
8/25/2013	0.02	AB	0.67	C	0.84	A	4.88	ABCDE	4.27	A	
9/16/2013	0.03	AB	0.74	C	0.61	A	5.95	A	4.64	A	
10/1/2013	0.02	B	0.76	C	0.71	A	5.09	ABCD	4.48	A	
11/1/2013	0.02	B	6.81	A	0.79	A	3.47	E	5.37	A	
12/1/2013	0.02	B	6.77	A	0.93	A	4.2	CDE	4.48	A	
ANOVA P	0.0809		<0.0001			0.879	<0.0001			0.4802	
T-test P						0.09158		0.552			

* SNK groupings are done by letter assignment where multilettered assignments are in multiple SNK groups

Table 16: Repeated measures ANOVA and SNK by date for physicochemical spring data

Date	pH*		C°*		TDS* (ppm)		cm ³ /sec*	
12/1/2012	7.07	BCD	19.32	ABCD	462.60	CD	580.00	A
1/1/2013	7.49	A	18.64	D	448.60	CD	852.00	A
2/1/2013	7.09	BCD	18.46	D	397.40	D	2462.00	A
3/1/2013	6.96	CD	18.25	D	607.50	AB	2007.00	A
4/29/2013	7.34	AB	18.90	CD	455.50	CD	1202.00	A
5/17/2013	7.26	ABC	19.14	BCD	369.60	D	1010.00	A
6/22/2013	7.32	AB	19.61	ABCD	413.80	D	998.00	A
7/11/2013	7.26	ABC	20.42	AB	645.67	A	1472.00	A
8/25/2013	7.32	AB	20.17	ABC	412.40	D	1147.00	A
9/16/2013	6.85	D	20.71	A	591.50	ABC	254.00	A
10/1/2013	6.97	CD	20.30	ABC	526.50	ABCD	2326.00	A
11/1/2013	6.93	D	20.15	ABC	502.33	BCD	1531.00	A
12/1/2013	5.41	E	18.57	D	387.83	D	3496.00	A
ANOVA P	<0.0001		<0.0001		<0.0001		0.4529	

* SNK groupings are done by letter assignment where multilettered assignments are in multiple SNK groups

Table 17: Repeated measures ANOVA and SNK grouping by date for anion analyses

Date	F ⁻		Cl ⁻		NO ₃		PO ₄ ⁻³		SO ₄ ²⁻		HCO ₃	
12/1/2012	0.47	BC	13.57	A	4.59	A	7.50	B	0.00	D	266.72	A
1/1/2013	0.44	BC	13.57	A	5.80	A	9.22	B	0.00	D	272.16	A
2/1/2013	0.23	C	11.17	A	5.55	A	1.27	C	22.89	A	283.65	A
3/1/2013	0.56	B	17.22	A	6.57	A	11.93	A	0.06	D	269.89	A
4/29/2013	0.53	BC	13.06	A	6.17	A	2.32	C	4.78	D	283.12	A
5/17/2013	0.55	BC	10.89	A	4.35	A	0.00	C	7.84	B	261.88	A
6/22/2013	0.83	A	15.11	A	5.74	A	0.00	C	8.94	B	257.34	A
7/11/2013	0.88	A	14.22	A	4.20	A	0.00	C	8.94	B	253.26	A
8/25/2013	0.40	BC	12.67	A	4.91	A	0.01	C	7.91	B	247.36	A
9/16/2013	0.44	BC	13.61	A	3.49	A	0.01	C	0.98	CD	267.88	A
10/1/2013	0.46	BC	13.10	A	4.69	A	0.00	C	7.02	BC	282.02	A
11/1/2013	0.29	BC	10.84	A	5.49	A	0.03	C	6.94	BC	245.20	A
12/1/2013	0.38	BC	13.61	A	3.64	A	0.00	C	6.65	BC	220.25	A
ANOVA P	<0.0001		0.0746		0.0494		<0.0001		<0.0001		0.2308	

* SNK groupings are done by letter assignment where multilettered assignments are in multiple SNK groups

4.3.1.4 Trace Element Repeated Measures Grouped by Sample Date

Al and Fe were the only two trace elements that were statistically different between soluble and total analyses among sample dates by t-test comparison (Table 18). Soluble and total B were not significantly different among sampling dates. Although there were differences in SNK groupings for B the repeated measures analyses between the soluble and total tests, the t-test comparisons make any differences found to be less significant.

Table 18: Repeated measures ANOVA and SNK grouping by date for Al, B, Cu and Fe analyses

Date	Al				B				Cu		Fe			
	Soluble		Total		Soluble		Total		Soluble	Soluble		Total		
12/1/2012	7.2	B	124.68	AB	37.4	B	43.64	CD	3.3	B	1.2	A	89.08	B
1/1/2013	8.02	B	99.7	AB	38.08	B	41.28	CD	3.3	B	1.2	A	62.7	B
2/1/2013	174.8	A	10.5	B	38.58	B	38.32	CD	3.3	B	99.94	A	11.1	B
3/1/2013	18.97	B	177.97	AB	52.43	A	56.28	B	3.3	B	1.2	A	47.72	B
4/29/2013	6	B	140.75	AB	35.83	B	34.3	D	3.3	B	1.2	A	85.13	B
5/17/2013	10.22	B	239.28	AB	40.5	B	43.56	D	145.7	A	1.2	A	126.74	B
6/22/2013	6	B	83.82	AB	2.4	C	45.3	BCD	5.98	B	8.24	A	69.88	B
7/11/2013	16.77	B	381.28	A	47.38	AB	75.42	A	3.3	B	1.2	A	386.32	A
8/25/2013	7.22	B	300.14	AB	37.68	B	50.62	BC	3.3	B	1.2	A	150.4	B
9/16/2013	6	B	198.62	AB	38.48	B	45.6	BCD	3.3	B	1.2	A	152.48	B
10/1/2013	6	B	10.5	B	2.4	C	4.05	E	4.42	B	122.27	A	91.85	B
11/1/2013	6	B	10.5	B	2.4	C	4.05	E	3.3	B	41.87	A	27.03	B
12/1/2013	6	B	10.5	B	2.4	C	4.05	E	3.3	B	41.87	A	32.03	B
ANOVA P	0.0083		0.0024		<0.0001		<0.0001		<0.0001		0.2663		0.0075	
T-test P			0.0032				0.2954						0.0167	

* SNK groupings are done by letter assignment where multilettered assignments are in multiple SNK groups

Table 19: Repeated measures ANOVA and SNK grouping for Mn and Zn analyses

Date	Mn		Zn		Total	
	Soluble		Soluble			
12/1/2012	2.88	AB	12.6	B	2.32	D
1/1/2013	1.86	B	5.04	C	35.26	A
2/1/2013	2.04	B	1.56	C	0.85	D
3/1/2013	3.892	AB	0.75	C	22.85	B
4/29/2013	2.925	AB	8.5	BC	10.225	CD
5/17/2013	2.53	B	19.12	A	1.68	D
6/22/2013	0.45	B	4.24	C	1.06	D
7/11/2013	3.117	AB	1.35	C	3.967	D
8/25/2013	10.68	A	12.74	B	3.46	D
9/16/2013	4.208	AB	4.617	C	1.275	D
10/1/2013	0.45	B	1.917	C	2.042	D
11/1/2013	0.45	B	0.3	C	11.817	C
12/1/2013	0.45	B	0.3	C	3.633	D
ANOVA P	0.032		<0.0001		<0.0001	
T-test P				0.5322		

Soluble Al concentration was only significantly higher in February when compared to the other sampling dates (Table 18). Total Al was highest in July and lowest in the late fall and winter of the sampling interval. The increase in total Al coincides with the other peaks in major ion increases for July, possibly resulting from a flushing event.

Soluble B concentrations were highest in March and below the LOD in the fall and winter of 2013 (Table 18). Total B concentrations peaked in July and were also below the LOD for fall and winter of 2013. Soluble Cu spiked in concentration in May, while for the remainder of the sampling events soluble Cu had values near the LOD. Total Fe concentrations were only significantly different for July, being higher in concentration than the other sampling events. Soluble Mn concentrations were highest

in August with the lowest values being in the winter of 2012 and 2013 (Table 19). Soluble Zn concentrations were highest in May and December 2012 and August 2013 of the sampling interval. The remaining months' Zn concentrations were not significantly different. Total Zn concentrations were highest in January and March; April and November were also elevated while the other months remained relatively constant.

4.3.2 Principal Component Analysis

4.3.2.1 Soluble Element Principal Component Analysis

Thirteen factors were used in the soluble PCA and are shown in Table 20. Five principal components (PC) were retained for analysis after review of eigenvalues from the soluble PCA. The conclusion of five components to be retained was based on the eigenvalue of each retained component being above 1, and that over 70% of the total dataset variation was accounted for using only these five components (Table 21). The magnitude of variable loadings for each component was the basis for deciding which variables were included in the analysis. The magnitudes of some analytes were highly influential on specific PC, with similar magnitudes, while the remaining analytes were less influential. Analytes were then grouped based on this pattern of magnitude analysis and spring chemical characteristics.

The 5 retained principal components for the soluble PCA are shown in Table 22. Principal component 1 was heavily loaded by Cl, Na, Mg, and S. K and pH had an inverse relationship; they have significant loadings on component 2. NO₃⁻ and

temperature were also inversely related and had significant impact on component 3. TDS had the most significant loading for component 4. Ca, F, and spring discharge were all significant factors of component 5.

Table 20: Table of PCA variables for soluble and total element data sets

PCA Dataset	Variables	Mean	Standard Deviation
Soluble Elements	Soluble B (ppm)	0.0284	0.0203
	Soluble Ca (ppm)	100.4657	23.0788
	Cl ⁻ (ppm)	13.3258	4.1645
	Fl ⁻ (ppm)	0.4967	0.264
	Soluble Mg (ppm)	20.0246	10.4133
	NO ₃ ⁻ (ppm)	4.969	2.3199
	Soluble K (ppm)	2.051	2.6751
	Soluble Na (ppm)	8.5936	4.3783
	Soluble S (ppm)	4.8493	1.9409
	pH	6.9576	0.5581
	C°	19.467	1.1248
	TDS (ppm)	484.457	119.318
	Spring Discharge (cm ³ /sec)	1716.869	2950.0281

Table 21: Soluble elements PCA eigenvalues of the correlation matrix

PC	Eigenvalue	Difference	Proportion	Cumulative
1	3.6202	1.3610	0.2785	0.2785
2	2.2592	0.7600	0.1738	0.4523
3	1.4992	0.3211	0.1153	0.5676
4	1.1782	0.0606	0.0906	0.6582
5	1.1176	0.1758	0.0860	0.7442
6	0.9418	0.2355	0.0724	0.8166
7	0.7063	0.2749	0.0543	0.8710
8	0.4314	0.0314	0.0332	0.9042
9	0.4000	0.0405	0.0308	0.9349
10	0.3595	0.1479	0.0277	0.9626
11	0.2117	0.0526	0.0163	0.9789
12	0.1591	0.0434	0.0122	0.9911
13	0.1157	N/A	0.0089	1.0000

Table 22: Component loadings for soluble PCA

Factor	Comp 1	Comp 2	Comp 3	Comp 4	Comp 5
Soluble B	0.4801	0.5512	0.1867	-0.0285	-0.1528
Soluble Ca	0.0170	0.4810	-0.3853	-0.2771	0.6547
Cl ⁻	0.7422	-0.3391	-0.0759	-0.1640	-0.1547
F ⁻	0.5925	0.0725	0.2116	0.2157	0.4752
Soluble Mg	0.7037	-0.5006	0.0245	0.0010	0.1084
NO ₃	0.2213	0.2378	0.6529	-0.4212	0.0338
Soluble K	-0.2560	-0.7904	0.0858	-0.1706	0.0281
Soluble Na	0.8784	0.1095	-0.0755	0.1517	-0.0882
Soluble S	0.8318	-0.0934	-0.0456	-0.2993	0.2003
pH	0.0810	0.7942	0.0575	0.0310	-0.3200
Temperature	-0.0110	0.1175	-0.7381	0.1556	0.1163
TDS	0.5221	-0.0788	-0.0149	0.6738	-0.1352
Spring Discharge	-0.3675	0.0192	0.5245	0.4784	0.4691
Eigenvalue	3.6202	2.2592	1.4992	1.1782	1.1176

Components 1 and 2 (Figure 34) describe nearly half (45%) of the overall variance observed for sampled springs. Springs south of Owl Mountain (Crayfish, Geocache, and Nolan Creek Springs) had higher concentrations of magnesium, chloride, sulphur, and sodium, which would indicate longer residence time for water in those systems than those to the north (Bear, Gnarly Root, and Road Springs) which are chemical signatures of shorter residence times. Similar groupings were seen between the north and south portions of Owl Mountain in component 2 loadings, where the springs to the north had higher pH and lower potassium concentrations. The southern springs exhibited lower pH and higher potassium concentrations. However, these trends were not seen for the last two sampling events (November and December 2013) where all samples had a negative component loading for both components. This change for all springs in November and December was possibly due to the observed shift of all springs to a more epigenetic chemical composition from the large rain event in June, lowering

the concentrations of the associated ions in component 1. These negative loadings indicate that on these sampling dates all springs had lower than average magnesium, chloride, sulphur, sodium, and pH but higher potassium. The increase in potassium was interesting, since there is reported to be minimal potassium in the formations through which the water is flowing. The source of the potassium may be related to suspended clay soil being washed into the aquifer and migrating through the karst system. As noted previously, the two springs with cave features (Geocache and Nolan Creek) are known to be sources of soil; they consistently had low values for component 2 loadings, indicating higher potassium concentration. The majority of sampling events had similar loadings for component 3 (an inverse relationship between nitrogen and temperature) apart from positive outliers for Gnarly Root and Crayfish in March 2013 as well as negative loading outliers for East Range Road in July, August, and September (Figure 35). As stated previously, the increases in nitrogen for Gnarly Root were most likely associated with cattle feces contaminating the spring pool. Component 4, which is associated with conductivity, had increases in eigenvalues for most springs in March, July, and September (Figure 36). Each of these increases in discharge and conductivity roughly coincided with rain events occurring approximately a month prior to the recorded increase. Component 5 did not show any discernable pattern with respect to date or locations for the sampled springs.

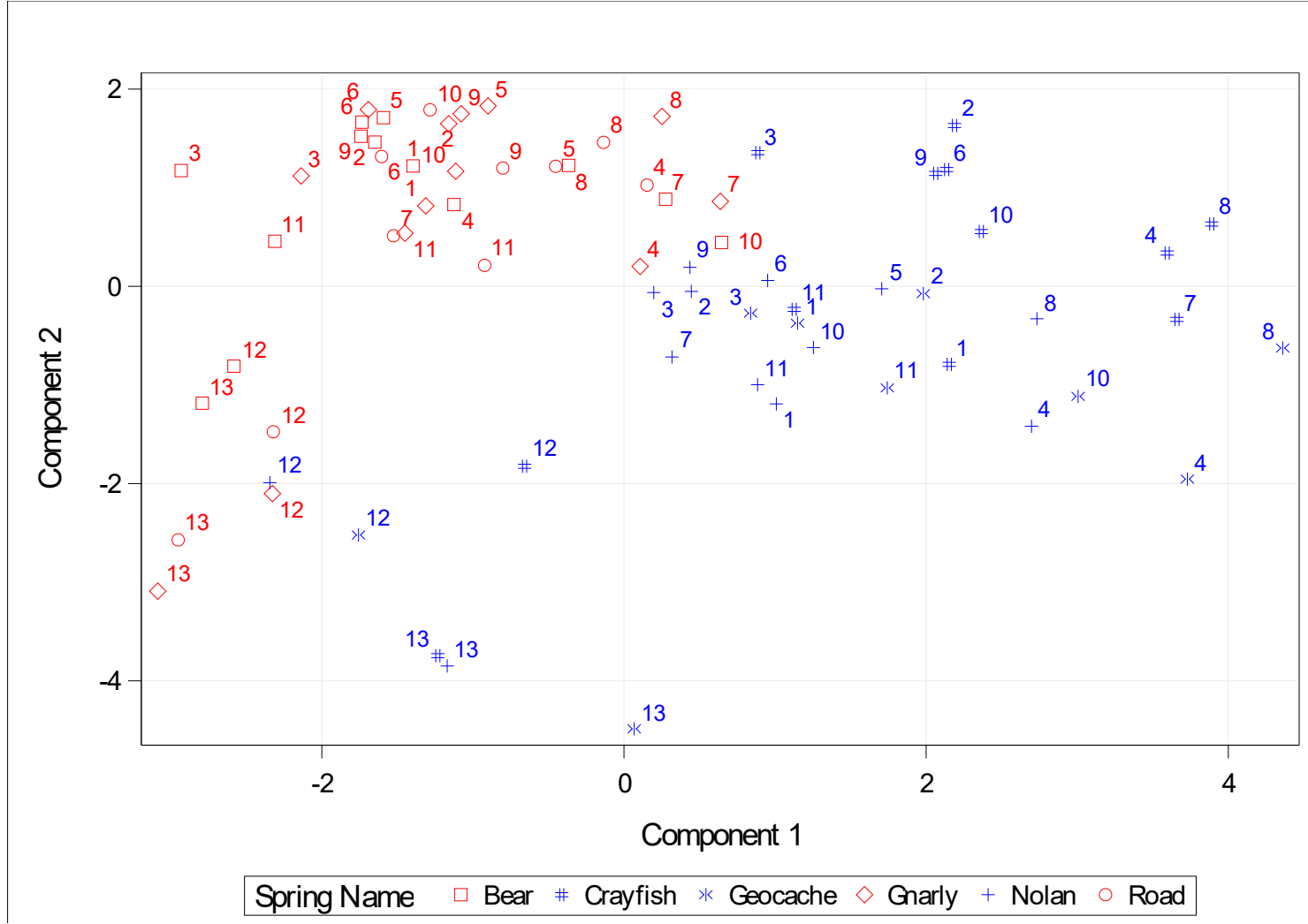


Figure 34: Soluble analytes PCA biplot of component 1 (Cl, Na, Mg, and S) and component 2 (pH and -|K|)

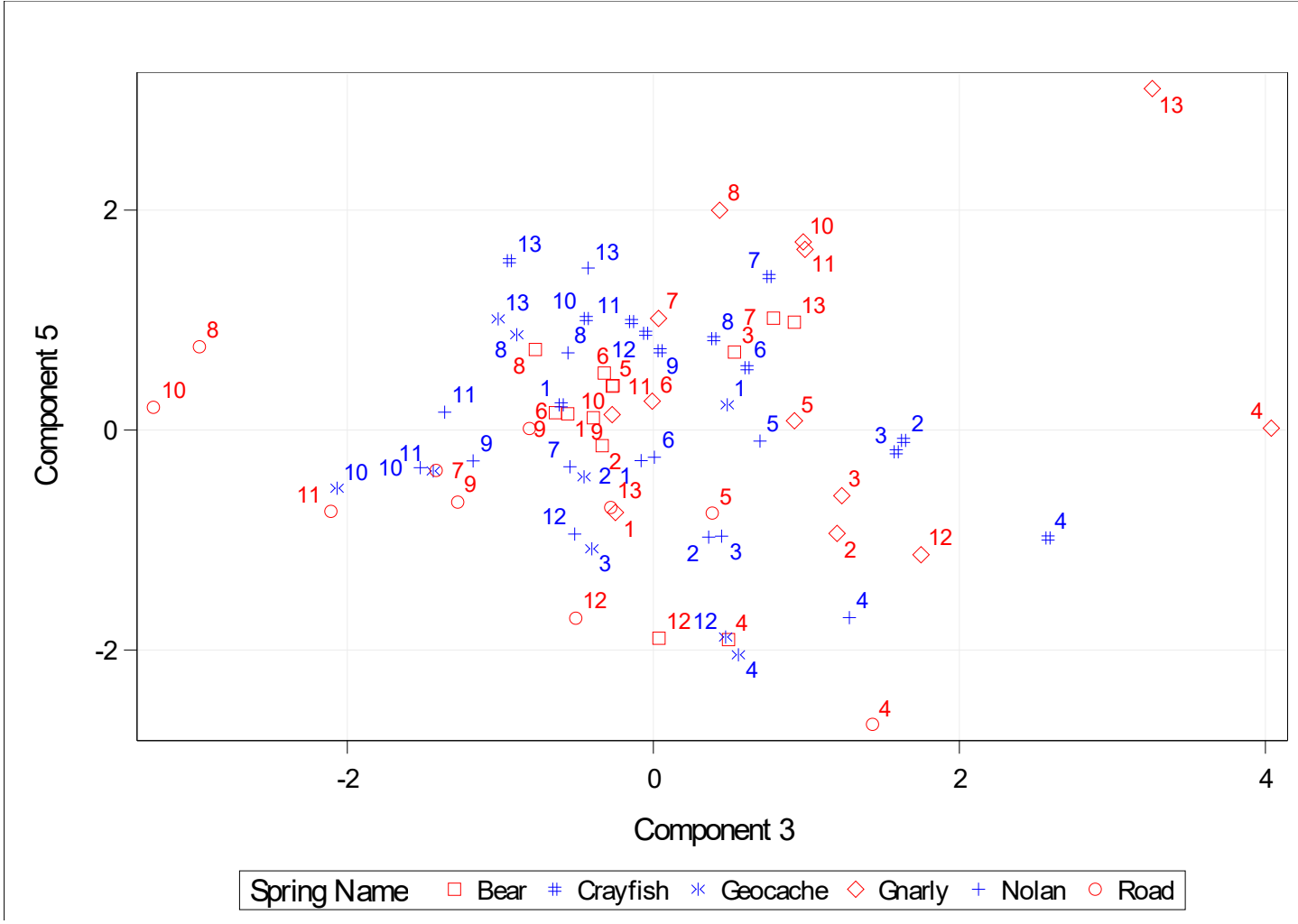
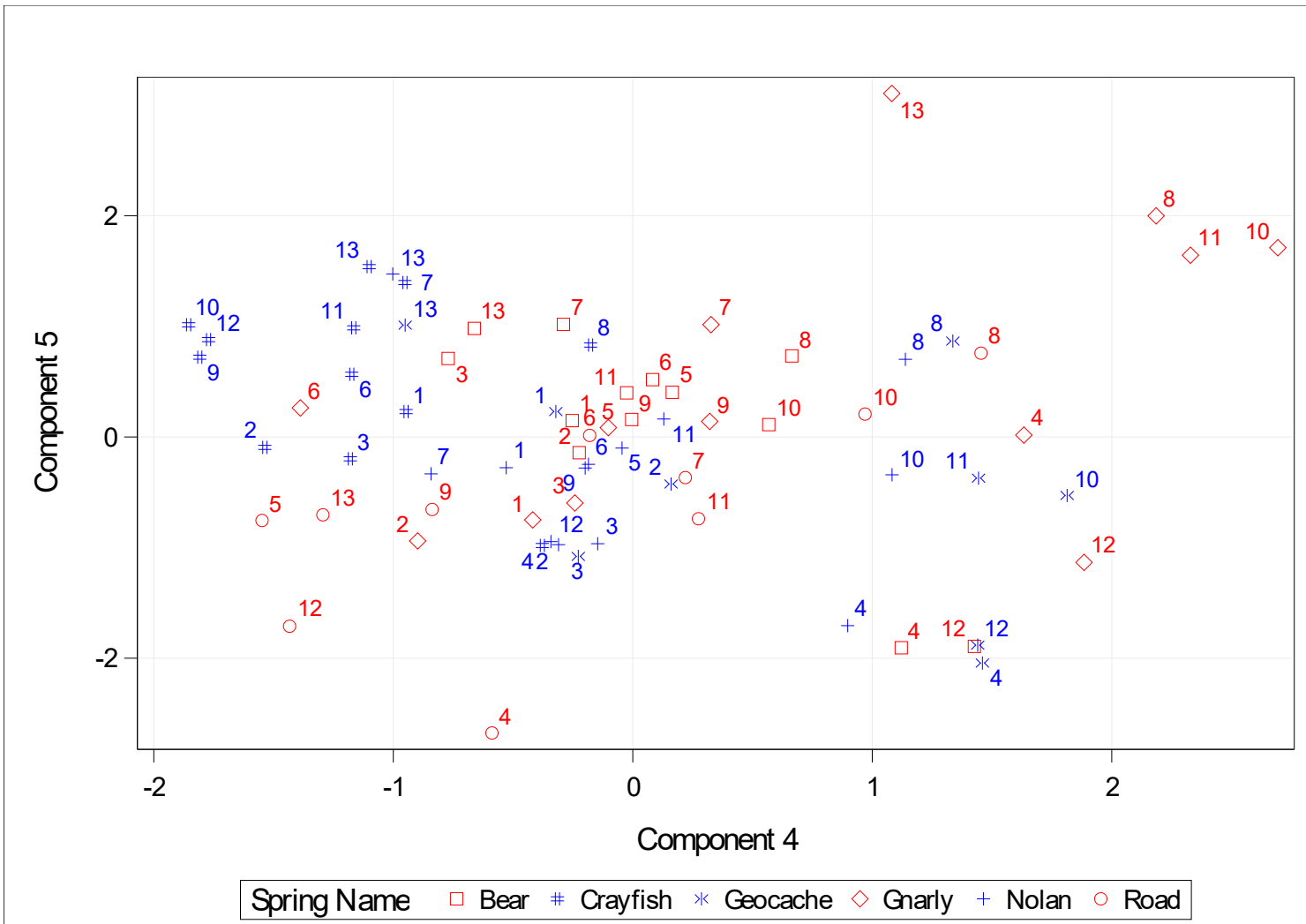


Figure 35: Soluble analytes PCA biplot for component 3 (NO₃ and -[C°]) and component 5 (Ca, F, and discharge)



4.3.2.2 Total Element Principal Component Analysis

For total element PCA there were 13 factors utilized for the analysis as shown in Table 23. Five principal components (PC) were retained for interpretation of the total element principal component analysis (Table 24). The retention of components was made based upon both the eigen value being greater than 1 combined with more than 70% of the observed variation being explained by these 5 components as shown in Table 25. The first PC indicated component loadings of Al, Fe, Na, and S. The second PC indicated an inverse correlation for Mg and K with respect to the loading value. This means that components with higher loadings will have lower concentrations of analytes, which is indicated by both analytes having negative loadings on PC 2. The third PC is affected by B, Zn, and pH. Spring discharge volume and conductivity are each loaded on the fourth and fifth components respectively.

Table 23: Total elements PCA dataset

PCA Dataset	Variables	Mean	Standard Deviation
Total Elements	Total Al (ppm)	0.137	0.2038
	Total B (ppm)	0.037	0.0236
	Total Ca (ppm)	129.354	35.4038
	Total Fe (ppm)	0.1045	0.1676
	Total Mg (ppm)	21.5581	12.7652
	Total K (ppm)	0.7866	0.4742
	Total Na (ppm)	10.6818	4.4084
	Total S (ppm)	2.1537	2.1537
	Total Zn (ppm)	0.011	0.011
	pH	0.5581	0.5581
	C°	1.1248	1.1248
	TDS (ppm)	484.457	119.318
	Spring Discharge (cm ³ /sec)	2950.028	2950.0281

Table 24: Total element PCA eigenvalues of the correlation matrix

PC	Eigenvalue	Difference	Proportion	Cumulative
1	3.8056	1.2833	0.2927	0.2927
2	2.5222	0.8786	0.1940	0.4868
3	1.6436	0.3285	0.1264	0.6132
4	1.3151	0.3290	0.1012	0.7144
5	0.9861	0.1983	0.0759	0.7902
6	0.7878	0.2258	0.0606	0.8508
7	0.5620	0.0917	0.0432	0.8940
8	0.4702	0.1104	0.0362	0.9302
9	0.3598	0.0987	0.0277	0.9579
10	0.2611	0.0663	0.0201	0.9780
11	0.1948	0.1392	0.0150	0.9929
12	0.0556	0.0195	0.0043	0.9972
13	0.0361		0.0028	1.0000

Table 25: Component loadings for retained factors for total element PCA

Factor	Comp 1	Comp 2	Comp 3	Comp 4	Comp 5
Total Al	0.7312	0.3921	0.2405	0.1519	-0.3000
Total B	0.5959	0.3617	0.5223	-0.0094	-0.1378
Total Ca	0.5497	0.5373	-0.2864	0.2537	0.1752
Total Fe	0.7297	0.5341	-0.0172	0.2653	-0.0706
Total Mg	0.6132	-0.6696	0.0272	-0.0468	-0.0280
Total K	0.4012	-0.6518	0.1794	0.2767	-0.2098
Total Na	0.7628	-0.5403	-0.2131	-0.1447	0.1052
Total S	0.7400	-0.1561	-0.1369	-0.2433	-0.1776
Total Zn	-0.0409	-0.2381	0.7067	-0.0141	0.3225
pH	-0.1508	0.4643	0.5954	-0.3866	-0.0295
C°	0.2767	0.4405	-0.4836	-0.3659	0.2831
TDS	0.4801	-0.0710	0.2111	0.1112	0.7509
Spring Discharge	-0.2882	0.0524	-0.0324	0.8381	0.0722
Eigenvalue	3.8056	2.5222	1.6436	1.3151	0.9861

The biplot of components 1 and 2 of the total element analysis shows a clear distinction between the springs to the north of Owl Mountain and those to the south (Figure 37). Springs to the north have lower concentrations of all indicated elements for the first (Al, Fe, Na, and S) as well as the second (Mg and K) factors, indicative of shorter water residence time. In contrast, springs to the south have higher concentrations of elements loaded on the first two components, indicating longer residence times. There was no discernible pattern of differences among sample locations based on the distribution of PC 3 values. However, there was some temporal variation among sampling dates. January and March of 2013 had higher loadings on PC 3 values, while in October, November, and December of 2013 the PC values were still high in magnitude but were negative, indicating lower concentrations (Figure 38). These changes are likely driven primarily by pH changes associated with the flushing event initiated by storms in June, which could have lowered spring discharge water pH in October through December 2013 (sample collections 11-13). Epigenetic waters flushing through the spring network could have moved the system away from equilibrium with the aquifer substrate, diluting the ionic strength of spring water, resulting in a more acidic pH. Discharge volume of the sampled springs greatly influences PC 4. PC 4 scores were relatively flat near zero. This is an indicator that discharge did not play a significant role in variation of the dataset, until sampling events in February (3), March (4), July (8), and September (10) through December (13) (Figure 38). Principal component 5, loaded highly by conductivity measurements, coincides with increases in discharge for July (8) and September (10) through December 2013 (13).

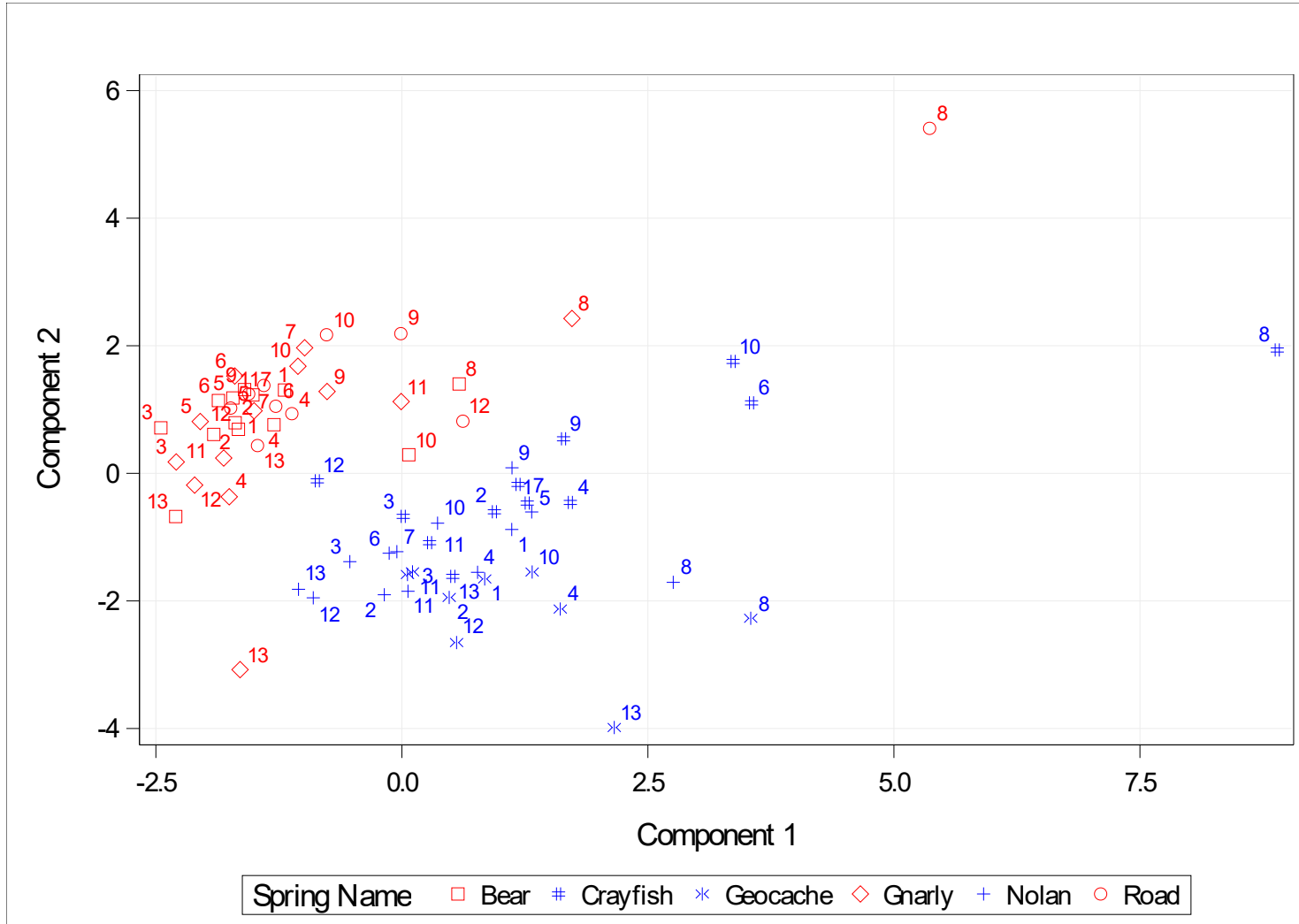


Figure 37: Total metal PCA biplot for component 1 (Al, Fe, Na, and S) and component 2 (-|Mg| and -|K|)

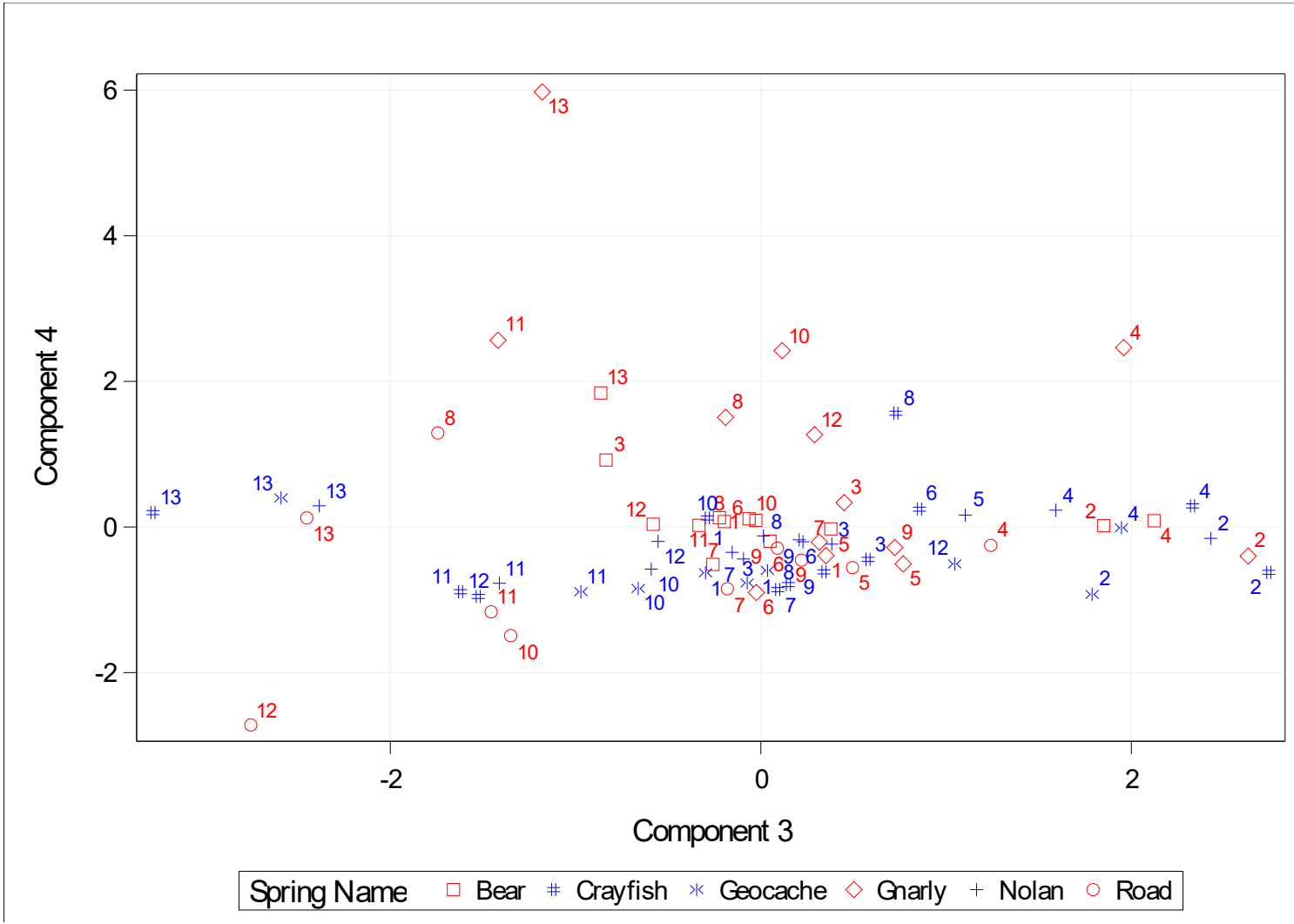


Figure 38: Total metal PCA biplot for component 3 (B, Zn, and pH) and component 4 (discharge)

5. DISCUSSION

5.1 Study Significance

The eastern peninsula of Ft. Hood is a rugged terrain covered by mixed juniper and oak shrubland, growing in calcareous clay loam to loamy soils, underlain by predominately carbonate rock of the lower Cretaceous (Walnut Clay, Comanche Peak, and Edwards Limestone), with extensive karst features throughout the study area. The karst features of specific interest of this study were the springs which are utilized by an endangered species the golden cheek warbler and a sub species of salamander *Plethodon albagula*. Despite water being essential for the wellbeing of wildlife, hydrology of the region has only recently begun to be studied in more detail by (Bryant, 2012) and (Faulkner, 2016). Historically, springs in the region discharged sufficient volumes of water perennially. However, drought conditions have significantly impacted spring discharge. Due to water becoming a limiting resource, desire to understand the spring hydrology has become more important.

The primary objective of this study was to identify and characterize the spring water chemistry of the eastern peninsula of Fort Hood Military Installation. During the course of the study there were 6 months with greater than average (5.66 cm for the 6 years prior) rainfall: January (8.65 cm), March (7.44 cm), April (11.76 cm), May (6.39

cm), July (16.85 cm) and September (10.17 cm) as shown in Figure 14. Sampling for the project ran from December 2012 to December 2013. Eight springs were sampled monthly. Two of the springs ran dry (Amphitheater and Cold Springs) and were excluded from the study. Three of the remaining springs were located to the north of the Owl Mountains, which comprise much of the peninsula (Bear, East Range Road, and Gnarly Root), one spring along the south west margin of the peninsula (Crayfish), and two springs in the Nolan Creek region to the south of the eastern peninsula (Nolan Creek and Geocache), across Belton Lake. Bear, Nolan Creek, and East Range Road Springs are underlain by the Edwards Formation, Crayfish and Geocache are located at the boundary of the Edwards and Comanche Peak formations. Gnarly Root Spring is underlain by the Walnut Clay Formation. The complete list of analytical parameters and averages for the study were referenced in Table 1.

5.2 Regulatory Standards Water Quality Review

All regulated chemical constituents were within the TCEQ limits (Table 5, Table 6, and Table 7) with the exception of Pb with MCL's below the LOD of the selected chemical analysis method. TDS also exceeded TCEQ limits for this segment, 1220 of the Brazos River basin. The TDS standard for the sampled springs may not necessarily be the most appropriate criteria, since the standard is for open pressure surface systems such as rivers and lakes (TCEQ 2012). These springs are closed to semi closed

pressurized systems that can naturally contain much higher concentrations of solutes. As these springs equilibrate with surface conditions and mix with surface waters, TDS values should become more consistent with TCEQ criteria.

5.3 Karst Hydrogeology Interpretation Using Geochemical

Evidence

The complex spring recharge mechanisms driven by the interplay between deeper seated hypogenetic hydrologic water flow with more rapid epigenetic flow regimes are not well understood and were the subject of this investigation. Water chemistry was used to characterize this hydrologic regime. A complex pattern of alternating spring water sources and recharge was evident from the pattern of ion concentrations observed over the study period. During periods of basal flow for the studied springs, where the spring water is near its steady state chemical concentration, the springs to the north of the study area (Bear, East Range Road, and Gnarly Root) had chemical compositions that can be attributed to more epigenetic flow regimes. Those to the south (Crayfish, Nolan Creek, and Geocache) had characteristics of longer residence times and more hypogenetic characteristics. The $\text{Ca}^{2+} / \text{Mg}^{2+}$ ratios of the northern springs are Ca dominant, while to the south, Mg concentrations were more prevalent (Table 2). Ca concentrations dominate epigenetic regimes due to Mg being in lower quantities in most carbonate formations and requiring longer residence time to

precipitate into solution. This condition limits soluble Mg in faster flowing systems, as found in many epigene systems (Dreybrodt and Eisenlohr 2000) (Drever, 1997) (Hem, 1985) (Kresic, Stevanovich, & Zoran, 2010). Other than increased Ca and minimal Mg concentrations from dissolution of carbonates, water in epigenetic regimes has similar chemical composition to surface waters when compared to deeper seated hypogenetic systems (Klimchouk, 2007). The standard ion index for the northern springs (Figure 16, Figure 19, and Figure 21) indicate HCO_3^- (dissolved into solution through carbon dioxide interaction with water) Ca^{2+} and to a lesser extent Mg^{2+} (being lesser than half the significance on the ion composition as calcium) were the dominant ions. The remaining elements being almost insignificant in contribution to ionic value. This contrasts with the southern springs with SII values for Mg^{2+} being nearly equal in the ionic composition (Figure 17, Figure 18, and Figure 20). Repeated measures ANOVA results confirmed the epigenetic nature of the northern springs, with a more hypogenetic character to the south. Ca was the only element in the northern springs in higher concentrations and greater chemical diversity than the southern springs (Table 11). Principal component analysis (PCA) also indicated an epigenetic regime with the northern springs having minimal loadings in general for soluble PCA component 1 (Mg, Cl, S and Na) and total PCA component 1 (Al, Fe, Na, and S). The springs to the south had the exact opposite loadings on the first components of the soluble and total element PCAs (Figure 34 and Figure 37). As this spring network is driven from its steady state through storm events, rising potentiometric surfaces in the different interrelated formations change the chemical indicators in these springs, allowing better inference into how these springs are related to differing water sources.

In karst systems, when large volumes of water are added, moving transitioning vadose zones into phreatic, there is an associated increase in chemical concentration of water leaving the system (Ford & Williams, 2007) at spring outlets. In simple epigenetic systems, this chemical concentration increase is accompanied by an increase in discharge proportional to the volume of water added to the system. In hypogenetically regulated systems, there may still be a chemical concentration increase at the onset of a flushing event; however, the accompanying discharge increase will be dampened by the semi-confined strata involved in the system, spreading the discharge signature over a longer time interval (Klimchouk, 2014). This hypogenetic regulated scheme was observed in the study area. There were 6 months of above average precipitation during the study period and with our sampling interval a discernable pattern of discharge correlating to precipitation events was not evident. In March, July, September, October, November, and December of 2013 Gnarly Root Spring discharge was a significant factor in the variance of the spring as illustrated by the total element PCA component 1 x 4 biplot. Repeated Measures ANOVA SNK groupings by date (Table 14, Table 16, and Table 18) for July results showed across the board increases in ion concentrations for Ca, Mg, Na, Al, B, Fe and TDS values at all spring sources. However, no definitive increase in discharge among all springs in July, was observed. This could be an indicator of significant pressure head increases in the hypogenetic segments of this spring network. The rise in ionic concentration peaks in the 8th sampling event in July and slowly reduces to the lowest ionic concentrations for all springs by the 13th event in December of 2013. This transition can be seen in the soluble PCA component 1 which is associated with Mg, Cl, S, and Na (Figure 34). During this period, the transition can

also be seen in the total element PCA results with increased loadings on component 1 (total Al, Na, and S) at their maximum in July and decreasing steadily until December 2013. Total element PCA component 2 (total Mg and K) is a possible indicator of suspended soils being pushed through the system. This is based upon soil characterizations summarized in (Faulkner, 2016) indicating calcareous clay soils are prevalent across the region. These clays contain potassium and magnesium due to the dolomitic Edwards limestone being the most prevalent caprock in the region. Concentration of these solids is lower at the onset of the ionic increase, marking the start of the flushing event, while soluble magnesium is high in the southern set of springs. As the flushing event progresses, soluble magnesium decreases as total magnesium increases, which likely indicates residence time changes for the spring network. The association of potassium and soils is supported by results from two springs (Geocache and Nolan Creek) that have associated cave systems, known to have soil within them (Bryant, 2012). These are both identified with having high total potassium concentrations from ANOVA tests (Table 11). There are also some indications of faster acting epigenetic mechanisms at work at Geocache and Nolan Creek Springs. At both springs in March, there is a fluctuation in their calcium SII values (Figure 26 and Figure 30) which is an indicator of an influx of meteoric water into the system. At the time of sampling, there was a rain event occurring, which most likely inundated the associated cave features of these two springs, diluting the calcium content at the spring orifices.

6. CONCLUSION

The Lower Cretaceous formations of Walnut Clay, Comanche Peak, and Edwards Limestone that underlay the Eastern Peninsula of Fort Hood Military Installation contain a complex network of karst springs. Overall water quality of the studied springs was within the TCEQ human and aquatic life primary contact water quality standards. TDS measurement for Geocache was the only analyte above the TCEQ standard. The TDS result being high is most likely due to the standard being designed for surface water bodies and not turbid groundwater springs. These karst springs show evidence of both hypogenetic and epigenetic modifications. Generally, the spring's epigenetic signature is predominant with varying hypogenetic characteristics. The springs to south displayed more hypogenetic influence than those to the north. As precipitation recharges these systems, on the order of three to six months after initiation, there is little to no fluctuation in discharge volume, indicating hypogenetically coupled recharge mechanisms. During sampling there was observed increases in precipitation with no significant discharge variation among most springs. This is despite indicating short residence time epigenetic chemical signatures. The model of the system as presented by Bryant (2012) and Faulkner (2016) is that of a terraced epigenetic system hydraulically linked with an older hypogenetic system. The springs appear to be a system where the hydrostatic pressure of the two segments are in competition. When the pressure is high in the epigenetic segment it overpowers the hypogenetic and the chemical signature is epigenetic. As the

meteoric water increases pressure on the system, an increase in ionic concentrations of soluble and total ions from all springs is observed on the order of months after the initiation of the rain event. This increased ionic activity decreases over time as the “fresh” influx of water flushes through the karst network, for soluble measurements, and the majority of total ion measurements, with the exception of those associated with particulate material drawn through the epigenetic segments of system such as suspended soil particles (Mg and K). These suspended soil particulates increase at the end of the sampling interval in total measurements but decrease in soluble measurements, indicating that these materials did not reside long enough in the karst network to precipitate into solution. As the epigenetic hydrostatic pressure decreases the hypogenetic waters begin to have a greater contribution and maintain the same relative discharge volumes at the spring orifice, but with differing chemical signatures. To determine what the exact correlation between the springs discharge and precipitation sampling intervals would need to be more frequent to validate our observations. Utilization of isotopic analysis would more definitively determine the actual ages of the waters being discharged from this karst network. These techniques could be utilized in additional studies to more comprehensively characterize these springs.

7. LITERATURE CITED

- Adkins, W. S. (1930). *Geology of Bell County Texas University of Texas Bulletin NO. 3016*. Austin, TX: University of Texas Austin.
- Amsbury, D. L. (1984). *A Field Guide to Lower Cretaceous Carbonate Strata in the Moffat Mound Area Near Lake Belton Bell County, Texas*. San Antonio: Gulf Coast Section/ Society of Economic Paleontologists and Mineralogists Foundation.
- Bell County. (2013). *Annual Drinking Water Quality Report*. Bell County.
- Belton, City of. (2013). *Annual Drinking Water Quality Report*. Belton: Belton, City of.
- Blakeley, R. (2011, February). *Paleogeography and Geologic Evolution of North America*. Retrieved from Paleogeography: <https://www2.nau.edu/rcb7/nam.html>
- Briuer, F. L. (2015, October 15). *Fort Hood*. Retrieved from Handbook of Texas Online: <https://tshaonline.org/handbook/online/articles/qbf25>
- Brown, J. L. (1972). *Paleoenvironment and Diagenetic History of the Moffat Mound, Edwards Formation, Central Texas*. Baton Rouge: Louisiana State University.
- Bryant, A. W. (2012). *Geologic and Hydrogeologic Characterization of Groundwater Resources in the Fredericksburg Group, North Nolan Creek Province, Bell County, Texas*. Nacogdoches: Stephen F Austin State University.
- Cattell, R. B. (1966). The Scree Test for the Number of Factors. In R. B. Cattell, *Multivariate Behavioral Research* (pp. 245-276).
- Chang, M. (2006). *Forest Hydrology, An Introduction to Water and Forests, 2nd. ed.* CRC Press.
- Charlson, R. J., & Rodhe, H. (1982). Factors Controlling the Acidity of Natural Rainwater. *Nature Vol 295*, 5851.
- Drever, I. J. (1997). *The Geochemistry of Natural Waters 3rd ed.* Upper Saddle River, NJ: Prentice Hall.
- Dreybrodt, W., & Eisenlohr, L. (2000). Limestone Dissolution Rates in Karst Environments. In A. B. Klimchouk, D. C. Ford, A. N. Palmer, & W. Dreybrodt,

- Speleogenesis: Evolution of Karst Aquifers* (pp. 136-148). Huntsville: National Speleological Society.
- Dunham, R. J. (1962). Classification of carbonate rocks according to depositional texture. *Classification of carbonate rocks: American Association of Petroleum Geologists Memoir*, 108-121.
- Faulkner, M. S. (2016). *An Investigation of Hydrogeologic, Stratigraphic, and Structural Controls on Acer Grandidentatum Communities in a Karst Landscape, Owl Mountain Province, Fort Hood Military Installion, Texas*. Nacogdoches: Stephen F Austin State University.
- Ford, D., & Williams, P. (2007). *Karst Hydrogeology and Geomorphology*. West Sussex: John Wiley and Sons Ltd.
- George, P. G., Mace, R. E., & Petrossian, R. (2011). *Aquifers of Texas*. Austin: Texas Water Development Board.
- Groundwater Database. (1995-2007). *Well Information Report for State Well Number 40-52-302*. Austin: Texas Water Development Board.
- Hem, J. D. (1985). *Study and Interpretation of the Chemical Characteristics of Natural Water vol 2254*. US Geological Survey, Department of the Interior.
- History of the Great Place*. (2007). Retrieved from Fort Hood History: <http://www.hood.army.mil/history.aspx>
- Junge, C. E., & Werby, R. T. (1958). The Concentration of Chloride, Sodium, Potassium, Calcium, and Sulfate in Rain Water Over the United States. *Journal of Meterology*, 15(5), 417-425.
- Klimchouk, A. (2000). Speleogenesis Under Deep Seated and Confined Settings. In A. B. Klimchouk, D. C. Ford, A. N. Palmer, & W. Dreybrodt, *Speleogenesis: Evolution of Karst Aquifers* (pp. 224-260). Huntsville: National Speleological Society.
- Klimchouk, A. (2007). *Hypogene Speleogenesis: Hydrogeological and Morphogenetic Perspective. Special Paper no. 1*. Carlsbad, NM: National Cave and Karst Research Institute.
- Klimchouk, A. (2014). The Methodological Strength of the Hydrogeological Approach to Distinguishing Hypogene Speleogenesis. *Hypogene Cave Morphologies, Selected Papers and Abstracts of the Symposium* (pp. 4-12). Leesburg, VA: Karst Waters Institute.

- Kresic, N., Bonacci, & Ognjen. (2010). Spring Discharge Hydrograph. In N. Kresic, *Groundwater Hydrology of Springs: Theory, Management, and Sustainability*. Butterworth-Heinemann Elsevier.
- Kresic, Stevanovich, N., & Zoran. (2010). *Groundwater Hydrology of Springs: Theory, Management, and Sustainability*. Butterworth-Heinemann Elsevier.
- Laidler, K. J. (1984). The Development of the Arrhenius Equation. *Journal of Chemical Education* vol 61, 494.
- Lenntech, V. B. (2013). *Water Conductivity*. Retrieved from <http://www.lenntech.com/applications/ultrapure/conductivity/water-conductivity.htm>
- Martin, T., Brockhoff, C., Creed, J., & Group, E. M. (1994). *Method 200.7 Determination of Metals and Trace Elements in Water and Wastes by Inductively Coupled Plasma-Atomic Emission Spectrometry Revision 4.4*. Cincinnati, OH: Environmental Monitoring Systems Laboratory Office of Research and Development; U.S. Environmental Protection Agency.
- Moore, C. H. (1964). *Stratigraphy of the Fredericksburg Division, South-Central Texas*. Austin, TX: Bureau of Economic Geology.
- Morse, J. W., & Arvidson, R. S. (2002). The Dissolution Kinetics of Major Sedimentary Carbonate Minerals. *Earth-Sci*, 51-84.
- Narasimhan, B., Srinivassan, R., Quiring, S., & Nielsen-Gammon, J. W. (2005). *Digital Climate Atlas of Texas*. Texas Water Development Board.
- National Oceanic and Atmospheric Administration. (2014, June 17). *National Climate Datasets*. Retrieved from National Climate Data Center: <http://www.ncdc.noaa.gov/cdo-web/datasets>
- National Resources Conservation Service. (2014 a). *Official Soil Descriptions*. Retrieved from National Soil Conservation Service: <https://soilseries.sc.egov.usda.gov/osdlist.aspx>
- National Resources Conservation Service. (2014 b). *Web Soil Survey*. Retrieved from National Resources Conservation Service: <https://websoilsurvey.sc.egov.usda.gov/App/HomePage.htm>
- Nelson, H. F. (1959). Deposition and Alteration of the Edwards Limestone, Central Texas. *Symposium on Edwards Limestone in Central Texas* (pp. 21-86). Austin: Bureau of Economic Geology.

- Pekins, C. E. (2007). *Conserving Biodiversity on Military Lands: A Guide for Natural Resources Managers*. NatureServe.
- Pfaff, J. D. (1993). *Determination of Inorganic Anions by Ion Chromatography*. Cincinnati, OH: Environmental Monitoring Systems Laboratory Office of Research and Development; U.S. Environmental Protection Agency.
- Rose, P. R. (1972). *Edwards Group, Surface and Subsurface, Central Texas*. Austin, TX: Bureau of Economic Geology.
- SAS. (2014). *Principal Component Analysis*. Retrieved from SAS Support: <https://support.sas.com/publishing/pubcat/chaps/55129.pdf>
- Sellards, E. H. (1930). Rocks Underlying Cretaceous in Balcones Fault Zone of Central Texas. *Bureau of Economic Geology* (pp. 819-827). Austin: Bureau of Economic Geology.
- Şen, Z. (2011). Standard Ion Index for Groundwater Quality Evolution. *Water Quality Expo Health vol 3*, 193-202.
- State Water Resources Board. (2007). *Electrical Conductivity/Salinity Fact Sheet*. Retrieved from State Water Resources Board: http://www.waterboards.ca.gov/water_issues/programs/swamp/docs/cwt/guidance/3130en.pdf
- Stevens, J. (1986). *Applied Multivariate Statistics for the Social Sciences*. Hillsdale: Lawrence Erlbaum Associates.
- Temple, City of. (2013). *Annual Drinking Water Quality Report*. Temple: Temple, City of.
- Texas Commission on Environmental Quality. (2012). *Chapter 307- Texas Surface Water Quality Standards*. Austin: Texas Commission on Environmental Quality.
- United States Geological Survey. (2018, May 16). *Texas Geologic Map Data*. Retrieved from United States Geological Survey: <https://mrdata.usgs.gov/geology/state/state.php?state=TX>
- University of California Davis. (2014). *Solubility of Salts/Solubility Equilibria*. California.
- US Army. (2013). *Water Quality Report*. Fort Hood: US Army.
- van der Ent, R. J., & Tuinenburg, O. A. (2017). The Residence Time of Water in the Atmosphere Revisited. *Hydrology and Earth System Sciences*, 779-790.

Walker, L. E. (1979). *Occurance, Availability, and Chemical Quality of Ground Water in the Edwards Plateau Region of Texas*. Austin: Texas Department of Water Resources.

White, W. B. (2010). Springwater Geochemistry. In Kresic, Stevanovich, Neven, & Zoran, *Groundwater Hydrology of Springs: Theory, Management, and Sustainability*. Butterworth-Heinemann Elsevier.

Williams, P. W. (1983). The Role of the Subcutaneous Zone in Karst Hydrology. *Journal of Hydrology* vol 61, 45-67.

8. APPENDIX

8.1 Field and Laboratory Results

8.1.1 Physicochemical Attributes Data Table

Table 26: Physicochemical attributes

Spring Name	Sample Date	pH	C°	µS/cm	cm/sec	DO %	cm/sec	cm wide	cm deep	Discharge cm3/sec
Bear	12-Dec	7.13	19.30	678.80	12.14	74.30	12.14	40.00	4.00	1942.88
Bear	13-Jan	7.36	19.20	653.10	15.30	81.00	15.30	40.00	4.00	2448.00
Bear	13-Feb	6.79	19.20	372.40	40.00	84.60	40.00	40.30	3.70	5964.40
Bear	13-Mar	7.43	19.10	899.40	14.68	86.90	14.68	40.00	4.00	2348.80
Bear	13-Apr	7.35	19.49	709.00	17.43	80.60	17.43	41.60	3.80	2756.06
Bear	13-May	7.31	19.51	630.00	21.43	80.80	21.43	41.20	3.80	3354.68
Bear	13-Jun	7.35	19.53	644.00	8.26	78.60	8.26	39.80	3.80	1249.25
Bear	13-Jul	6.84	19.80	907.80	7.90	73.90	7.90	37.40	3.80	1122.75
Bear	13-Aug	7.36	19.56	660.00	15.18	71.90	15.18	40.00	4.10	2489.36
Bear	13-Sep	6.86	19.50	947.10	16.12	70.80	16.12	36.00	3.80	2205.22
Bear	13-Oct	7.18	19.42	710.30	14.98	78.30	14.98	39.60	3.90	2313.51

Table 26: Physicochemical attributes continued

Spring Name	Sample Date	pH	C°	µS/cm	cm/sec	DO %	cm/sec	cm wide	cm deep	Discharge cm3/sec
Bear	13-Nov	6.84	19.70	945.10	12.69	69.50	12.69	32.00	3.60	1461.89
Bear	13-Dec	5.62	16.80	630.70	16.80	72.80	16.80	42.00	4.30	3034.08
Bear Average	N/A	7.03	19.24	722.13	16.38	77.23	16.38	39.22	3.89	2514.68
Crayfish	12-Dec	7.10	19.50	768.00	1.21	90.50	1.21	23.00	8.00	223.19
Crayfish	13-Jan	7.74	18.80	751.00	5.10	90.20	5.10	23.00	8.00	938.40
Crayfish	13-Feb	7.43	18.50	741.50	23.00	91.00	23.00	8.00	12.23	2250.32
Crayfish	13-Mar	6.93	18.50	1048.00	3.41	98.70	3.41	23.00	8.00	627.44
Crayfish	13-May	7.16	19.24	736.00	1.46	81.60	1.46	22.90	8.10	271.38
Crayfish	13-Jun	7.17	19.24	801.00	2.26	82.40	2.26	23.10	8.00	416.82
Crayfish	13-Jul	6.73	19.53	1175.20	3.11	72.20	3.11	23.00	8.20	586.55
Crayfish	13-Aug	7.16	19.60	617.00	0.76	75.30	0.76	23.00	8.00	140.21
Crayfish	13-Sep	6.61	20.33	621.30	0.65	68.20	0.65	22.90	6.40	95.26
Crayfish	13-Oct	6.82	20.20	649.30	7.22	71.30	7.22	14.90	3.40	365.77
Crayfish	13-Nov	6.77	20.10	754.40	6.43	86.30	6.43	14.80	3.60	342.59
Crayfish	13-Dec	5.22	19.90	598.50	12.85	70.40	12.85	14.60	3.90	731.68
Crayfish Average	N/A	6.90	19.45	771.77	5.62	81.51	5.62	19.68	7.15	582.47
Geocache	12-Dec	6.88	19.30	794.10	2.22	74.60	2.22	9.00	4.00	79.81
Geocache	13-Jan	7.40	19.40	763.40	6.50	85.70	6.50	9.00	4.00	234.00
Geocache	13-Feb	6.96	18.70	662.70	9.00	96.60	9.00	4.00	2.35	84.60
Geocache	13-Mar	6.60	18.60	1096.00	1.72	79.80	1.72	9.00	4.00	61.92
Geocache	13-Jul	6.78	19.70	1012.40	1.79	94.90	1.79	8.90	3.40	54.17
Geocache	13-Sep	6.71	20.40	1206.90	6.16	55.50	6.16	9.10	4.20	235.44
Geocache	13-Oct	6.82	20.10	1114.20	4.67	58.60	4.67	8.90	4.10	170.41
Geocache	13-Nov	6.75	19.70	1056.30	5.15	67.20	5.15	7.60	2.90	113.51

Table 26: Physicochemical attributes continued

Spring Name	Sample Date	pH	C°	µS/cm	cm/sec	DO %	cm/sec	cm wide	cm deep	Discharge cm3/sec
Geocache	13-Dec	5.15	19.10	650.70	8.87	63.40	8.87	9.40	4.20	350.19
Geocache Average	N/A	6.67	19.44	928.52	5.12	75.14	5.12	8.32	3.68	153.78
Gnarly Root	12-Dec	7.31	18.90	650.50	0.44	74.20	0.44	50.00	10.00	219.50
Gnarly Root	13-Jan	7.77	17.80	641.10	0.70	73.10	0.70	50.00	10.00	350.00
Gnarly Root	13-Feb	7.22	17.90	626.40	50.00	73.10	50.00	10.00	5.90	2950.00
Gnarly Root	13-Mar	6.98	16.70	896.20	17.12	77.30	17.12	50.00	10.00	8560.00
Gnarly Root	13-Apr	7.57	18.91	681.00	3.35	78.90	3.35	51.40	9.10	1568.24
Gnarly Root	13-May	7.56	19.71	240.00	1.71	75.60	1.71	50.20	6.10	522.68
Gnarly Root	13-Jun	7.68	20.20	675.00	7.80	86.70	7.80	50.40	7.40	2910.16
Gnarly Root	13-Jul	7.28	21.30	931.30	13.26	82.80	13.26	50.10	10.40	6908.99
Gnarly Root	13-Aug	7.65	20.45	658.00	5.24	84.10	5.24	49.60	8.80	2288.27
Gnarly Root	13-Sep	7.16	20.40	930.90	20.62	76.30	20.62	51.60	11.40	12129.51
Gnarly Root	13-Oct	7.14	20.10	933.70	18.65	72.40	18.65	50.30	11.10	10412.85
Gnarly Root	13-Nov	7.17	19.10	924.40	12.58	67.40	12.58	50.30	10.10	6391.02
Gnarly Root	13-Dec	5.34	17.30	579.40	25.57	65.80	25.57	52.40	11.80	15810.44
Gnarly Root Average	N/A	7.22	19.14	720.61	13.62	75.98	13.62	47.41	9.39	5463.21
Nolan Creek	12-Dec	6.95	19.60	725.70	8.95	87.90	8.95	20.20	2.40	433.94
Nolan Creek	13-Jan	7.20	18.00	699.20	6.35	82.60	6.35	19.80	2.30	289.18
Nolan Creek	13-Feb	7.05	18.00	702.60	20.00	87.40	20.00	22.10	2.40	1060.80
Nolan Creek	13-Mar	6.73	18.00	1008.00	9.86	84.10	9.86	19.60	2.10	405.84
Nolan Creek	13-Apr	7.19	18.38	771.00	9.36	79.00	9.36	21.10	2.20	434.37
Nolan Creek	13-May	7.12	18.53	657.00	17.40	71.00	17.40	20.60	2.50	896.31
Nolan Creek	13-Jun	7.13	19.30	484.00	9.97	71.40	9.97	19.40	2.10	406.05
Nolan Creek	13-Jul	6.81	19.70	1038.40	3.46	76.60	3.46	19.80	1.90	130.17

Table 26: Physicochemical attributes continued

Spring Name	Sample Date	pH	C°	µS/cm	cm/sec	DO %	cm/sec	cm wide	cm deep	Discharge cm3/sec
Nolan Creek	13-Aug	7.17	20.61	606.90	16.52	66.50	16.52	20.40	2.40	808.83
Nolan Creek	13-Sep	6.66	20.80	991.80	9.79	66.10	9.79	20.10	2.20	432.91
Nolan Creek	13-Oct	6.77	20.60	746.15	14.65	66.80	14.65	19.90	2.30	670.53
Nolan Creek	13-Nov	6.79	20.20	498.70	18.60	67.50	18.60	19.80	2.30	847.04
Nolan Creek	13-Dec	5.19	19.00	651.10	22.65	65.10	22.65	20.10	2.20	1001.58
Nolan Creek Average	N/A	6.83	19.29	736.97	12.89	74.77	12.89	20.22	2.25	601.35
East Range Road	13-Mar	7.11	18.60	749.50	2.76	76.80	2.76	7.60	1.90	39.85
East Range Road	13-Apr	7.24	18.82	686.20	3.08	55.30	3.08	7.60	2.10	49.13
East Range Road	13-May	7.15	18.72	625.40	0.46	47.00	0.46	7.60	1.20	4.17
East Range Road	13-Jun	7.26	19.76	630.50	0.64	48.10	0.64	7.80	1.50	7.49
East Range Road	13-Jul	6.70	22.50	989.10	1.91	85.40	1.91	7.60	1.90	27.58
East Range Road	13-Aug	7.27	20.65	680.70	0.49	54.10	0.49	7.50	1.70	6.22
East Range Road	13-Sep	7.10	22.80	847.20	3.28	84.10	3.28	7.40	1.80	43.69
East Range Road	13-Oct	7.10	21.40	786.90	1.58	67.90	1.58	7.60	1.70	20.41
East Range Road	13-Nov	7.27	22.10	531.20	2.17	91.70	2.17	7.50	1.90	30.92
East Range Road	13-Dec	5.93	19.30	527.40	3.34	79.90	3.34	7.50	1.90	47.60
East Range Road Average	N/A	7.01	20.47	705.41	1.97	69.03	1.97	7.57	1.76	27.71

8.1.2 Soluble Elements Data Tables

Table 27: Major soluble element analysis (mg/L)

Spring Name	Sample Date	Ca	K	Mg	Na	P	S
Bear	12-Dec	124.500	0.904	8.004	5.968	0.018	4.119
Bear	13-Jan	121.000	0.755	8.381	5.920	0.018	3.590
Bear	13-Feb	117.700	0.535	7.861	5.475	0.018	2.753
Bear	13-Mar	67.700	0.616	8.328	6.018	0.018	3.448
Bear	13-Apr	125.900	0.487	8.628	6.025	0.018	3.314
Bear	13-May	124.900	0.445	8.529	5.926	0.018	3.434
Bear	13-Jun	103.700	0.550	10.470	9.200	0.018	4.180
Bear	13-Jul	128.700	0.382	10.670	7.264	0.018	4.334
Bear	13-Aug	123.200	0.397	8.897	6.121	0.018	3.775
Bear	13-Sep	113.700	0.683	19.940	10.080	0.018	5.852
Bear	13-Oct	113.520	0.850	11.630	0.009	0.018	3.290
Bear	13-Nov	47.400	0.840	11.650	0.009	0.018	2.770
Bear	13-Dec	113.900	0.870	11.610	0.009	0.018	3.710
Bear Average	N/A	109.679	0.640	10.354	5.233	0.018	3.736
Crayfish	12-Dec	115.900	6.810	24.150	12.080	0.018	8.282
Crayfish	13-Jan	109.500	1.080	24.280	11.060	0.018	7.793
Crayfish	13-Feb	110.600	1.288	23.250	10.200	0.018	6.354
Crayfish	13-Mar	63.540	1.401	26.620	12.540	0.018	9.237
Crayfish	13-May	118.500	0.906	25.110	11.450	0.018	7.732
Crayfish	13-Jun	106.400	0.940	29.890	14.890	0.018	9.780
Crayfish	13-Jul	125.700	0.802	30.520	13.790	0.042	10.030

Table 27: Major soluble element analysis (mg/L) continued

Spring Name	Sample Date	Ca	K	Mg	Na	P	S
Crayfish	13-Aug	127.600	0.742	25.600	11.940	0.018	8.357
Crayfish	13-Sep	123.600	0.700	26.660	12.270	0.018	9.599
Crayfish	13-Oct	105.500	0.980	23.840	10.460	0.018	7.770
Crayfish	13-Nov	113.850	8.170	27.070	0.820	0.018	7.180
Crayfish	13-Dec	106.400	7.470	32.450	0.790	0.018	5.040
Crayfish Average	N/A	110.591	2.607	26.620	10.191	0.020	8.096
Geocache	12-Dec	99.440	3.917	31.230	14.260	0.018	5.796
Geocache	13-Jan	97.340	1.085	32.430	13.900	0.018	5.419
Geocache	13-Feb	94.120	1.032	31.350	13.590	0.039	4.451
Geocache	13-Mar	42.130	1.291	37.620	16.810	0.018	6.368
Geocache	13-Jul	108.700	0.987	39.050	17.770	0.018	6.837
Geocache	13-Sep	102.900	0.846	34.980	16.570	0.018	6.635
Geocache	13-Oct	96.730	0.800	32.880	15.580	0.018	6.240
Geocache	13-Nov	42.040	8.550	19.790	5.410	0.018	2.130
Geocache	13-Dec	103.130	7.840	38.520	6.410	0.018	5.380
Geocache Average	N/A	87.392	2.928	33.094	13.367	0.020	5.473
Gnarly Root	12-Dec	107.800	2.109	14.170	5.904	0.018	3.150
Gnarly Root	13-Jan	105.600	0.498	14.650	6.221	0.018	3.014
Gnarly Root	13-Feb	100.400	0.535	13.590	5.596	0.018	2.255
Gnarly Root	13-Mar	58.510	0.964	15.120	8.001	0.018	3.894
Gnarly Root	13-Apr	110.200	0.498	15.460	6.097	0.066	2.652
Gnarly Root	13-May	109.000	0.443	15.350	6.108	0.055	2.720
Gnarly Root	13-Jun	111.700	0.570	17.640	11.170	0.018	3.710
Gnarly Root	13-Jul	113.900	0.525	18.270	7.102	0.038	3.389

Table 27: Major soluble element analysis (mg/L) continued

Spring Name	Sample Date	Ca	K	Mg	Na	P	S
Gnarly Root	13-Aug	107.000	0.436	15.550	6.237	0.043	3.283
Gnarly Root	13-Sep	107.400	0.770	16.060	7.013	0.074	3.809
Gnarly Root	13-Oct	105.600	0.500	14.650	6.240	0.018	3.010
Gnarly Root	13-Nov	42.040	8.550	19.790	5.410	0.018	2.130
Gnarly Root	13-Dec	98.320	8.460	18.780	5.040	0.018	3.020
Gnarly Root Average	N/A	98.267	1.912	16.083	6.626	0.032	3.080
Nolan Creek	12-Dec	94.870	6.121	27.290	12.080	0.018	5.252
Nolan Creek	13-Jan	92.030	1.284	27.010	10.820	0.018	4.808
Nolan Creek	13-Feb	93.460	1.107	28.680	11.250	0.018	4.091
Nolan Creek	13-Mar	50.230	1.249	32.000	14.040	0.018	5.706
Nolan Creek	13-Apr	97.110	1.111	30.370	12.210	0.018	4.917
Nolan Creek	13-May	100.800	1.195	27.200	11.920	0.018	5.149
Nolan Creek	13-Jun	90.310	1.590	28.830	12.740	0.018	5.650
Nolan Creek	13-Jul	109.100	1.288	33.640	13.440	0.018	6.050
Nolan Creek	13-Aug	100.600	1.327	28.090	11.100	0.018	4.926
Nolan Creek	13-Sep	95.670	1.146	29.440	11.510	0.018	5.701
Nolan Creek	13-Oct	98.710	0.840	35.280	12.050	0.018	5.790
Nolan Creek	13-Nov	59.080	5.890	24.320	3.070	0.018	3.700
Nolan Creek	13-Dec	106.440	7.470	32.450	0.790	0.018	5.040
Nolan Creek Average	N/A	91.416	2.432	29.585	10.540	0.018	5.137
East Range Road	13-Mar	62.480	0.492	2.771	9.906	0.018	3.314
East Range Road	13-Apr	120.700	0.565	7.851	5.808	0.060	3.622
East Range Road	13-May	122.200	0.453	7.983	5.641	0.018	3.753
East Range Road	13-Jun	100.400	0.560	9.400	8.670	0.018	4.430

Table 27: Major soluble element analysis (mg/L) continued

Spring Name	Sample Date	Ca	K	Mg	Na	P	S
East Range Road	13-Jul	134.100	0.396	2.810	9.980	0.018	4.047
East Range Road	13-Aug	118.300	0.439	8.364	5.773	0.018	4.082
East Range Road	13-Sep	129.400	0.320	2.098	8.530	0.018	4.080
East Range Road	13-Oct	100.400	0.560	9.400	8.670	0.018	4.430
East Range Road	13-Nov	59.280	8.880	2.860	1.860	0.018	2.890
East Range Road	13-Dec	80.020	8.480	2.620	2.940	0.018	3.010
East Range Road Average	N/A	102.728	2.115	5.616	6.778	0.022	3.766

Table 28: Soluble anion analysis of sampled springs (mg/L)

Spring Name	Sample Date	F ⁻	Cl ⁻	NO ₃ ⁻	PO ₄ ³⁻	SO ₄ ²⁻	HCO ₃ ⁻
Bear	12-Dec	0.291	10.717	3.563	6.059	N/A	294.840
Bear	13-Jan	0.221	10.350	3.808	5.899	N/A	250.990
Bear	13-Feb	0.122	7.778	5.539	1.076	14.795	241.920
Bear	13-Mar	0.220	11.348	3.965	7.860	N/A	294.840
Bear	13-Apr	0.401	8.394	4.371	N/A	5.263	317.520
Bear	13-May	0.396	8.604	3.702	N/A	4.989	285.770
Bear	13-Jun	1.161	14.541	8.114	N/A	6.931	267.620
Bear	13-Jul	0.603	9.743	3.744	N/A	5.800	176.900
Bear	13-Aug	0.273	8.678	3.453	N/A	5.087	258.550
Bear	13-Sep	0.374	13.236	4.201	N/A	N/A	225.290
Bear	13-Oct	0.410	10.340	4.450	N/A	5.450	285.770

Table 28: Soluble anion analysis of sampled springs (mg/L) continued

Spring Name	Sample Date	F ⁻	Cl ⁻	NO ₃ ⁻	PO ₄ ³⁻	SO ₄ ²⁻	HCO ₃ ⁻
Bear	13-Nov	0.150	8.580	3.820	N/A	5.020	214.700
Bear	13-Dec	0.260	9.220	4.020	N/A	5.030	189.000
Bear Average	N/A	0.376	10.118	4.365	5.223	6.485	254.130
Crayfish	12-Dec	0.607	19.990	3.505	11.170	N/A	264.600
Crayfish	13-Jan	0.607	15.338	10.625	16.080	N/A	257.040
Crayfish	13-Feb	0.334	12.121	9.554	2.091	39.392	297.860
Crayfish	13-Mar	0.730	16.028	11.083	18.297	N/A	182.950
Crayfish	13-May	0.707	14.235	7.982	N/A	15.091	260.060
Crayfish	13-Jun	1.171	20.087	9.046	N/A	17.873	273.670
Crayfish	13-Jul	0.660	15.879	8.580	N/A	17.048	219.240
Crayfish	13-Aug	0.569	15.591	7.718	N/A	17.208	223.780
Crayfish	13-Sep	0.532	15.795	7.496	N/A	N/A	319.030
Crayfish	13-Oct	0.710	14.240	7.980	N/A	15.090	317.520
Crayfish	13-Nov	0.380	12.550	8.050	N/A	14.700	246.460
Crayfish	13-Dec	0.480	14.500	3.240	N/A	8.140	250.990
Crayfish Average	N/A	0.624	15.530	7.905	11.909	18.068	259.430
Geocache	12-Dec	0.624	9.191	7.172	4.215	N/A	261.580
Geocache	13-Jan	0.668	18.637	3.574	10.492	N/A	294.840
Geocache	13-Feb	0.252	15.638	2.779	1.445	26.151	326.590
Geocache	13-Mar	0.645	23.748	3.413	14.969	N/A	317.520
Geocache	13-Jul	1.223	21.910	1.857	N/A	10.636	322.060
Geocache	13-Sep	0.431	20.856	0.723	N/A	N/A	261.580
Geocache	13-Oct	0.400	14.440	2.870	N/A	7.580	263.090
Geocache	13-Nov	0.360	8.020	5.010	N/A	3.690	252.500

Table 28: Soluble anion analysis of sampled springs (mg/L) continued

Spring Name	Sample Date	F ⁻	Cl ⁻	NO ₃ ⁻	PO ₄ ³⁻	SO ₄ ²⁻	HCO ₃ ⁻
Geocache	13-Dec	0.420	19.530	1.920	N/A	9.720	266.110
Geocache Average	N/A	0.558	16.886	3.258	7.780	11.555	285.100
Gnarly Root	12-Dec	0.284	10.844	3.594	5.912	N/A	269.140
Gnarly Root	13-Jan	0.335	9.602	7.140	5.071	N/A	276.700
Gnarly Root	13-Feb	0.199	7.182	5.931	0.617	10.960	267.620
Gnarly Root	13-Mar	0.900	12.720	7.658	8.896	0.167	297.860
Gnarly Root	13-Apr	0.673	8.371	6.749	1.219	4.022	284.260
Gnarly Root	13-May	0.637	8.042	5.337	N/A	3.743	276.700
Gnarly Root	13-Jun	1.048	17.440	6.249	N/A	5.073	244.940
Gnarly Root	13-Jul	1.170	9.944	5.697	N/A	4.035	189.000
Gnarly Root	13-Aug	0.581	8.348	4.950	N/A	3.624	266.110
Gnarly Root	13-Sep	0.584	8.664	4.279	N/A	N/A	341.710
Gnarly Root	13-Oct	0.650	10.420	5.700	N/A	5.050	264.600
Gnarly Root	13-Nov	0.360	8.020	5.010	N/A	3.690	261.580
Gnarly Root	13-Dec	0.500	9.860	5.140	N/A	3.960	204.120
Gnarly Root Average	N/A	0.609	9.958	5.649	4.343	4.432	264.950
Nolan Creek	12-Dec	0.551	17.113	5.123	10.126	N/A	243.430
Nolan Creek	13-Jan	0.358	13.932	3.840	8.573	N/A	281.230
Nolan Creek	13-Feb	0.260	13.106	3.944	1.110	23.127	284.260
Nolan Creek	13-Mar	0.660	20.812	5.188	13.538	N/A	309.960
Nolan Creek	13-Apr	0.812	16.776	5.440	N/A	9.668	297.860
Nolan Creek	13-May	0.567	15.406	3.135	N/A	9.384	232.850
Nolan Creek	13-Jun	0.417	14.901	3.772	N/A	8.942	254.020
Nolan Creek	13-Jul	0.992	16.387	3.575	N/A	9.676	284.260

Table 28: Soluble anion analysis of sampled springs (mg/L) continued

Spring Name	Sample Date	F ⁻	Cl ⁻	NO ₃ ⁻	PO ₄ ³⁻	SO ₄ ²⁻	HCO ₃ ⁻
Nolan Creek	13-Aug	0.399	14.306	3.241	0.065	8.724	278.210
Nolan Creek	13-Sep	0.410	14.910	2.652	0.069	0.000	222.260
Nolan Creek	13-Oct	0.420	14.900	3.770	N/A	8.940	309.960
Nolan Creek	13-Nov	0.250	9.180	2.900	N/A	6.480	231.340
Nolan Creek	13-Dec	0.480	14.500	3.240	N/A	8.140	247.970
Nolan Creek Average	N/A	0.506	15.094	3.832	5.580	9.308	267.510
East Range Road	13-Mar	0.219	18.687	8.125	8.040	0.172	216.220
East Range Road	13-Apr	0.219	18.687	8.125	8.040	0.172	232.850
East Range Road	13-May	0.425	8.170	1.606	N/A	5.990	254.020
East Range Road	13-Jun	0.377	8.556	1.515	N/A	5.896	246.460
East Range Road	13-Jul	0.620	11.479	1.744	N/A	6.460	328.100
East Range Road	13-Aug	0.159	16.431	5.179	N/A	4.888	210.170
East Range Road	13-Sep	0.305	8.221	1.572	N/A	5.857	237.380
East Range Road	13-Oct	0.179	14.277	3.377	N/A	N/A	275.180
East Range Road	13-Nov	0.220	18.690	8.120	0.170	8.040	264.600
East Range Road	13-Dec	0.160	14.070	4.290	N/A	4.920	163.300
East Range Road Average	N/A	0.288	13.727	4.365	5.416	4.711	242.830

Table 29: Trace metal soluble element analysis (mg/L)

Spring Name	Sample Date	Al	As	B	Cu	Fe	Mn	Pb	Zn
Bear	Dec-12	0.0060	0.0242	0.0348	0.0033	0.0012	0.0041	0.0218	0.0064
Bear	Jan-13	0.0060	0.0242	0.0355	0.0033	0.0012	0.0038	0.0218	0.0034
Bear	Feb-13	0.0206	0.0242	0.0291	0.0033	0.0224	0.0005	0.0218	0.0013
Bear	Mar-13	0.0060	0.0242	0.0424	0.0033	0.0012	0.0011	0.0218	0.0003
Bear	Apr-13	0.0060	0.0242	0.0328	0.0033	0.0012	0.0025	0.0218	0.0053
Bear	May-13	0.0060	0.0242	0.0346	0.0688	0.0012	0.0005	0.0218	0.0077
Bear	Jun-13	0.0060	0.0242	0.0024	0.0033	0.0012	0.0005	0.0218	0.0003
Bear	Jul-13	0.0060	0.0242	0.0404	0.0033	0.0012	0.0011	0.0218	0.0006
Bear	Aug-13	0.0060	0.0242	0.0288	0.0033	0.0012	0.0017	0.0218	0.0103
Bear	Sep-13	0.0060	0.0242	0.0400	0.0033	0.0012	0.0030	0.0218	0.0054
Bear	Oct-13	0.0060	0.0242	0.0024	0.0033	0.0012	0.0005	0.0218	0.0003
Bear	Nov-13	0.0060	0.0242	0.0024	0.0033	0.0012	0.0005	0.0218	0.0003
Bear	Dec-13	0.0060	0.0242	0.0024	0.0033	0.0012	0.0005	0.0218	0.0003
Bear Average	N/A	0.0071	0.0242	0.0252	0.0083	0.0028	0.0015	0.0218	0.0032
Crayfish	Dec-12	0.0060	0.0242	0.0521	0.0033	0.0012	0.0018	0.0218	0.0092
Crayfish	Jan-13	0.0060	0.0242	0.0569	0.0033	0.0012	0.0010	0.0218	0.0045
Crayfish	Feb-13	0.5911	0.0242	0.0536	0.0033	0.2413	0.0058	0.0218	0.0030
Crayfish	Mar-13	0.0433	0.0242	0.0769	0.0033	0.0012	0.0005	0.0218	0.0003
Crayfish	May-13	0.0158	0.0242	0.0587	0.0611	0.0012	0.0025	0.0218	0.0186
Crayfish	Jun-13	0.0060	0.0242	0.0024	0.0033	0.0100	0.0005	0.0218	0.0003
Crayfish	Jul-13	0.0060	0.0242	0.0643	0.0033	0.0012	0.0077	0.0218	0.0031
Crayfish	Aug-13	0.0060	0.0242	0.0525	0.0033	0.0012	0.0297	0.0218	0.0170
Crayfish	Sep-13	0.0060	0.0242	0.0542	0.0033	0.0012	0.0026	0.0218	0.0036
Crayfish	Oct-13	0.0060	0.0242	0.0024	0.0033	0.7000	0.0005	0.0218	0.0003
Crayfish	Nov-13	0.0060	0.0242	0.0024	0.0033	0.0500	0.0005	0.0218	0.0003
Crayfish	Dec-13	0.0060	0.0242	0.0024	0.0033	0.0500	0.0005	0.0218	0.0003
Crayfish Average	N/A	0.0587	0.0242	0.0399	0.0081	0.0883	0.0044	0.0218	0.0050

Table 29: Trace metal soluble element analysis (mg/L) continued

Spring Name	Sample Date	Al	As	B	Cu	Fe	Mn	Pb	Zn
Geocache	Dec-12	0.0120	0.0242	0.0288	0.0033	0.0012	0.0027	0.0218	0.0140
Geocache	Jan-13	0.0060	0.0242	0.0313	0.0033	0.0012	0.0022	0.0218	0.0053
Geocache	Feb-13	0.1387	0.0242	0.0413	0.0033	0.1335	0.0013	0.0218	0.0012
Geocache	Mar-13	0.0310	0.0242	0.0464	0.0033	0.0012	0.0142	0.0218	0.0003
Geocache	Jul-13	0.0060	0.0242	0.0476	0.0033	0.0012	0.0018	0.0218	0.0016
Geocache	Sep-13	0.0060	0.0242	0.0300	0.0033	0.0012	0.0005	0.0218	0.0026
Geocache	Oct-13	0.0060	0.0242	0.0024	0.0033	0.0200	0.0005	0.0218	0.0003
Geocache	Nov-13	0.0060	0.0242	0.0024	0.0033	0.0500	0.0005	0.0218	0.0003
Geocache	Dec-13	0.0060	0.0242	0.0024	0.0033	0.0500	0.0005	0.0218	0.0003
Geocache Average	N/A	0.0242	0.0242	0.0258	0.0033	0.0288	0.0027	0.0218	0.0029
Gnarly Root	Dec-12	0.0060	0.0242	0.0400	0.0033	0.0012	0.0027	0.0218	0.0115
Gnarly Root	Jan-13	0.0060	0.0242	0.0329	0.0033	0.0012	0.0009	0.0218	0.0036
Gnarly Root	Feb-13	0.0819	0.0242	0.0316	0.0033	0.0592	0.0022	0.0218	0.0014
Gnarly Root	Mar-13	0.0060	0.0242	0.0441	0.0033	0.0012	0.0019	0.0218	0.0003
Gnarly Root	Apr-13	0.0060	0.0242	0.0412	0.0033	0.0012	0.0027	0.0218	0.0013
Gnarly Root	May-13	0.0173	0.0242	0.0349	0.4014	0.0012	0.0013	0.0218	0.0289
Gnarly Root	Jun-13	0.0060	0.0242	0.0024	0.0100	0.0100	0.0005	0.0218	0.0200
Gnarly Root	Jul-13	0.0060	0.0242	0.0504	0.0033	0.0012	0.0039	0.0218	0.0003
Gnarly Root	Aug-13	0.0121	0.0242	0.0367	0.0033	0.0012	0.0020	0.0218	0.0074
Gnarly Root	Sep-13	0.0060	0.0242	0.0401	0.0033	0.0012	0.0168	0.0218	0.0085
Gnarly Root	Oct-13	0.0060	0.0242	0.0024	0.0033	0.0012	0.0005	0.0218	0.0003
Gnarly Root	Nov-13	0.0060	0.0242	0.0024	0.0033	0.0500	0.0005	0.0218	0.0003
Gnarly Root	Dec-13	0.0060	0.0242	0.0024	0.0033	0.0500	0.0005	0.0218	0.0003
Gnarly Root Average	N/A	0.0132	0.0242	0.0278	0.0344	0.0138	0.0028	0.0218	0.0065
Nolan Creek	Dec-12	0.0060	0.0242	0.0313	0.0033	0.0012	0.0031	0.0218	0.0219
Nolan Creek	Jan-13	0.0161	0.0242	0.0338	0.0033	0.0012	0.0014	0.0218	0.0084
Nolan Creek	Feb-13	0.0418	0.0242	0.0373	0.0033	0.0433	0.0005	0.0218	0.0009

Table 29: Trace metal soluble element analysis (mg/L) continued

Spring Name	Sample Date	Al	As	B	Cu	Fe	Mn	Pb	Zn
Nolan Creek	Mar-13	0.0060	0.0242	0.0392	0.0033	0.0012	0.0036	0.0218	0.0003
Nolan Creek	Apr-13	0.0060	0.0242	0.0324	0.0033	0.0012	0.0026	0.0218	0.0183
Nolan Creek	May-13	0.0060	0.0242	0.0385	0.0354	0.0012	0.0038	0.0218	0.0154
Nolan Creek	Jun-13	0.0060	0.0242	0.0024	0.0033	0.0100	0.0005	0.0218	0.0003
Nolan Creek	Jul-13	0.0706	0.0242	0.0381	0.0033	0.0012	0.0028	0.0218	0.0022
Nolan Creek	Aug-13	0.0060	0.0242	0.0360	0.0033	0.0012	0.0025	0.0218	0.0130
Nolan Creek	Sep-13	0.0060	0.0242	0.0322	0.0033	0.0012	0.0012	0.0218	0.0024
Nolan Creek	Oct-13	0.0060	0.0242	0.0024	0.0033	0.0012	0.0005	0.0218	0.0003
Nolan Creek	Nov-13	0.0060	0.0242	0.0024	0.0033	0.0500	0.0005	0.0218	0.0003
Nolan Creek	Dec-13	0.0060	0.0242	0.0024	0.0033	0.0500	0.0005	0.0218	0.0003
Nolan Creek Average	N/A	0.0145	0.0242	0.0253	0.0058	0.0126	0.0018	0.0218	0.0065
East Range Road	Mar-13	0.0215	0.0242	0.0656	0.0033	0.0012	0.0021	0.0218	0.0030
East Range Road	Apr-13	0.0060	0.0242	0.0369	0.0033	0.0012	0.0039	0.0218	0.0091
East Range Road	May-13	0.0060	0.0242	0.0358	0.1618	0.0012	0.0046	0.0218	0.0250
East Range Road	Jun-13	0.0060	0.0242	0.0024	0.0100	0.0100	0.0005	0.0218	0.0003
East Range Road	Jul-13	0.0060	0.0242	0.0435	0.0033	0.0012	0.0014	0.0218	0.0003
East Range Road	Aug-13	0.0060	0.0242	0.0344	0.0033	0.0012	0.0175	0.0218	0.0160
East Range Road	Sep-13	0.0060	0.0242	0.0344	0.0033	0.0012	0.0012	0.0218	0.0052
East Range Road	Oct-13	0.0060	0.0242	0.0024	0.0100	0.0100	0.0005	0.0218	0.0100
East Range Road	Nov-13	0.0060	0.0242	0.0024	0.0033	0.0500	0.0005	0.0218	0.0003
East Range Road	Dec-13	0.0060	0.0242	0.0024	0.0033	0.0500	0.0005	0.0218	0.0003
East Range Road Average	N/A	0.0076	0.0242	0.0260	0.0205	0.0127	0.0033	0.0218	0.0070

8.1.3 Total Element Data Tables

Table 30: Total major element analysis (mg/L)

Spring Name	Sample Date	Ca	K	Mg	Na	P	S
Bear	12-Dec	138.80	0.44	9.19	6.45	0.02	3.30
Bear	13-Jan	124.30	0.51	8.26	5.75	0.05	2.99
Bear	13-Feb	119.60	0.49	8.20	5.72	0.02	3.47
Bear	13-Mar	125.60	0.56	8.00	5.90	0.02	2.98
Bear	13-Apr	128.40	0.35	8.67	6.01	0.02	3.01
Bear	13-May	132.20	0.43	8.94	6.25	0.02	3.06
Bear	13-Jun	141.10	0.36	10.03	6.84	0.02	3.48
Bear	13-Jul	191.20	0.49	13.56	9.77	0.02	4.43
Bear	13-Aug	125.50	0.38	8.87	6.23	0.02	3.24
Bear	13-Sep	120.20	0.56	20.43	9.94	0.02	4.58
Bear	13-Oct	133.79	0.51	7.54	6.86	0.02	3.38
Bear	13-Nov	142.60	0.43	2.14	6.84	0.02	3.39
Bear	13-Dec	136.42	0.51	2.10	7.02	0.02	3.45
Bear Average	N/A	135.36	0.46	8.92	6.89	0.02	3.44
Crayfish	12-Dec	127.60	1.01	29.41	12.83	0.02	7.52
Crayfish	13-Jan	121.00	1.17	26.31	11.74	0.02	7.11
Crayfish	13-Feb	106.50	0.98	23.84	10.46	0.02	7.77
Crayfish	13-Mar	124.40	1.22	22.66	10.44	0.08	6.82
Crayfish	13-May	142.40	1.08	29.51	13.17	0.02	7.94
Crayfish	13-Jun	135.40	0.71	28.49	12.67	0.02	7.94
Crayfish	13-Jul	239.50	1.28	45.70	20.67	0.06	12.07

Table 30: Total major element analysis (mg/L) continued

Spring Name	Sample Date	Ca	K	Mg	Na	P	S
Crayfish	13-Aug	133.20	0.85	25.50	11.96	0.02	7.48
Crayfish	13-Sep	140.90	0.66	27.34	12.16	0.02	7.83
Crayfish	13-Oct	127.60	1.01	29.41	12.83	0.02	7.52
Crayfish	13-Nov	117.89	0.17	23.72	11.06	0.02	4.73
Crayfish	13-Dec	162.64	0.61	31.84	15.35	0.02	6.60
Crayfish Average	N/A	139.92	0.90	28.64	12.95	0.03	7.61
Geocache	12-Dec	111.60	1.08	37.82	16.24	0.02	5.20
Geocache	13-Jan	110.40	1.24	36.26	15.49	0.02	5.11
Geocache	13-Feb	93.97	1.06	31.66	13.75	0.05	5.92
Geocache	13-Mar	109.00	1.23	35.81	16.11	0.02	5.08
Geocache	13-Jul	158.40	1.35	51.80	23.79	0.02	7.14
Geocache	13-Sep	107.80	0.84	36.59	17.27	0.02	5.30
Geocache	13-Oct	93.35	0.73	31.83	15.02	0.02	4.61
Geocache	13-Nov	110.40	1.24	36.26	15.49	0.02	5.11
Geocache	13-Dec	155.00	1.35	51.80	23.79	0.02	7.14
Geocache Average	N/A	116.66	1.12	38.87	17.44	0.02	5.62
Gnarly Root	12-Dec	114.40	0.38	15.42	5.95	0.02	2.32
Gnarly Root	13-Jan	114.40	0.52	15.18	6.38	0.02	2.57
Gnarly Root	13-Feb	101.00	0.48	14.07	5.78	0.02	2.82
Gnarly Root	13-Mar	113.00	0.61	13.80	6.83	0.02	3.17
Gnarly Root	13-Apr	113.20	0.23	15.70	6.07	0.02	2.36
Gnarly Root	13-May	121.10	0.36	16.64	6.45	0.05	2.48
Gnarly Root	13-Jun	118.10	0.25	16.56	6.27	0.02	2.46
Gnarly Root	13-Jul	192.30	0.55	25.62	10.19	0.02	3.74

Table 30: Total major element analysis (mg/L) continued

Spring Name	Sample Date	Ca	K	Mg	Na	P	S
Gnarly Root	13-Aug	115.40	0.87	15.97	6.49	0.02	2.68
Gnarly Root	13-Sep	113.10	0.32	15.94	6.03	0.05	2.59
Gnarly Root	13-Oct	188.70	0.55	25.62	10.19	0.02	3.74
Gnarly Root	13-Nov	104.17	0.77	16.15	5.83	0.02	2.32
Gnarly Root	13-Dec	124.40	2.67	19.07	8.37	0.02	2.91
Gnarly Root Average	N/A	125.64	0.66	17.36	6.99	0.02	2.78
Nolan Creek	12-Dec	118.00	1.13	36.02	14.19	0.02	5.07
Nolan Creek	13-Jan	102.90	1.38	29.83	11.81	0.02	4.38
Nolan Creek	13-Feb	91.13	1.03	28.47	11.09	0.02	5.21
Nolan Creek	13-Mar	100.30	1.16	29.92	12.92	0.02	4.43
Nolan Creek	13-Apr	116.50	1.09	33.69	13.35	0.02	4.83
Nolan Creek	13-May	105.90	1.24	28.63	12.54	0.02	4.68
Nolan Creek	13-Jun	114.60	1.55	30.14	11.99	0.02	4.76
Nolan Creek	13-Jul	149.10	1.61	44.34	17.67	0.02	6.18
Nolan Creek	13-Aug	106.80	1.53	27.64	10.93	0.02	4.37
Nolan Creek	13-Sep	96.51	1.05	28.97	11.07	0.02	4.33
Nolan Creek	13-Oct	100.26	1.14	38.98	15.44	0.02	4.08
Nolan Creek	13-Nov	93.74	1.85	28.53	10.96	0.02	3.19
Nolan Creek	13-Dec	88.85	0.16	31.77	13.19	0.02	3.29
Nolan Creek Average	N/A	106.51	1.23	32.07	12.86	0.02	4.52
East Range Road	13-Mar	124.10	0.43	1.99	8.66	0.02	2.86
East Range Road	13-Apr	124.30	0.24	7.96	5.75	0.02	3.34
East Range Road	13-May	134.50	0.51	8.64	6.16	0.02	3.61
East Range Road	13-Jun	127.00	0.30	8.88	6.29	0.02	3.54

Table 30: Total major element analysis (mg/L) continued

Spring Name	Sample Date	Ca	K	Mg	Na	P	S
East Range Road	13-Jul	326.00	0.53	4.78	14.44	0.08	5.49
East Range Road	13-Aug	125.80	0.60	8.26	5.98	0.02	3.59
East Range Road	13-Sep	136.30	0.24	2.10	8.45	0.02	3.19
East Range Road	13-Oct	126.30	0.30	8.88	6.29	0.02	3.54
East Range Road	13-Nov	149.62	0.28	2.63	14.93	0.02	13.46
East Range Road	13-Dec	174.34	0.26	2.79	10.95	0.02	3.51
East Range Road Average	N/A	154.83	0.37	5.69	8.79	0.02	4.61

Table 31: Total trace element analysis (µg/L)

Spring Name	Sample Date	Al	As	B	Cu	Fe	Mn	Pb	Zn
Bear	12-Dec	79.50	18.00	43.20	2.85	96.50	0.45	12.30	2.60
Bear	13-Jan	67.30	18.00	40.00	2.85	74.80	0.45	12.30	34.30
Bear	13-Feb	10.50	18.00	29.10	2.85	11.10	0.45	12.30	0.45
Bear	13-Mar	110.20	18.00	47.80	2.85	11.10	1.60	12.30	29.90
Bear	13-Apr	70.10	18.00	31.60	2.85	47.20	1.40	12.30	10.60
Bear	13-May	10.50	18.00	35.30	2.85	11.10	0.45	12.30	1.40
Bear	13-Jun	10.50	18.00	38.10	2.85	11.10	0.45	12.30	0.45
Bear	13-Jul	104.30	18.00	68.90	2.85	54.90	1.70	12.30	3.00
Bear	13-Aug	70.00	18.00	42.00	2.85	27.90	0.45	12.30	1.40
Bear	13-Sep	127.90	18.00	47.80	2.85	93.60	2.90	12.30	1.00
Bear	13-Oct	10.50	18.00	4.05	2.85	50.00	0.45	12.30	10.00
Bear	13-Nov	10.50	18.00	4.05	2.85	11.10	0.45	12.30	10.00

Table 31: Total trace element analysis (µg/L) continued

Spring Name	Sample Date	Al	As	B	Cu	Fe	Mn	Pb	Zn
Bear	13-Dec	10.50	18.00	4.05	2.85	30.00	0.45	12.30	10.00
Bear Average	N/A	53.25	18.00	33.53	2.85	40.80	0.90	12.30	8.85
Crayfish	12-Dec	118.50	18.00	63.30	2.85	66.50	1.60	12.30	1.90
Crayfish	13-Jan	209.80	18.00	60.00	2.85	97.50	2.00	12.30	35.30
Crayfish	13-Feb	10.50	18.00	51.90	2.85	11.10	0.90	12.30	1.10
Crayfish	13-Mar	294.10	18.00	75.60	6.90	151.90	1.70	12.30	25.40
Crayfish	13-May	863.90	18.00	65.10	2.85	388.20	9.20	12.30	2.20
Crayfish	13-Jun	105.50	18.00	63.60	2.85	49.40	1.30	12.30	0.45
Crayfish	13-Jul	1077.00	18.00	107.60	2.85	877.40	63.70	12.30	3.50
Crayfish	13-Aug	416.40	18.00	61.60	2.85	175.40	5.90	12.30	4.40
Crayfish	13-Sep	763.70	18.00	62.00	2.85	533.60	31.40	12.30	2.40
Crayfish	13-Oct	10.50	18.00	4.05	2.85	70.00	0.45	12.30	0.45
Crayfish	13-Nov	10.50	18.00	4.05	2.85	50.00	0.45	12.30	0.45
Crayfish	13-Dec	10.50	18.00	4.05	2.85	30.00	0.45	12.30	0.45
Crayfish Average	N/A	324.24	18.00	51.90	3.19	208.42	9.92	12.30	6.50
Geocache	12-Dec	61.90	18.00	36.50	2.85	52.40	0.90	12.30	2.60
Geocache	13-Jan	42.20	18.00	33.90	2.85	26.70	1.10	12.30	36.30
Geocache	13-Feb	10.50	18.00	40.80	2.85	11.10	1.30	12.30	0.45
Geocache	13-Mar	151.50	18.00	63.40	2.85	50.00	1.00	12.30	29.70
Geocache	13-Jul	84.50	18.00	72.50	11.50	56.90	1.90	12.30	8.40
Geocache	13-Sep	27.00	18.00	36.00	2.85	11.10	0.45	12.30	0.90
Geocache	13-Oct	10.50	18.00	4.05	2.85	11.10	0.45	12.30	0.45
Geocache	13-Nov	10.50	18.00	4.05	2.85	30.00	0.45	12.30	40.00
Geocache	13-Dec	10.50	18.00	4.05	10.00	60.00	0.45	12.30	10.00

Table 31: Total trace element analysis (µg/L) continued

Spring Name	Sample Date	Al	As	B	Cu	Fe	Mn	Pb	Zn
Geocache Average	N/A	45.46	18.00	32.81	4.61	34.37	0.89	12.30	14.31
Gnarly Root	12-Dec	138.10	18.00	34.60	2.85	98.30	4.00	12.30	2.30
Gnarly Root	13-Jan	98.30	18.00	32.70	2.85	69.10	2.40	12.30	34.00
Gnarly Root	13-Feb	10.50	18.00	30.20	2.85	11.10	2.00	12.30	1.80
Gnarly Root	13-Mar	101.50	18.00	41.60	2.85	11.10	0.45	12.30	20.30
Gnarly Root	13-Apr	10.50	18.00	35.20	2.85	11.10	1.00	12.30	8.90
Gnarly Root	13-May	128.20	18.00	44.40	2.85	113.30	2.30	12.30	1.60
Gnarly Root	13-Jun	177.20	18.00	45.50	2.85	202.40	6.70	12.30	1.40
Gnarly Root	13-Jul	383.10	18.00	60.60	2.85	336.30	12.80	12.30	4.20
Gnarly Root	13-Aug	188.50	18.00	52.40	2.85	109.60	3.00	12.30	5.60
Gnarly Root	13-Sep	177.30	18.00	49.60	2.85	170.30	4.50	12.30	1.90
Gnarly Root	13-Oct	10.50	18.00	4.05	10.00	340.00	10.00	12.30	0.45
Gnarly Root	13-Nov	10.50	18.00	4.05	10.00	30.00	0.45	12.30	10.00
Gnarly Root	13-Dec	10.50	18.00	4.05	2.85	11.10	0.45	12.30	0.45
Gnarly Root Average	N/A	111.13	18.00	33.77	3.95	116.44	3.85	12.30	7.15
Nolan Creek	12-Dec	225.40	18.00	40.60	2.85	131.70	2.60	12.30	2.20
Nolan Creek	13-Jan	80.90	18.00	39.80	2.85	45.40	1.00	12.30	36.40
Nolan Creek	13-Feb	10.50	18.00	39.60	2.85	11.10	6.80	12.30	0.45
Nolan Creek	13-Mar	216.10	18.00	58.30	2.85	26.70	1.20	12.30	15.10
Nolan Creek	13-Apr	427.60	18.00	37.20	2.85	231.20	4.70	12.30	11.20
Nolan Creek	13-May	86.90	18.00	33.30	2.85	51.60	2.50	12.30	2.10
Nolan Creek	13-Jun	58.80	18.00	38.60	2.85	34.70	1.30	12.30	1.60
Nolan Creek	13-Jul	151.00	18.00	60.70	2.85	83.20	3.00	12.30	1.90
Nolan Creek	13-Aug	411.60	18.00	50.10	2.85	200.00	5.30	12.30	1.90

Table 31: Total trace element analysis (µg/L) continued

Spring Name	Sample Date	Al	As	B	Cu	Fe	Mn	Pb	Zn
Nolan Creek	13-Sep	64.90	18.00	37.60	2.85	52.50	0.45	12.30	0.45
Nolan Creek	13-Oct	10.50	18.00	4.05	2.85	30.00	0.45	12.30	0.45
Nolan Creek	13-Nov	10.50	18.00	4.05	2.85	30.00	0.45	12.30	10.00
Nolan Creek	13-Dec	10.50	18.00	4.05	2.85	50.00	0.45	12.30	0.45
Nolan Creek Average	N/A	135.78	18.00	34.46	2.85	75.24	2.32	12.30	6.48
East Range Road	13-Mar	194.40	18.00	51.00	2.85	35.50	2.00	12.30	16.70
East Range Road	13-Apr	54.80	18.00	33.20	2.85	51.00	2.30	12.30	10.20
East Range Road	13-May	106.90	18.00	39.70	2.85	69.50	5.10	12.30	1.10
East Range Road	13-Jun	67.10	18.00	40.70	2.85	51.80	4.60	12.30	1.40
East Range Road	13-Jul	487.80	18.00	82.20	2.85	909.20	12.40	12.30	2.80
East Range Road	13-Aug	414.20	18.00	47.00	2.85	239.10	24.30	12.30	4.00
East Range Road	13-Sep	30.90	18.00	40.60	2.85	53.80	0.45	12.30	1.00
East Range Road	13-Oct	10.50	18.00	4.05	2.85	50.00	0.45	12.30	0.45
East Range Road	13-Nov	10.50	18.00	4.05	2.85	11.10	0.45	12.30	0.45
East Range Road	13-Dec	10.50	18.00	4.05	2.85	11.10	0.45	12.30	0.45
East Range Road Average	N/A	138.76	18.00	34.66	2.85	148.21	5.25	12.30	3.86

8.2 Statistics Data Tables

8.2.1 t-test Results

Table 32: Major element t-tests among springs

	Calcium		Potassium		Magnesium		Sodium		Sulphur	
	Soluble	Total	Soluble	Total	Soluble	Total	Soluble	Total	Soluble	Total
Mean	100.01	129.82	2.11	0.79	20.23	21.93	8.79	10.99	4.88	4.76
Variance	89.78	298.44	0.65	0.12	124.42	177.72	9.48	17.32	3.31	2.92
F value	3.32		5.23		1.43		1.83		1.13	
P _f	0.11		0.05		0.35		0.26		0.45	
T value	-3.71		3.67		-0.24		-1.04		0.12	
P _t	4.07E-03		7.92E-03		0.82		0.32		0.91	

Table 33: Trace element t-tests among springs

	Aluminum		Boron		Iron		Zinc	
	Soluble	Total	Soluble	Total	Soluble	Total	Soluble	Total
Mean	20.87	134.77	28.34	36.85	25.69	103.91	5.17	7.86
Variance	381.36	10219.29	32.93	54.80	866.35	4536.50	3.12	12.58
F value	26.80		1.66		5.24		4.04	
P _f	0.001		0.29		0.05		0.08	
T value	-2.71		-2.23		-2.61		-1.66	
P _t	4.23E-02		5.02E-02		3.51E-02		0.13	

Table 34: Major element t-tests among sample dates

	Calcium		Potassium		Magnesium		Sodium		Sulphur	
	Soluble	Total	Soluble	Total	Soluble	Total	Soluble	Total	Soluble	Total
Mean	101.40	128.35	1.96	0.78	19.87	21.37	8.63	10.51	4.82	4.64
Variance	388.19	669.65	5.37	0.02	5.38	16.23	8.60	4.83	0.64	0.52
F value	1.73		256.05		3.02		1.78		1.23	
P _f	0.18		1.58E-12		0.03		0.17		0.36	
T value	-2.99		1.83		-1.16		-1.85		0.60	
P _t	6.40E-03		0.09		0.26		0.08		0.55	

Table 35: Trace element t-tests among sample dates

	Aluminum		Boron		Iron		Zinc	
	Soluble	Total	Soluble	Total	Soluble	Total	Soluble	Total
Mean	21.48	137.56	28.92	37.42	102.50	24.91	5.62	7.73
Variance	2141.22	14217.86	358.84	462.11	9266.14	1704.91	35.16	107.53
F value	0.15		1.29		5.43		3.06	
P _f	1.29E-03		0.33		3.20E-03		0.03	
T value	-3.27		-1.07		-2.67		-0.64	
P _t	3.22E-03		0.30		0.02		0.53	

8.2.2 Soluble Element PCA Biplots

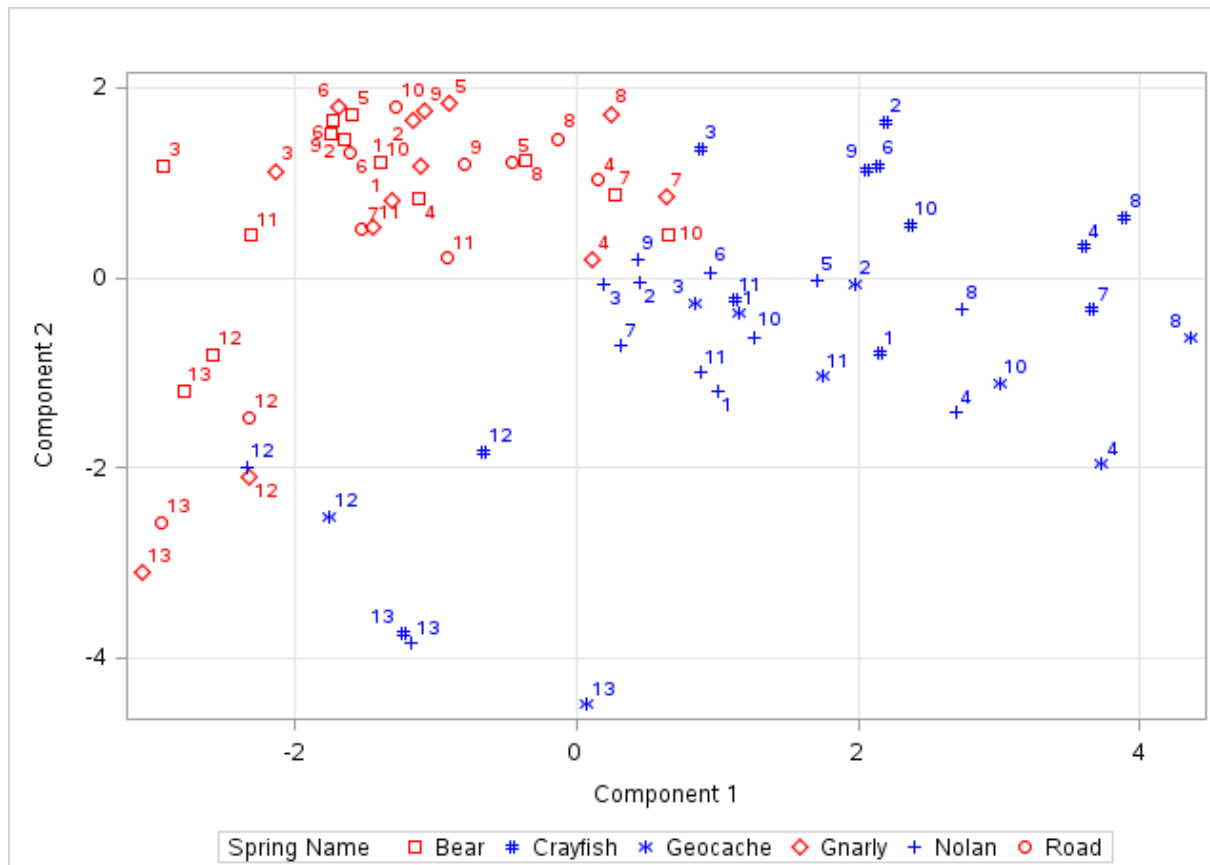
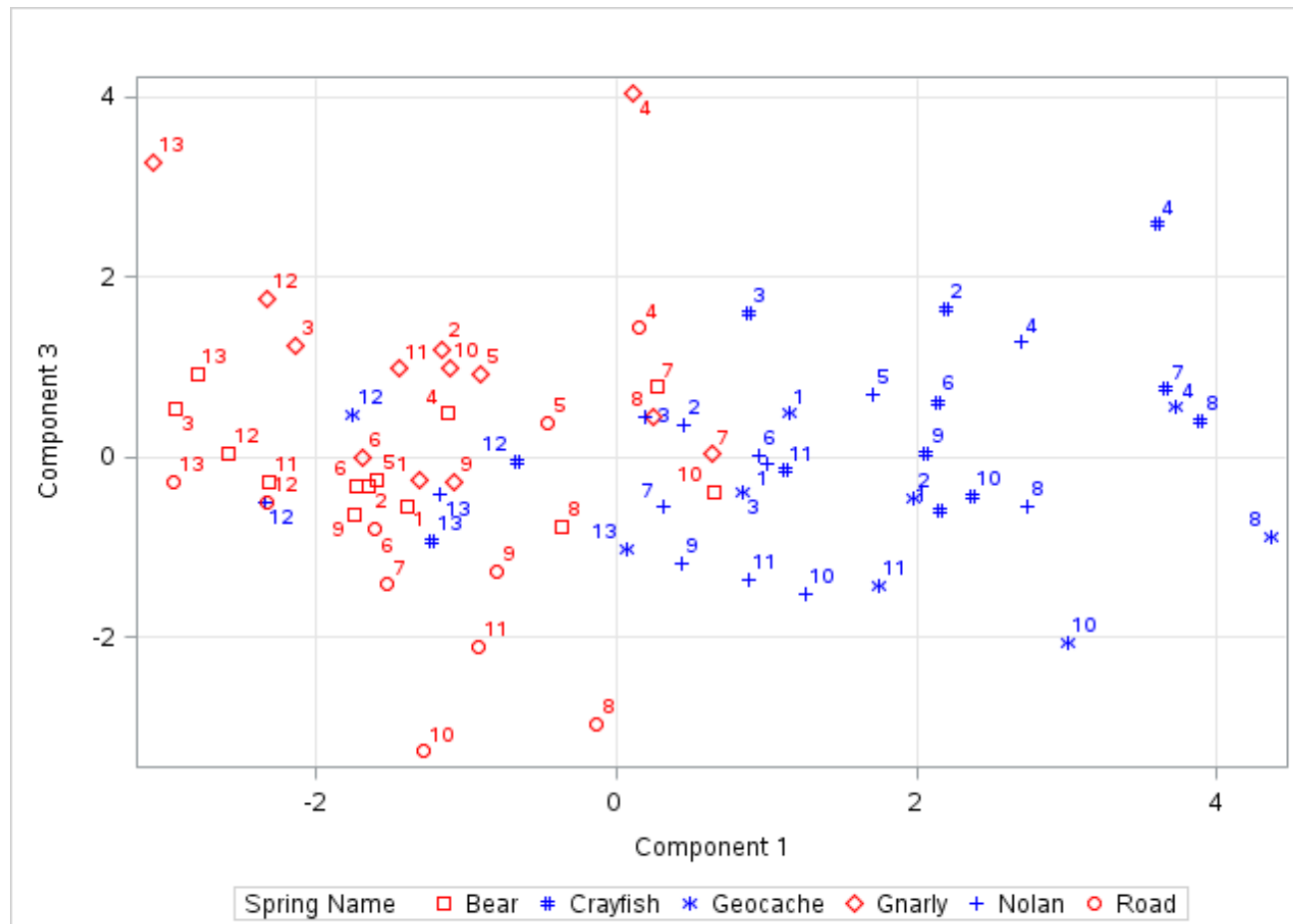


Figure 39: Soluble element PCA biplot of component 1 (Cl, Na, Mg, and S) x component 2 (K and inverse pH)



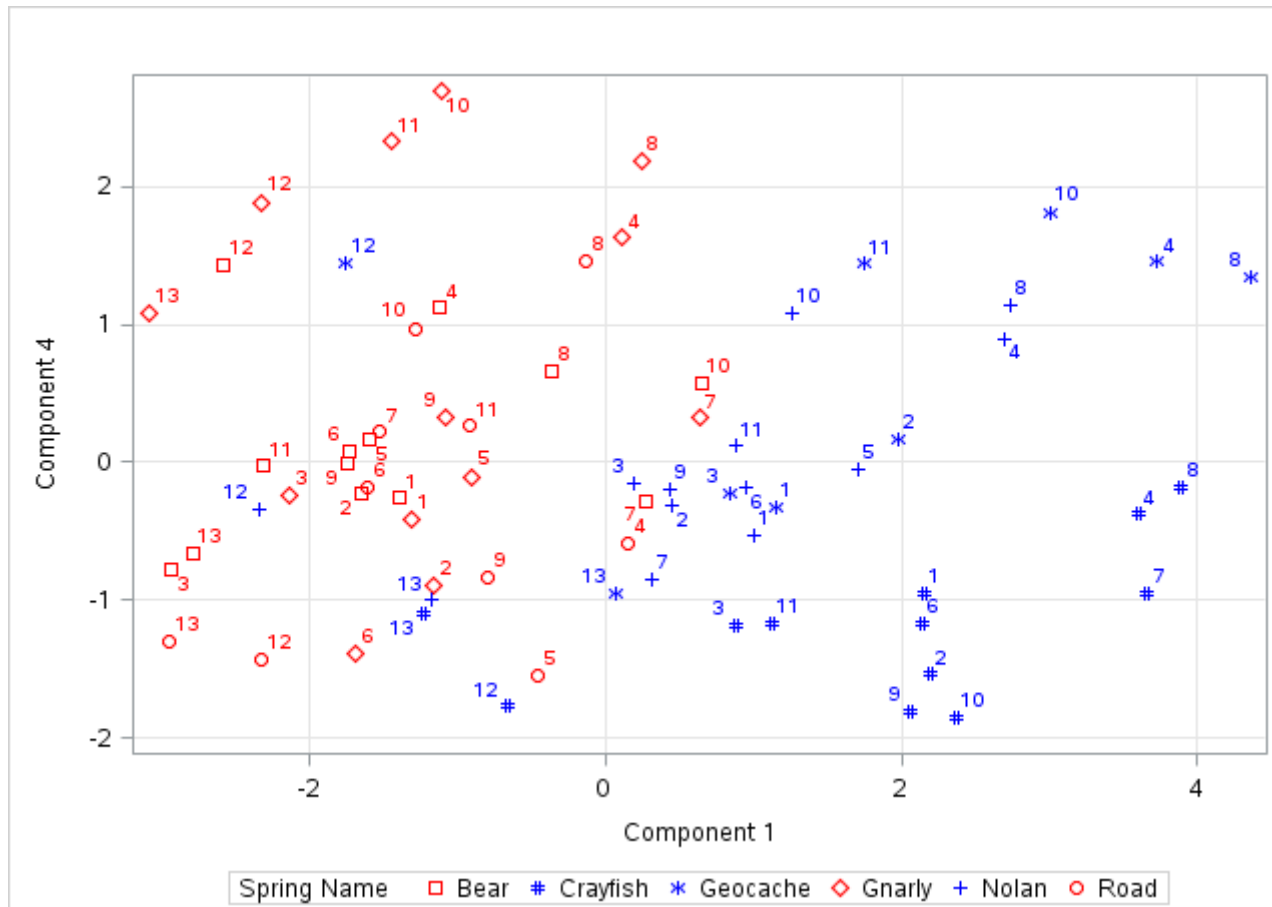


Figure 41: Soluble element PCA biplot component 1 (Cl, Na, Mg, and S) x component 4 (conductivity)

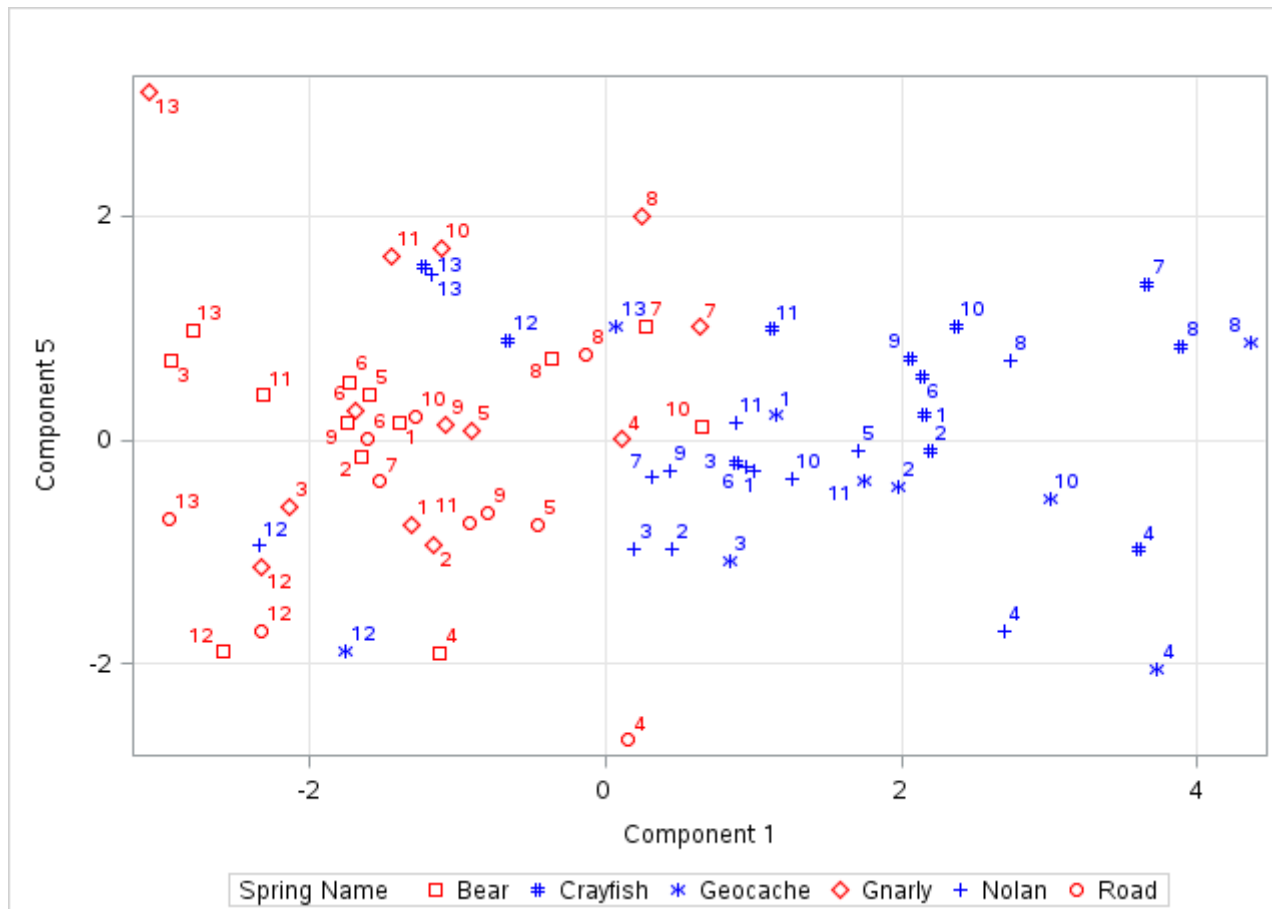


Figure 42: Soluble element PCA biplot component 1 (Cl, Na, Mg, and S) x component 5 (Ca, F, and discharge)

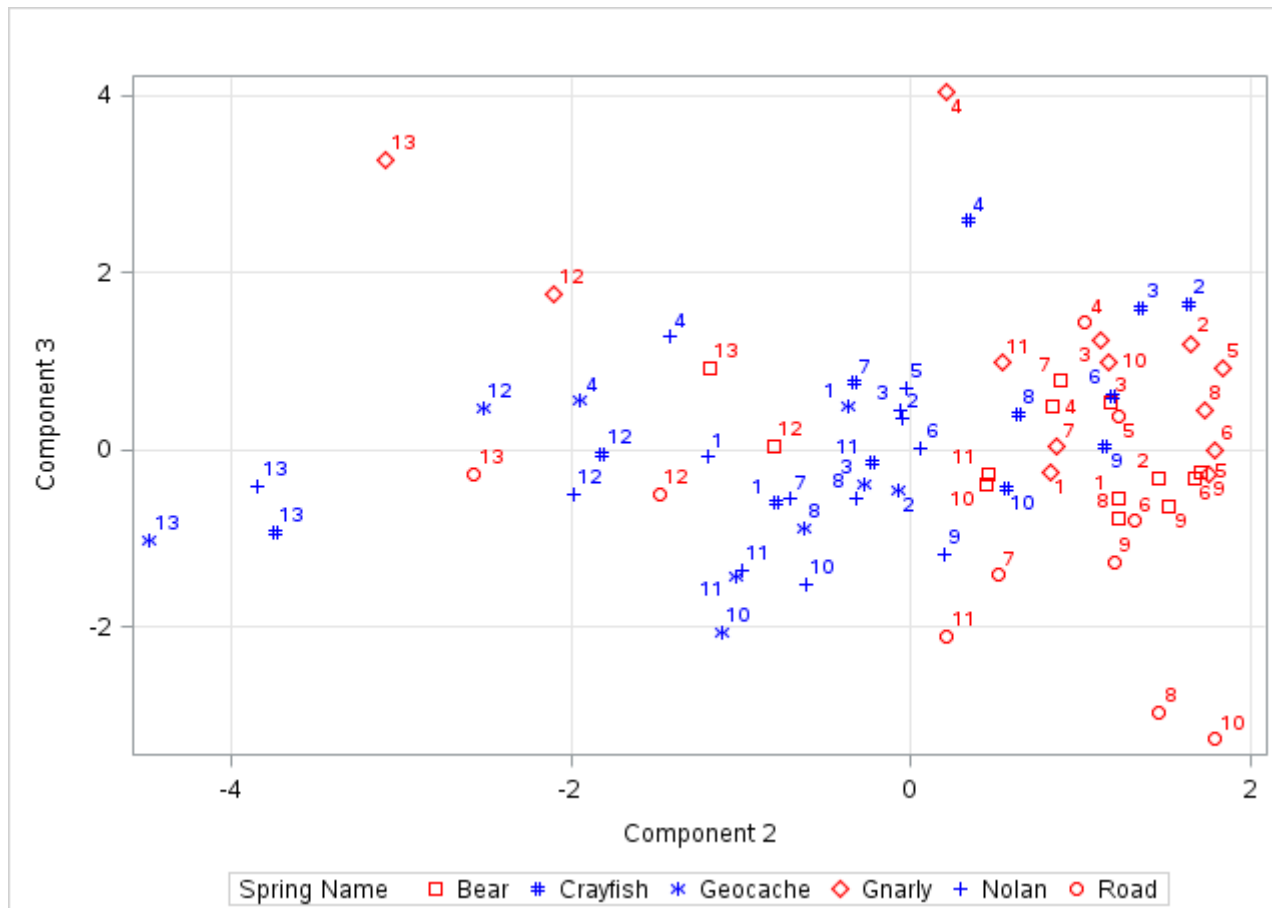


Figure 43: Soluble element PCA biplot component 2 (K and inverse pH) x component 3 (N and inverse temperature)

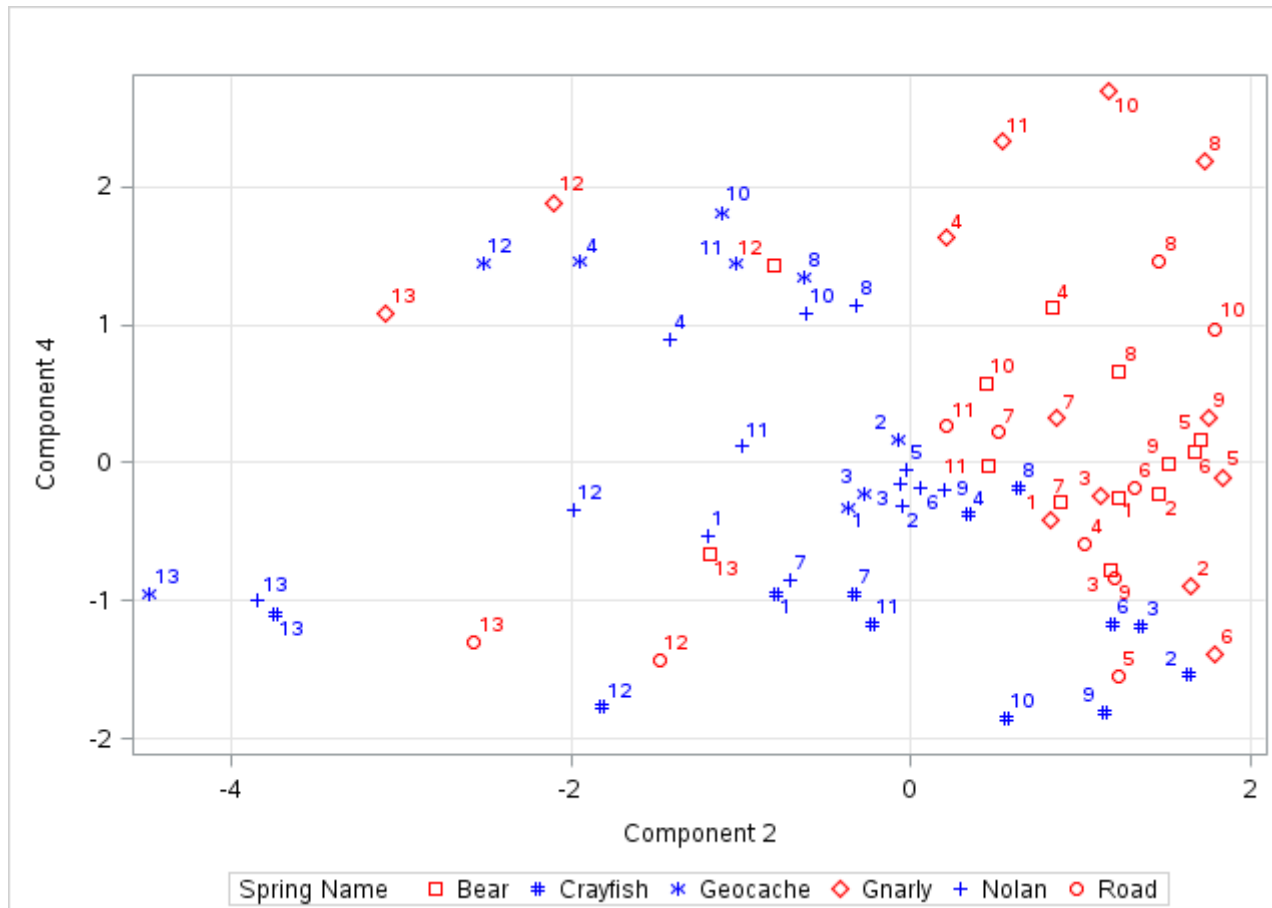


Figure 44: Soluble element PCA biplot component 2 (K and inverse pH) x component 4 (conductivity)

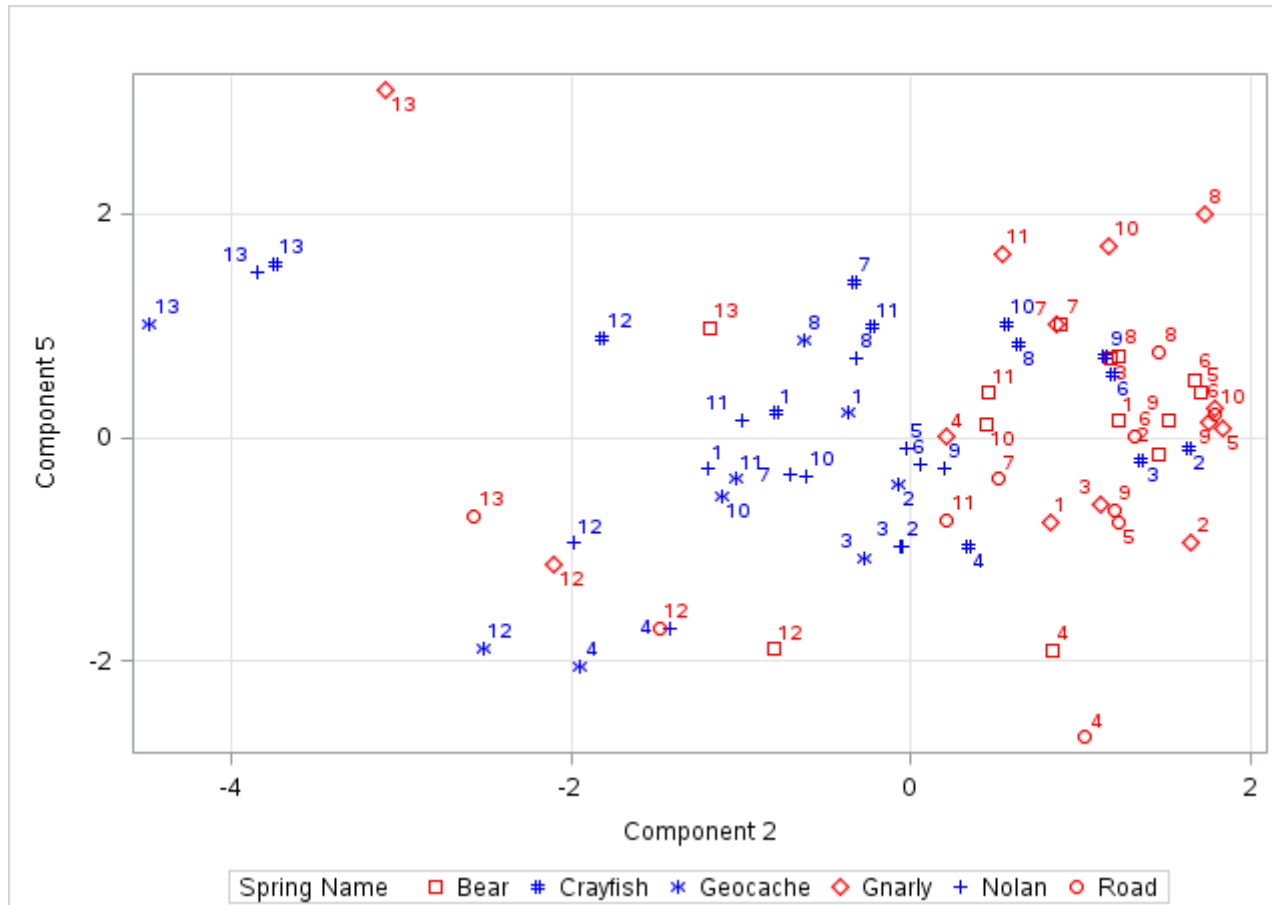


Figure 45: Soluble element PCA biplot component 2 (K and inverse pH) x component 5 (Ca, F, and discharge)

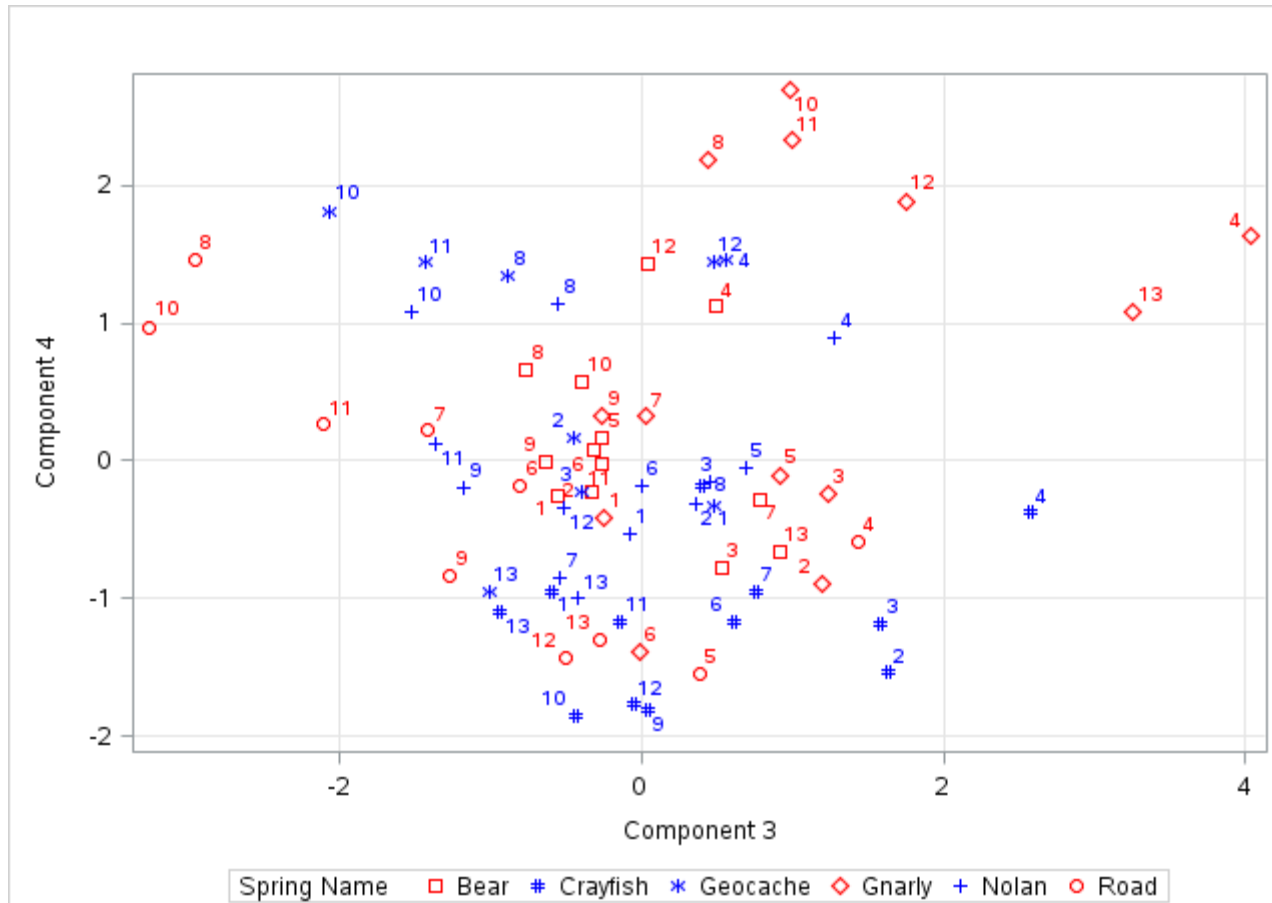


Figure 46: Soluble element PCA biplot component 3 (N and inverse temperature) x component 4 (conductivity)

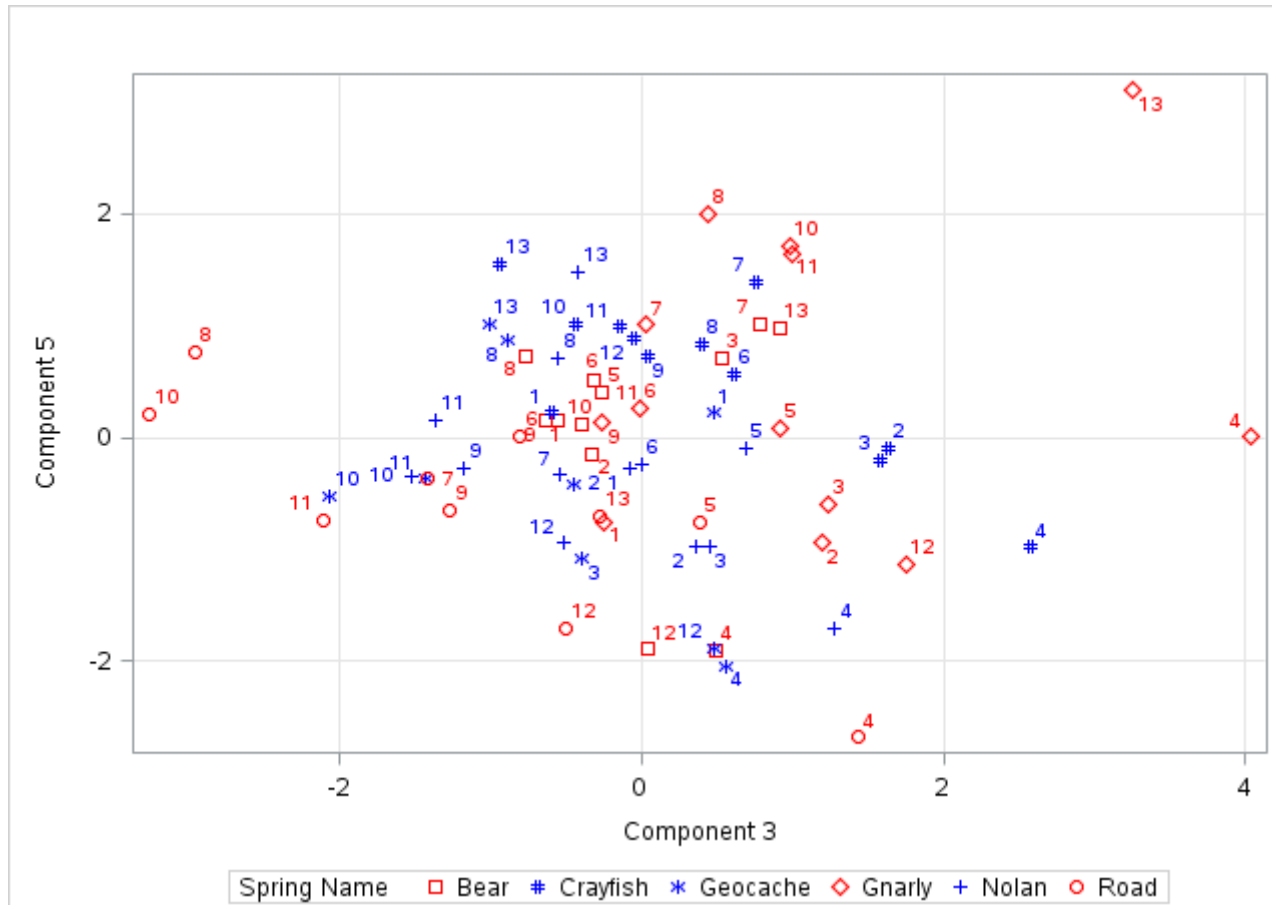
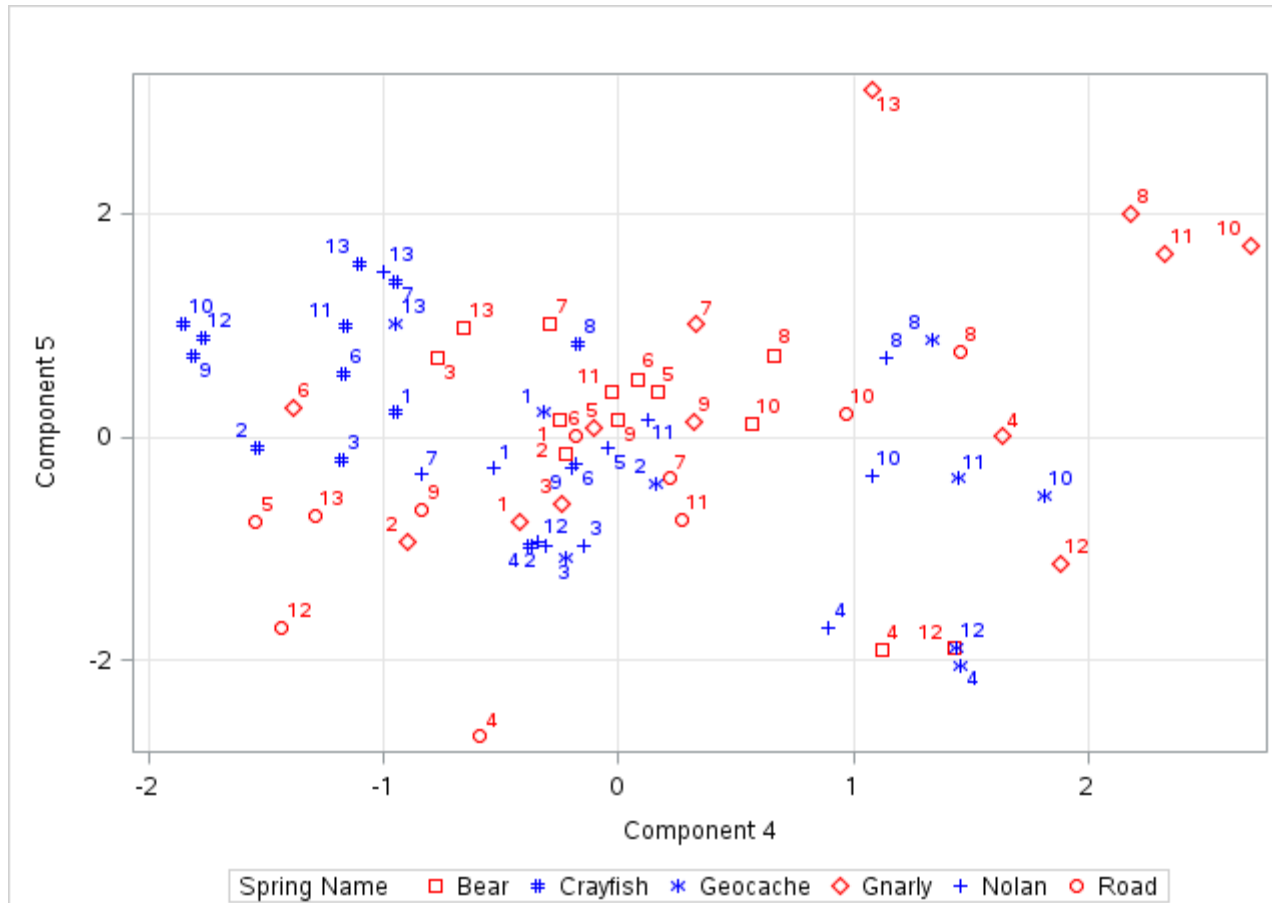


Figure 47: Soluble element PCA biplot component 3 (N and inverse temperature) x component 5 (Ca, F, and discharge)



8.2.3 Total Element PCA Biplots

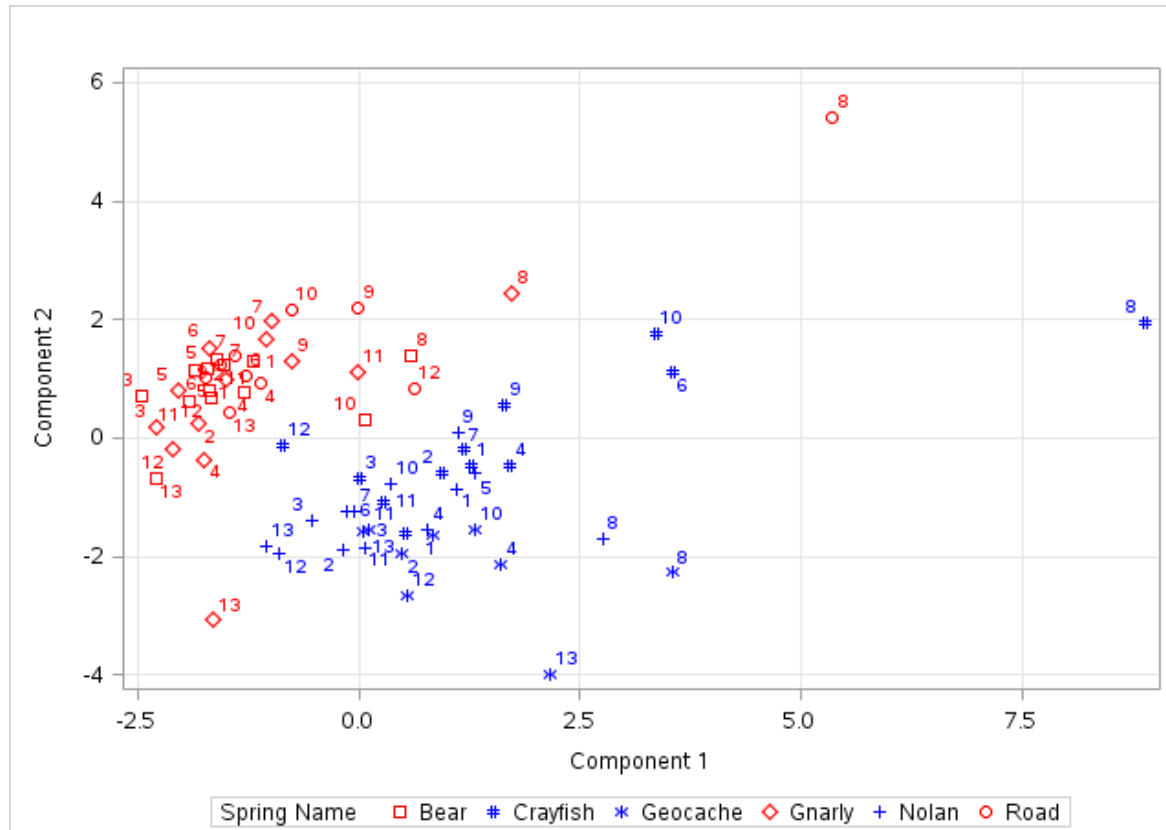


Figure 49: Total element PCA biplot component 1 (Al, Fe, Na, and S) x component 2 (Mg and inverse K)

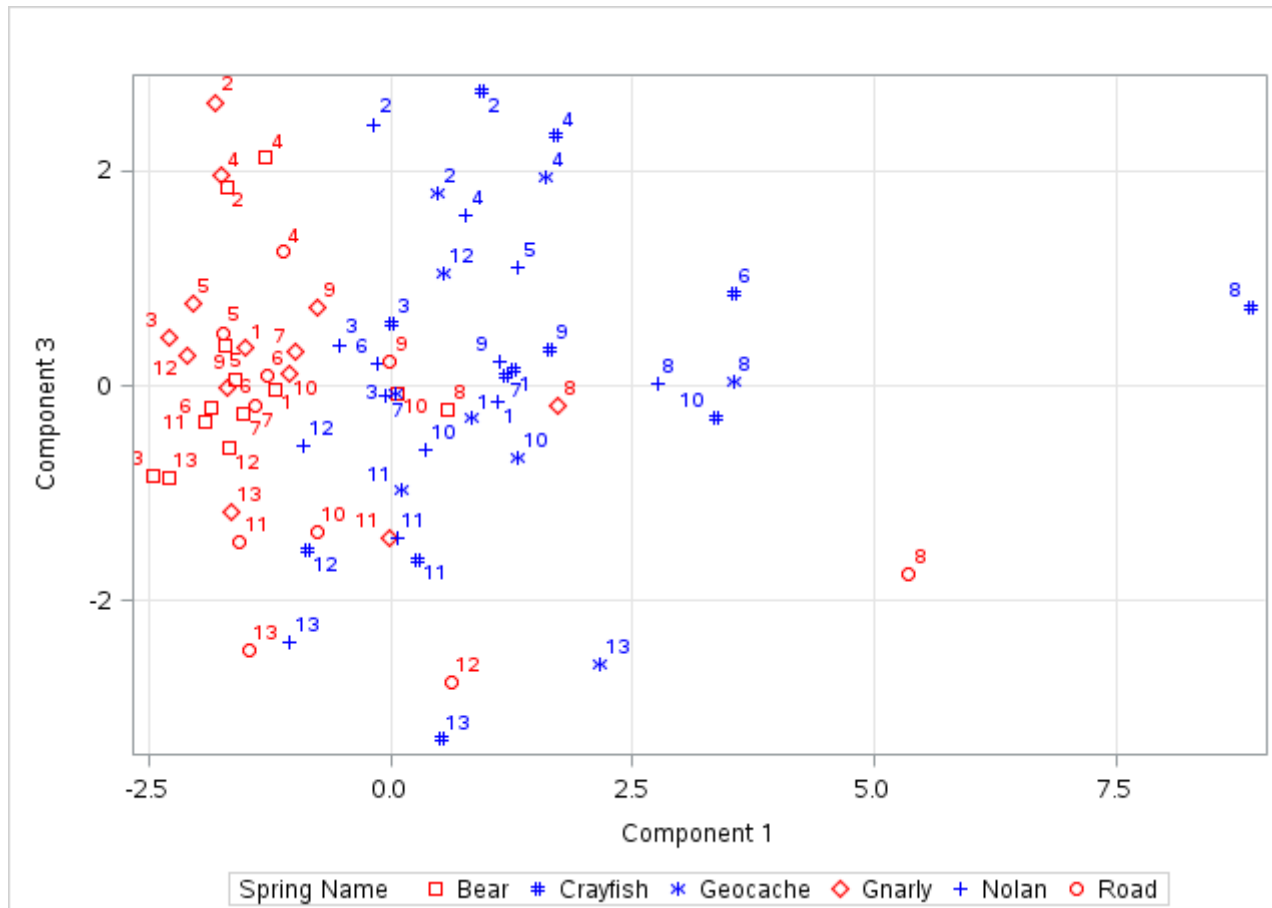


Figure 50: Total element PCA biplot component 1 (Al, Fe, Na, and S) x component 3 (B, Zn, and pH)

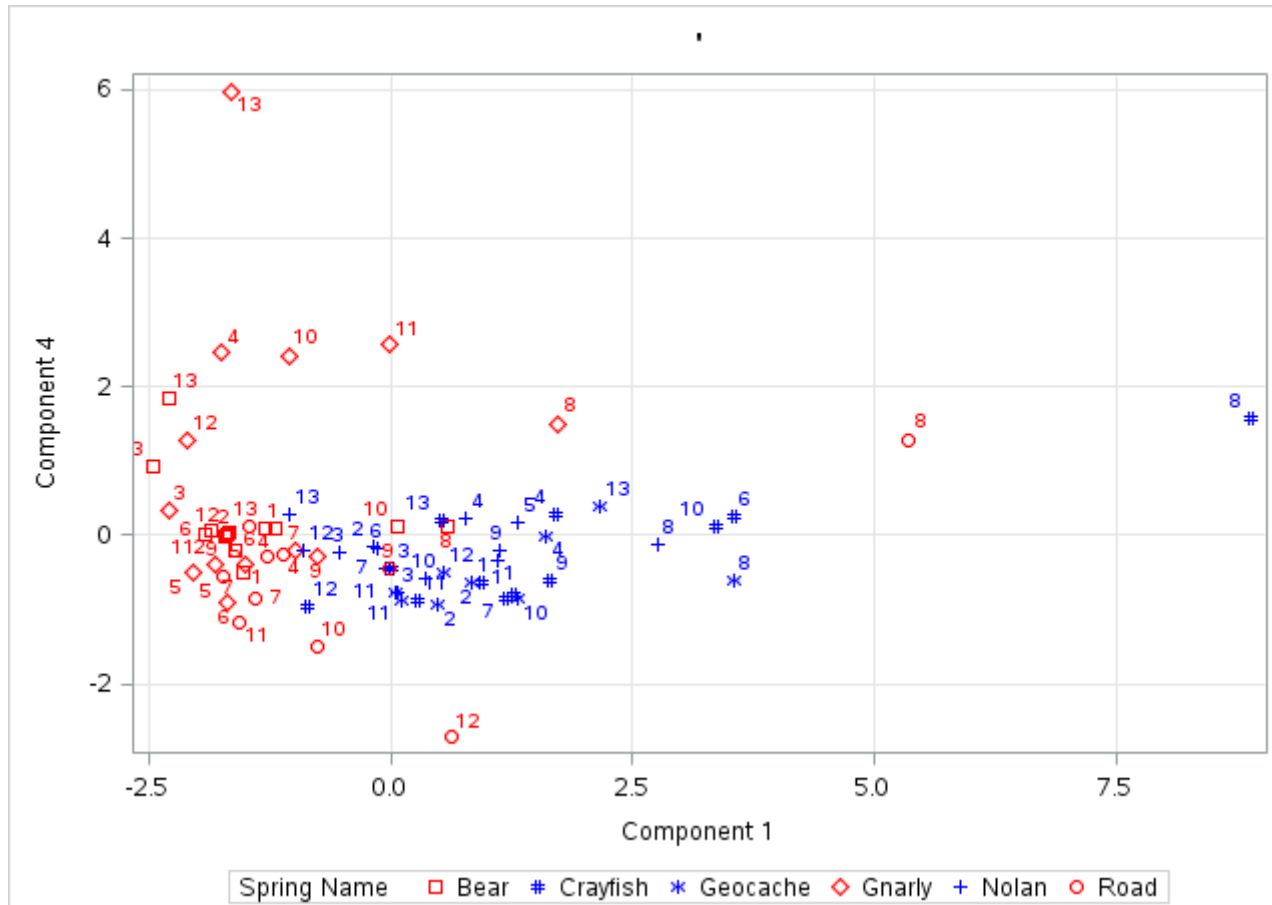


Figure 51: Total element PCA biplot component 1 (Al, Fe, Na, and S) x component 4 (discharge)

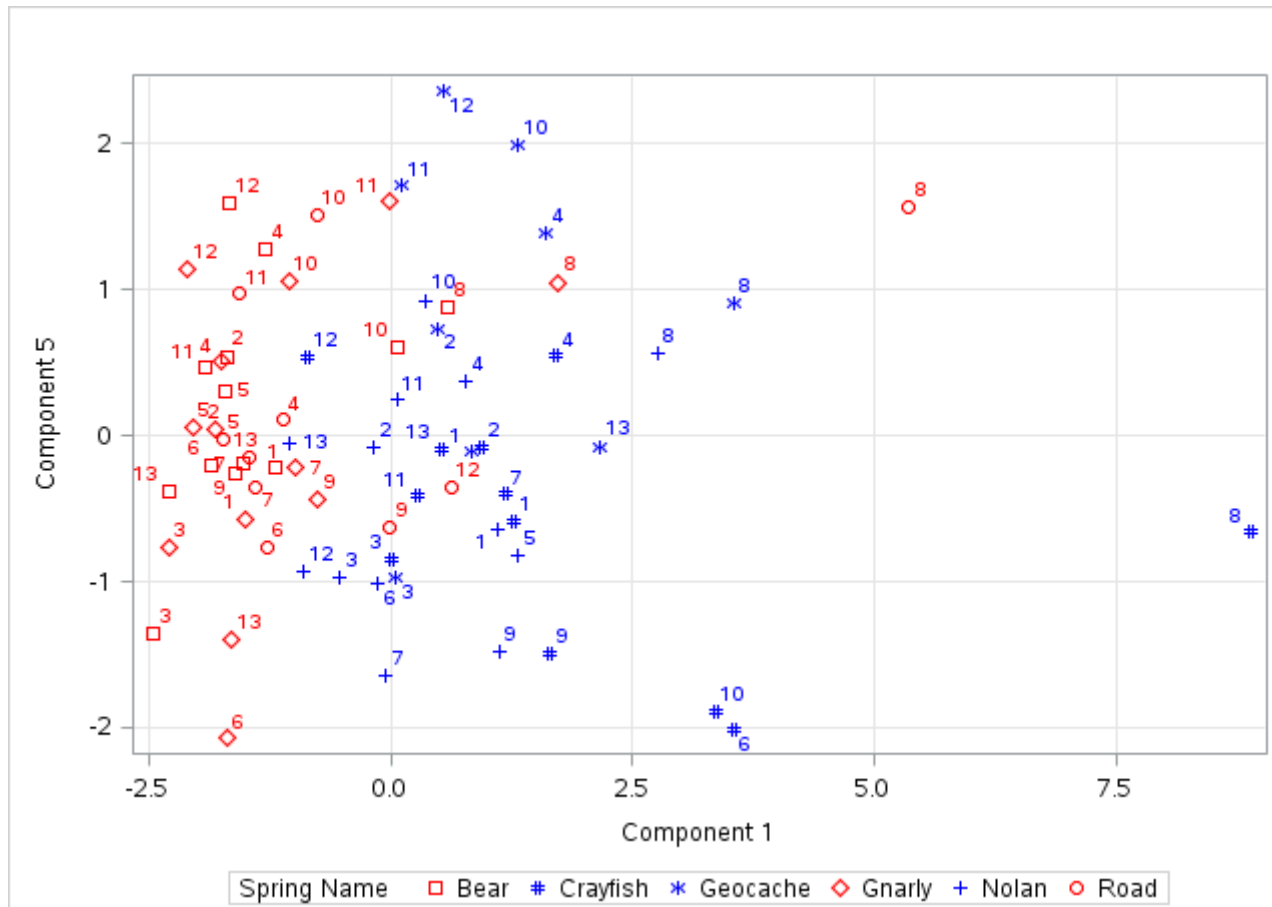


Figure 52: Total element PCA biplot component 1 (Al, Fe, Na, and S) x component 5 (conductivity)

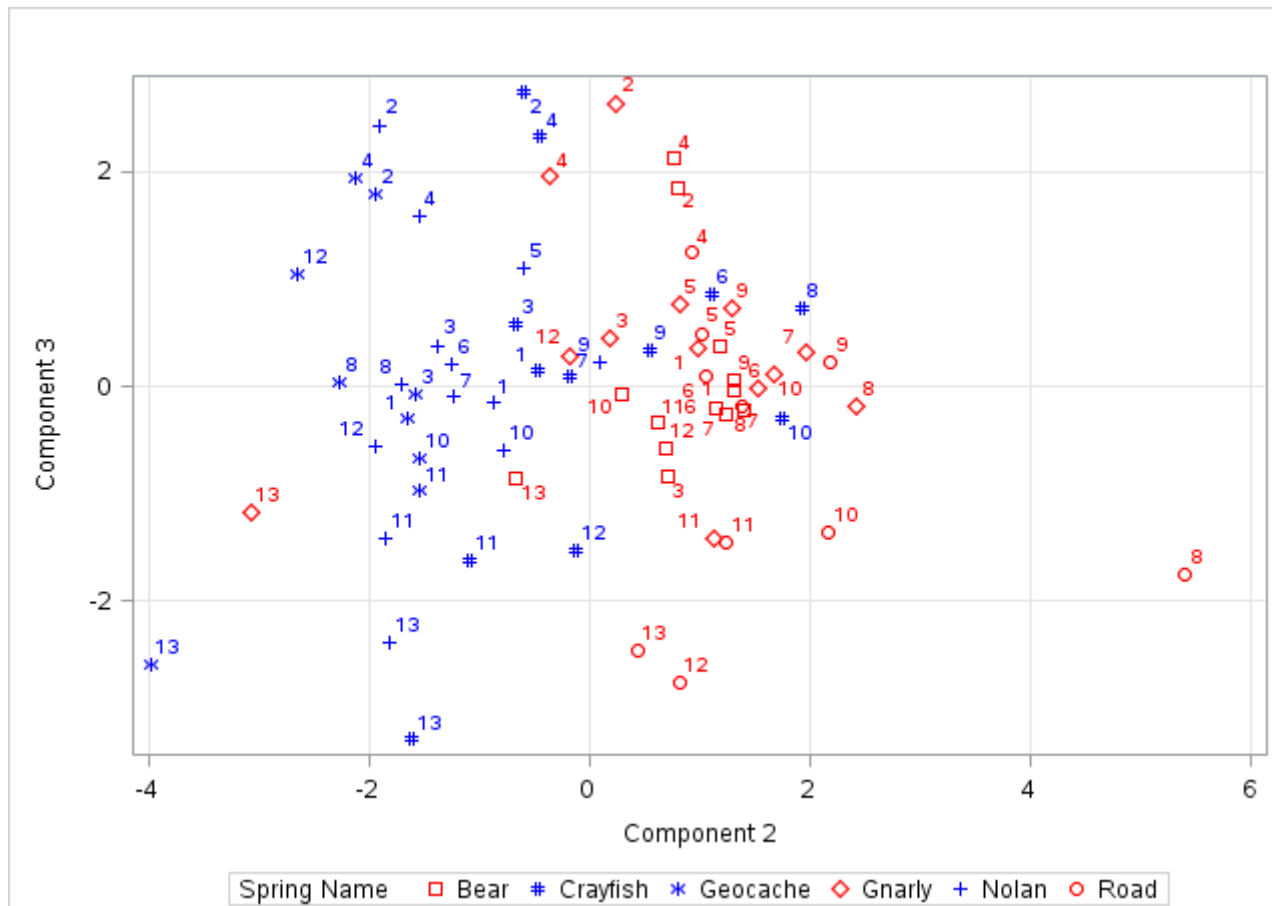


Figure 53: Total element PCA biplot component 2 (Mg and inverse K) x component 3 (B, Zn, and pH)

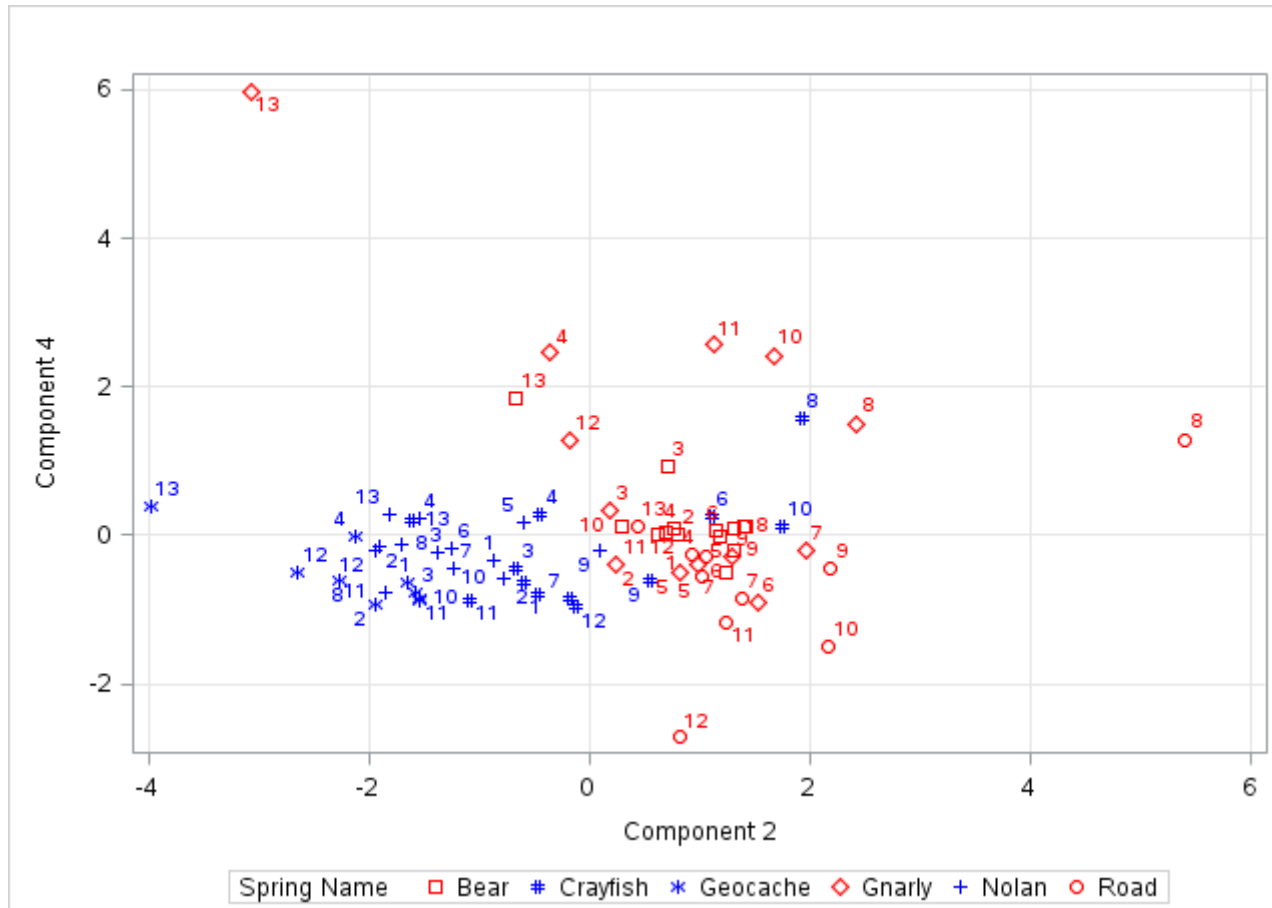


Figure 54: Total element PCA biplot component 2 (Mg and inverse K) x component 4 (discharge)

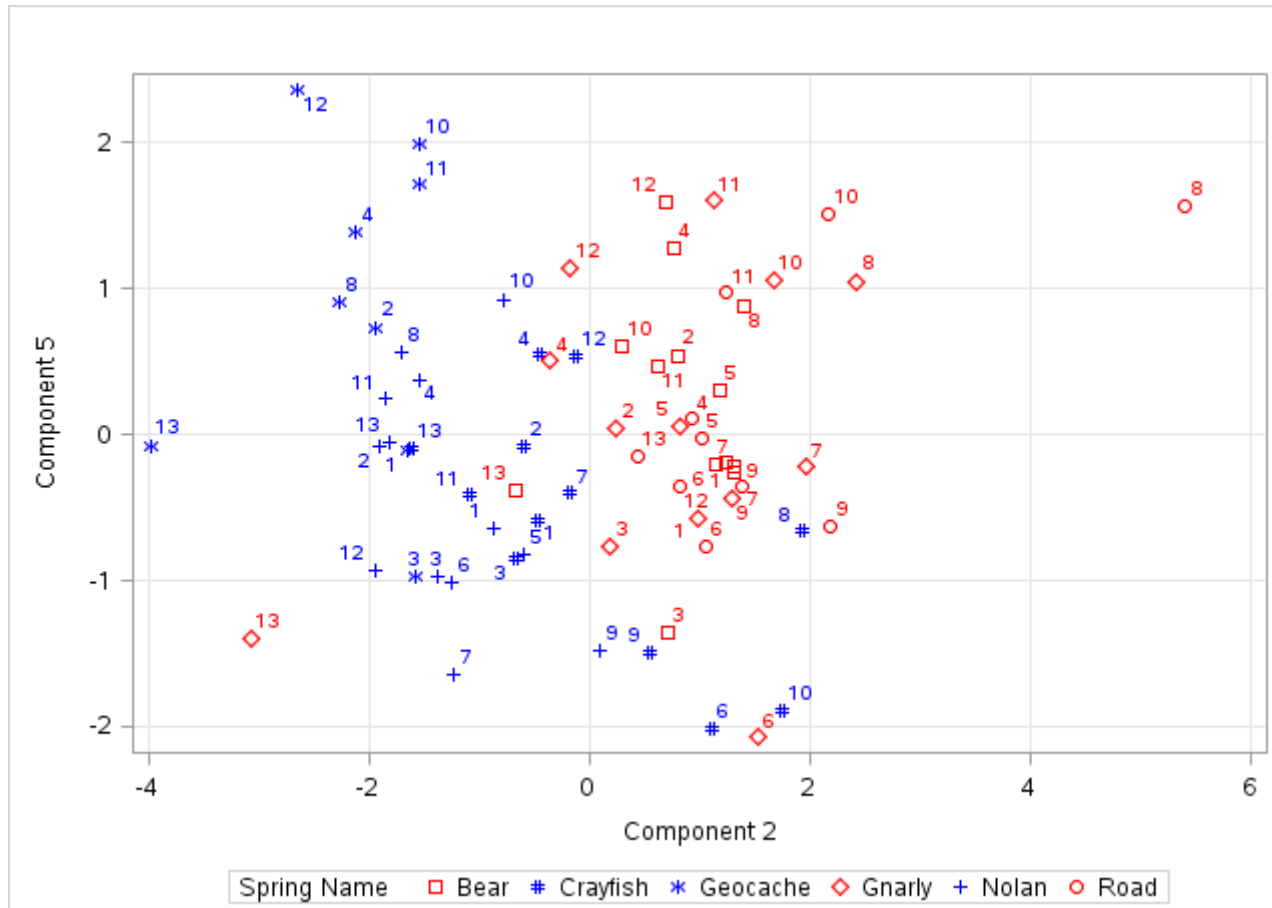


Figure 55: Total element PCA biplot component 2 (Mg and inverse K) x component 5 (conductivity)

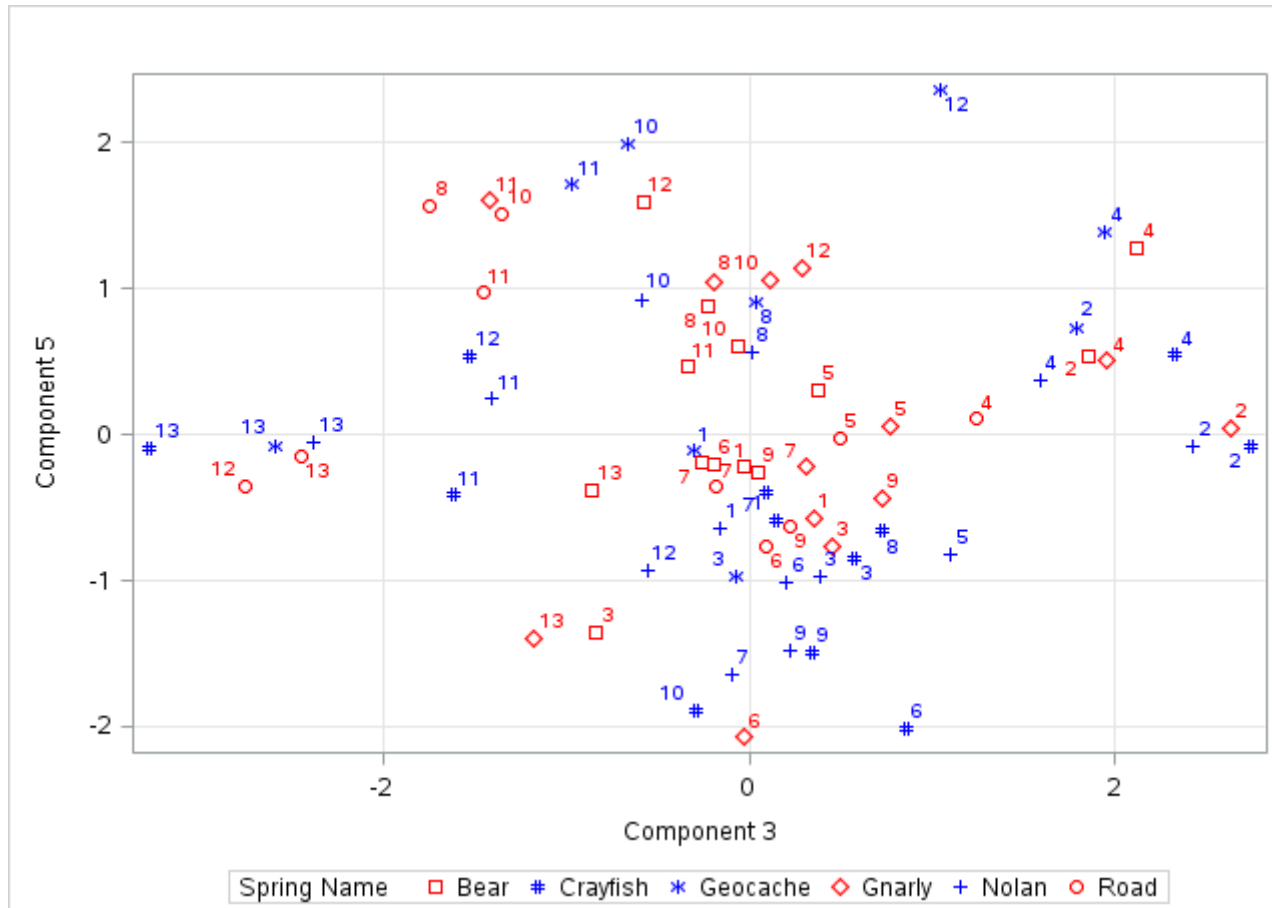


Figure 57: Total element PCA biplot component 3 (B, Zn, and pH) x component 5 (conductivity)

9. VITA

William Scribner Welles is from Orland Park, Illinois and attended Carl Sandburg High School and transferred to Ombudsman in Crestwood, Illinois graduating in 2001. After high school he graduated from Universal Technical Institute with an auto mechanics certificate in 2003. Returning to academia he took courses at Moraine Valley Community College (MVCC) and graduated from University of Illinois at Chicago (UIC) with a BS in chemistry and a minor in earth and environmental science in 2010. While at MVCC he was a lab teaching assistant. He continued his laboratory experiences by working in two laboratories while at UIC, the organic geochemistry laboratory and a physiology laboratory. William then enrolled at Stephen F. Austin State University (SFA) seeking a master's in environmental science. While attending SFA he began working at the Nacogdoches Central Appraisal District as a geographic information system (GIS) analyst He is now working at the Dallas Central Appraisal District (DCAD) as a senior GIS specialist.

Permanent Address: 10914 Palace Way
 Dallas, TX 75218

Style Manual Designation: JAWRA

This thesis was typed by William S. Welles